Leibniz Institute of Virology

University Medical Center Hamburg-Eppendorf

The role of the tissue-damage signaling protein HMGB1 in cytomegalovirus infection

Dissertation

Submitted to the

Department of Biology

Faculty of Mathematics, Informatics and Natural Sciences

University of Hamburg

In fulfillment of the requirements for the degree of

Doctor of Natural Sciences (Dr. rer. nat.)

by

Irke Waßmann

born in Hamburg, Germany

Hamburg, November 2024

Prof. Dr. Wolfram Brune (First Reviewer)

Prof. Dr. Tim Gilberger (Second Reviewer)

Date of disputation: 21.03.2025

This study was conducted between August 2020 and June 2024 at the Leibniz Institute of Virology (LIV) and the University Medical Center Hamburg-Eppendorf (UKE) under the supervision of Prof. Dr. Wolfram Brune and PD Dr. med. Peter Hübener.

Contents

1. Zusammenfassung

Das Protein High Mobility Group Box 1 (HMGB1) ist ein hochgradig multifunktionales und hoch-exprimiertes Molekül, das für seine Beteiligung an verschiedenen DNA-assoziierten Prozessen sowie für seine Rolle als schadensassoziiertes Signalmolekül (*damage-associated molecular pattern,* DAMP) bekannt ist. Obwohl ursprünglich im Zellkern konzentriert, kann HMGB1 in das Zytoplasma translozieren und durch aktive Sekretion, Zelltod oder Gewebeverletzungen in das extrazelluläre Milieu freigesetzt werden. Extrazelluläres HMGB1 ist ein potentes Signalmolekül, das bei sterilen Gewebeschäden sowie Infektionen regulatorisch auf zahlreiche Entzündungsprozesse wirkt. Die Auswirkungen des HMGB1-vermittelten Signals auf die Abwehr von Krankheitserregern und die Beseitigung von Viren sind jedoch noch wenig erforscht. Jüngste Forschungsergebnisse deuten darauf hin, dass HMGB1 vielseitige Funktion hat. So kann es zum einen die Virusreplikation unterstützen, wenn es intrazellulär vorhanden ist. Zum anderen ist aber auch bekannt, dass es die Virusausbreitung einschränkt, insbesondere wenn es in den extrazellulären Raum freigesetzt wird. Allerdings konzentrieren sich die meisten Studien auf RNA-Viren, während das Wissen über den Einfluss von HMGB1 auf den Lebenszyklus und die Ausbreitung von DNA-Viren sehr limitiert ist.

Da HMGB1 vielfältige und gegensätzliche Funktionen ausüben kann, soll in dieser Studie die Rolle von HMGB1 während der Infektion mit einem DNA-Virus, dem Cytomegalovirus (CMV), weiter untersucht und sein Beitrag zur Virusausbreitung und/oder -eliminierung bewertet werden. Um die Auswirkungen von HMGB1 auf die CMV-Replikation zu untersuchen, wird das etablierte Maus-CMV (MCMV)-Infektionsmodell zusammen mit transgenen HMGB1-defizienten Mäusen und murinen Zellkulturen mit veränderter HMGB1-Expression verwendet.

Die Ergebnisse der vorliegenden Studie deuten darauf hin, dass HMGB1 die frühe MCMV-Transkription unterstützt und mit hoher Wahrscheinlichkeit mit viralen Genomen interagieret, da es im Kern infizierter Zellen verbleibt und sich in viralen Replikationskompartimenten anreichert. Im Gegensatz dazu konnte hier gezeigt werden, dass extrazelluläres HMGB1, welches von MCMV-infizierten Zellen freigesetzt wird, die Virusreplikation zelltyp-abhängig inhibiert. Insbesondere in Makrophagen löst die Virus-vermittelte Freisetzung von HMGB1 den Zelltod aus, was das virale Wachstum in diesen Zellen begrenzt. In Übereinstimmung mit diesen *in*

vitro Daten, konnte gezeigt werden, dass HMGB1 auch *in vivo* die frühe MCMV-Replikation unterstützt. In späteren Phasen der Infektion hingegen scheint das Vorhandensein von HMGB1 die Virusreplikation und/oder -verbreitung negativ zu beeinflussen.

2. Abstract

High mobility group box 1 (HMGB1) protein is a highly multifunctional and abundant molecule known for its engagement in various DNA-associated processes and for its role as a damage-associated molecular pattern (DAMP). Initially concentrated in the cell nucleus, HMGB1 can translocate into the cytoplasm and be released into the extracellular milieu by active secretion, cell death or tissue injury. Extracellular HMGB1 is a potent signaling molecule regulating numerous inflammatory processes in the context of sterile tissue damage as well as infections. However, the impact of HMGB1-mediated signaling on pathogen defense and viral clearance remains poorly understood. Recent research suggests that HMGB1 has versatile functions. Indeed, it could support viral replication when present intracellularly but it is also known to restrict viral spread especially when it is released into the extracellular space. However, most studies focus on RNA viruses, while knowledge about the influence of HMGB1 on the life cycle and spread of DNA viruses is remarkably small.

Since HMGB1 can exert diverse and opposing functions, the aim of this study is to further investigate the role of HMGB1 during infection with a DNA virus, the cytomegalovirus (CMV), and to evaluate its contribution to viral progression and/or elimination. In order to investigate the impact of HMGB1 on CMV replication, the well-established mouse CMV (MCMV) infection model is used alongside transgenic HMGB1-deficient mice and murine cell cultures with altered HMGB1 expression.

The results obtained in the present study indicate that HMGB1 supports early MCMV transcription and is highly likely to interact with viral genomes, as it remains in the nucleus of infected cells and locates to viral replication compartments. In contrast, the data shows that extracellular HMGB1 released by MCMV-infected cells inhibits viral replication in a cell type-dependent manner. In macrophages in particular, virus-triggered release of HMGB1 induces cell death, which limits viral growth in these cells. In agreement with these *in vitro* results, HMGB1 was shown to support early MCMV replication *in vivo*. However, at later stages of infection, the presence of HMGB1 seems to negatively affect viral replication and/or dissemination.

3. Introduction

3.1 Cytomegalovirus

3.1.1 Cytomegalovirus epidemiology

In 1881, Hugo Ribbert was the first to describe cells with intranuclear inclusions in kidney sections from a stillborn child with syphilis, thus not knowingly documenting the first observation of human cytomegalovirus (HCMV) infection. Independent observations throughout the following decades suggested a group of viruses causing these intranuclear inclusions and various pathologies. Today those viruses are known as members of the *Herpesviridae* family, more specifically, the *Betaherpesvirnae* subfamily. In the early 1950s, due to major developments in cell culture techniques, Weller and Smith were able to isolate CMV from human and mouse cultures (reviewed in [1]).

HCMV is one of the most common human herpes viruses worldwide, with serum prevalence ranging from 45 % to almost 100 % depending on factors such as age, socio-economic status, and geographical location (reviewed in [2]). CMV enters the host via various routes, e.g. via the urogenital tract, the upper digestive tract, or the respiratory tract. Transmission of the virus can occur via direct contact with body fluids like saliva, urine, blood, semen, and breast milk or through blood transfusions and organ transplantations. Moreover, HCMV can be transmitted from mother to fetus through the placental barrier causing congenital infections. While immunocompetent adults often experience subclinical or mild illness, immunocompromised individuals, e.g. cancer patients, HIV-infected patients or transplant recipients are at greater risk of severe manifestations [1, 3, 4]. Congenital HCMV infections can lead to severe complications such as microcephaly, hearing loss, neurological abnormalities, or even miscarriage. CMV is the most common infectious cause of birth defects in the United States. With one in 200 babies born with a congenital CMV infection and about 10 to 15 % of CMV-infected babies developing long-term diseases, CMV is a major burden on public health systems [5, 6]. Despite the severity of CMV infections, only a few treatment options are available, including drugs like ganciclovir, valganciclovir, foscarnet, cidofovir, and letermovir [7, 8]. These drugs, targeting viral replication and packaging, have limitations due to their associated toxicities, such as myelosuppression, nephrotoxicity, retinal detachment, neutropenia, and anemia, and the increasing development of resistance

[9]. While organ transplant recipients are particularly susceptible to severe HCMV courses, drug treatment is often problematic due to the high toxicity [9]. There is a clear need for better treatment and prevention of CMV infections to reduce the burden on the population and healthcare systems. While there are currently clinical trials for CMV vaccines, none have been approved yet. Many challenges remain in developing new therapeutic agents and effective preventive measures.

3.1.2 Cytomegalovirus structure and life cycle

Herpes viruses belong to the large, enveloped DNA viruses. Although they share certain essential biological and morphological characteristics that distinguish them from other viruses, they are further divided into three subfamilies: alpha, beta, and gamma herpes virus. Known human-pathogenic members of the *Alphaherpesvirinae* are for example herpes simplex virus (HSV) and varicella zoster virus, while Epstein-Barr virus (EBV) and Karposi's sarcoma-associated herpesvirus (KSHV) are representatives of the *Gammaherpesvirinae.* CMV on the other hand is the prototype virus of the *Betaherpesvirinae*.

CMV virions are about 150 – 200 nm in diameter [10] and consist of the viral genome, nucleocapsid, tegument, and a lipid bilayer membrane (Figure 1). With 230 to 240 kb, CMV carries the largest linear double-stranded DNA genome among all human herpesviruses. It encodes up to 200 viral proteins [11-13]. The genome is embedded in the icosahedral nucleocapsid, which is surrounded by the tegument, a protein-rich layer containing several viral proteins as well as viral and cellular RNAs [14]. Finally, CMV particles are enveloped by a lipid bilayer, which derives from host cell membranes and carries various viral glycoproteins [15].

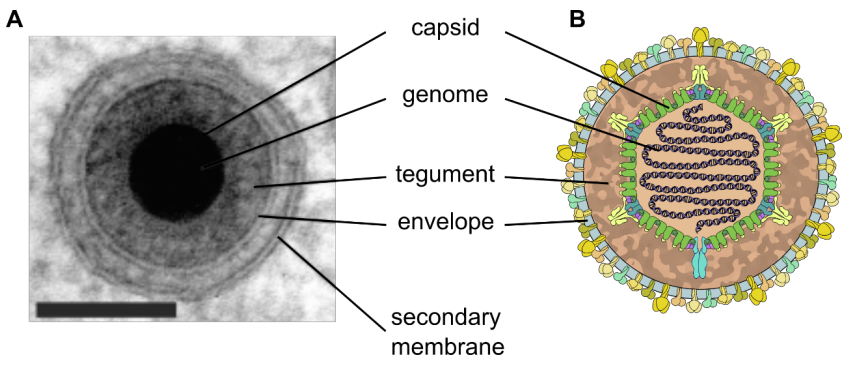

Figure 1: Cytomegalovirus virion structure.
Shown are an electron micrograph image (A, adapted from Read et al., [16]) and a schematic cytomegalovirus virion (B, SwissBioPics - accessed through webpage https://viralzone.expasy.org /180?outline=all_by_species).

One of the key features of the herpesviruses is their ability to undergo lytic as well as latent replication. Both are initiated by the virus entry into the host cell, which requires viral glycoproteins as mediators. In the case of HCMV, the glycoprotein complex gH/gL/gO binds to the cellular receptor platelet-derived growth factor receptor alpha (PDGFRα) mediating attachment to fibroblasts [17]. In contrast, attachment and entry into myeloid cells as well as endothelial and epithelial cells is mediated by the interaction of the pentamer complex gL/gH/pUL128/pUL130/pUL131 with neuropilin-2 [18] (Figure 2). Upon attachment, the viral fusion protein gB, gets activated and promotes fusion of the viral envelope either with the plasma membrane or the membrane of endosomes after the virion entered via endocytosis or micropinocytosis. This ultimately leads to the release of the nucleocapsid and tegument proteins into the host cytoplasm (reviewed in [19]). During lytic replication, nucleocapsid and selected tegument proteins are then transported towards the nucleus by hijacking the cellular microtubule network ([20]). Since CMV capsids are too large to enter the nucleus, only the viral DNA is injected into the nucleus, once the nucleocapsid arrives at the nuclear pore complex. In addition to the viral DNA, selected tegument proteins, such as pp71 and pUL38 of HCMV, also enter the nucleus inhibiting host cell immune responses [21-23] and promoting the expression of immediate early (IE) genes, which are the first viral proteins to be expressed only few hours after infection. IE gene products are crucial for driving lytic replication by enabling the expression of early (E) genes. Proteins encoded by early genes, in turn, ensure replication of the viral genome by the rolling circle mechanism initiated at the genomic region “origin of lytic replication” (oriLyt). Additionally, many early proteins support the expression of late (L) genes and regulate immune responses to ensure survival. For example, they can have certain homologies to cellular cytokines and chemokines or their receptors in order to antagonize their functions (reviewed in [24]).

The late genes encode for structural proteins, necessary for the formation of new viral particles. Some structural proteins encapsulate the viral genome within the nucleus and form the nucleocapsid [25], which is then released from the nucleus by a mechanism called nuclear egress. Once in the cytoplasm, tegumentation and envelopment takes place in cytoplasmic assembly compartments [26]. Finally, viral particles are released from the cell at the plasma membrane (Figure 2).

During CMV latency, which is supported by undifferentiated cells such a myeloid progenitor cells, no viral progeny is produced. After entering the cell and injecting the viral genome into the nucleus, the genome gets circularized and chromatinized. The resulting episome is mostly in a transcriptionally inactive state. During latency, only a specific subset of viral genes is expressed like US28, UL111A, and LUNA, which maintain genome integrity, the latent state, and immune evasion [27, 28].

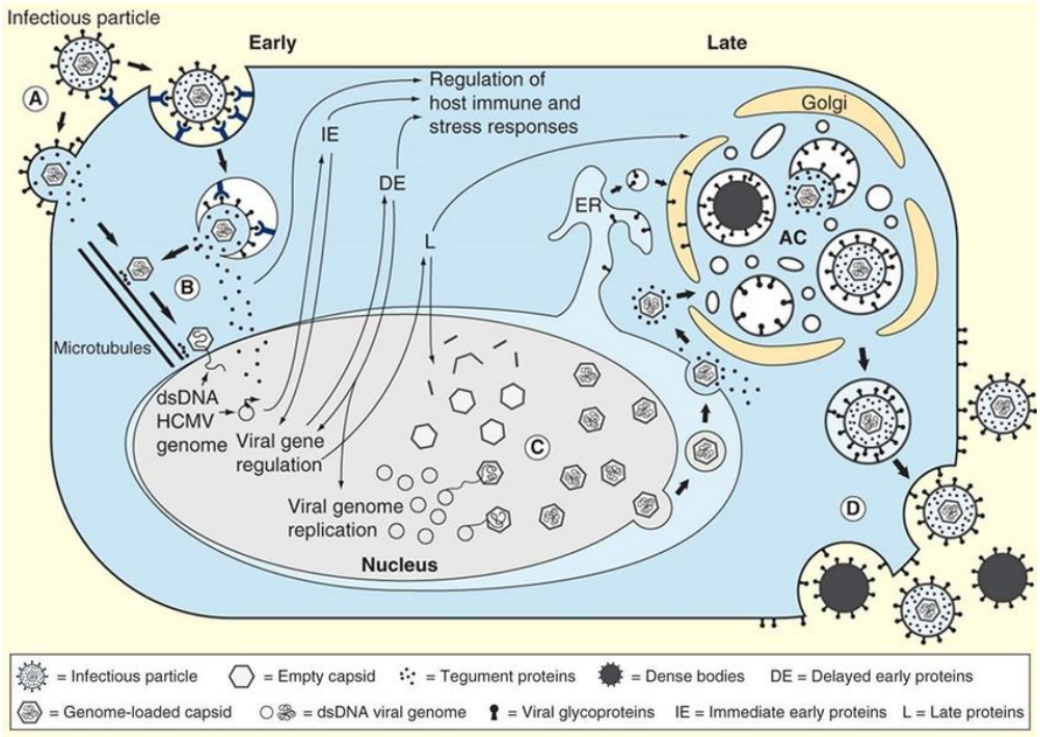

Figure 2: Cytomegalovirus lytic replication.
A) Infectious particles enter the cell through interaction with cellular receptors and membrane fusion at the plasma membrane, endocytosis, or macropinocytosis. **B)** The capsid travels to the nucleus, where the genome is injected and circularized. Tegument proteins initiate the expression of viral immediate early (IE) genes, followed by early (E) genes, which initiate viral genome replication and late (L) gene expression. **C)** Upon late gene expression, capsid assembly in the nucleus followed by nuclear egress to the cytosol take place. After tegumentation, capsids acquire their envelope by budding into intracellular vesicles at the viral assembly compartment (AC). **D)** Enveloped infectious particles are released along with non-infectious dense bodies. Modified from Beltran and Cristea, 2014 [29].

3.1.3 Replication compartments and liquid-liquid phase separation

As mentioned before, following the entry of CMV into the host cell, the viral genome is injected into the cell nucleus where transcription and replication are taking place. As for a wide range of DNA viruses, these processes do not occur all over the nucleus but rather in concentrated compartments called viral replication compartments (RC) (reviewed in [30]). Compartmentalization like this is not a virus-specific phenomenon but is indeed known to be an essential feature of every living cell and organism to ensure optimal conditions for biological reactions and

processes. In addition to membrane-enclosed compartments, numerous membrane-less compartments were discovered in eukaryotic cells, such as P-bodies and stress granules. Recently it has been shown that HCMV pUL112-113 proteins, also known as Early-1 (E1) proteins, initiate the formation of membrane-less viral RCs in the host cell nucleus by liquid-liquid-phase separation (LLPS) [31]. Isoforms of pUL112-113 contain a multivalent interaction domain and an intrinsically disordered region (IDR), both known to be required for phase separation [32-34]. Upon expression of pUL112-113, they cluster at the viral genome, subsequently leading to the induction of LLPS and the formation of early RCs with liquid properties. These compartments build up the optimal environment for viral DNA replication by recruiting important factors such as the viral DNA polymerase and are therefore essential for the successful production of new virions [31]. However, not only viral proteins are found to be in proximity or within the RCs. Host cell factors like proteasome subunits and RNA polymerase II have been found in HCMV RCs ([30, 35, 36]). Despite the importance of the RC, the exact composition and the contribution of host cell proteins to the formation and function of RCs are still largely unknown.

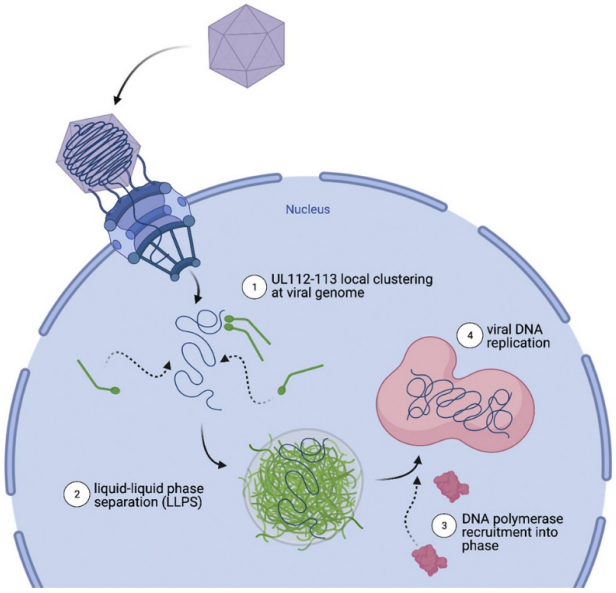

Figure 3: HCMV exploits liquid-liquid phase separation for the formation of the replication compartments. Schematic representation of the formation of viral replication compartments by HCMV pUL112-113 clustering at the viral genome, initiating liquid-liquid phase separation, and recruiting viral components to facilitate viral replication. Source: Caragliano *et al.*, Cell Rep 2022 [31]

3.1.4 Species specificity and cell tropism

In order to successfully infect a host and produce viral progeny, viruses need to adapt to the properties of their host. Due to the genetic background and evolutionary

adaptation the cellular environment has unique features depending on the host species. As a consequence of the co-evolution of viruses and their host, mechanisms have evolved in the host species to restrict viral replication. However, viruses have simultaneously developed countermeasures to enable productive infection in the respective host species. Due to this co-evolutionary adaptation viruses are often able to only infect certain host species [37]. In the case of CMV, high species specificity can be observed since CMV only replicates in cells of their own or closely related host species. For example, HCMV is only able to replicate in human cells as well as chimpanzee fibroblasts, while murine CMV (MCMV) infects cells from mice and rats [38, 39]. CMVs are able to enter cells from distant species and initiate expression of IE and E genes, however, viral DNA replication and late gene expression are severely impaired or absent in those cells [40, 41]. Due to the narrow host range of HCMV, it is impossible to study certain aspects of viral pathogenesis in animal models. Nevertheless, HCMV shares not only genetic similarities with MCMV but also similar tissue tropism and pathogenesis. Moreover, immune responses to CMV are comparable in humans and mice. Therefore, MCMV infection of mice is commonly used to model and study HCMV infections [42-44].

In their natural host, CMV has a broad cell tropism, meaning that it is able to enter and productively infect many different cell types *in vitro* as well as *in vivo [45]*. Epithelial cells of the respiratory or gastrointestinal tract are the first cells to be infected by CMV *in vivo* [46, 47]. From there the virus can spread to adjacent fibroblasts. Both, epithelial cells and fibroblasts are permissive for CMV and support viral replication. However, they are also specialized in protecting the host from invading pathogens that are recognized by pattern recognition receptors and therefore secrete pro-inflammatory cytokines and other factors that trigger the host defense response (reviewed in [48]). If the virus succeeds in counteracting this, the infection progresses and endothelial cells become infected. Subsequently, endothelial cells release CMV into the blood leading to viremia and infection of circulating cells. In addition, the permeability of the endothelial barrier increases with infection, which in turn increases the interaction with immune cells and their migration from the blood into the tissue [49]. Circulating blood monocytes can be infected by CMV but do not support productive lytic replication. However, they are important reservoirs for CMV since they can be latently infected. Upon migration into the tissue and differentiation from monocytes into macrophages, lytic replication can take place

[50]. Therefore, monocytes/macrophages are important target cells for CMV enabling its spread to various organs like lungs, spleen, salivary glands, or liver. This dissemination can occur biphasically, where CMV is first replicating in organs with high replication efficiency (e.g. liver) before it spreads to further organs in a secondary viremia [46]. MCMV is known to reach high virus titer in the liver [51] therefore causing complications like hepatitis in both, immunocompetent and immunocompromised patients. When CMV finally reaches and infects salivary glands or epithelial cells, e.g. of the urogenital tract or the gastrointestinal tract, the virus enters body fluids and excretions, through which it can be transmitted to a new host.

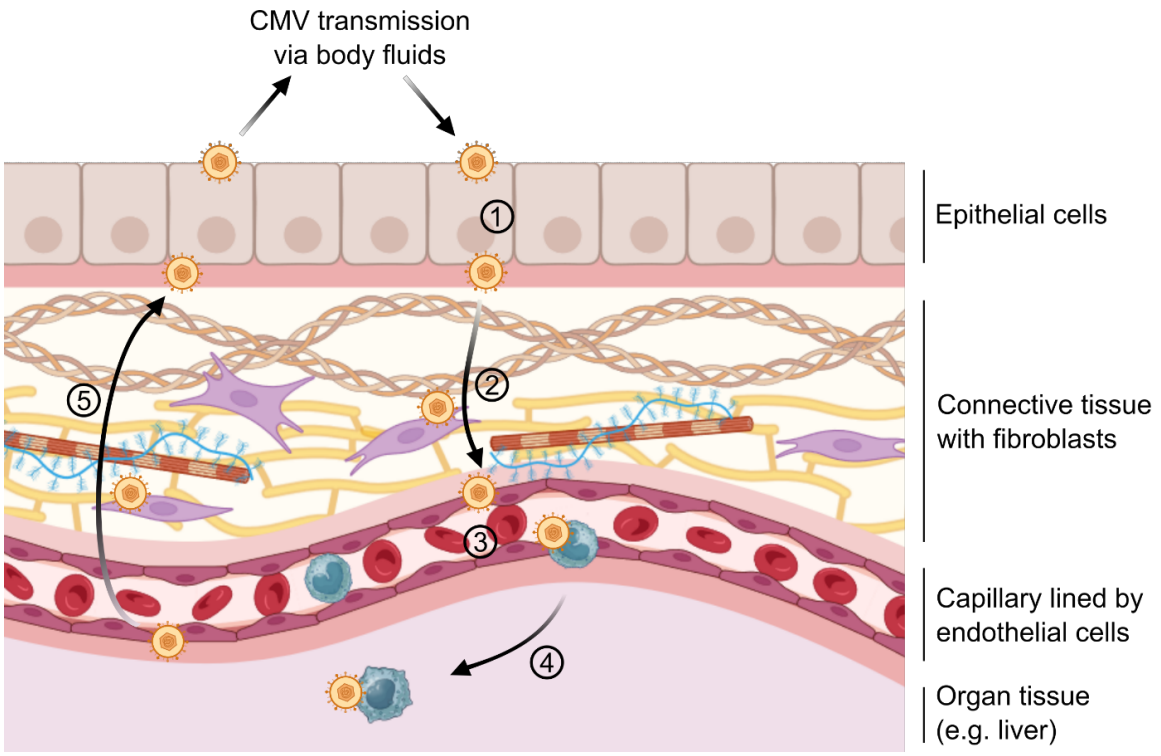

Figure 4: Cytomegalovirus dissemination and cell tropism.
Cytomegalovirus is commonly transmitted via body fluids (e.g. saliva) and enters the host by infecting epithelial cells in the respiratory or gastrointestinal tract (1). CMV is then released into the connective tissue where it can productively infect fibroblast and endothelial cells (2). By infection of endothelial cells, CMV enters the bloodstream causing viremia and infects non-permissive monocytes (3). However, monocytes migrate into organ tissue and differentiate into macrophages, which support productive lytic replication of CMV, leading to infection of multiple organs (4). When CMV reaches epithelial cells again it can be released into body fluids and exposed to the environment (5).

3.2 Manipulation of programmed cell death pathways by cytomegalovirus

3.2.1 Programmed cell death

Programmed cell death (PCD) has many faces and comes in the form of apoptosis, pyroptosis, and necroptosis amongst others. Different PCD pathways can be grouped into caspase-dependent and –independent or inflammatory and non-inflammatory. However, all those pathways share the same goal: maintaining cellular homeostasis by removing old or abnormal cells from the organism. In addition, infected cells can also be eliminated from an organism by PCD. Therefore, PCD is a central mechanism of defense against intracellular pathogens.

Viruses in general are known to induce various pathways leading to different forms of cell death. Sensing of viral components (e.g. viral RNA and DNA) or infection-induced cellular stress as well as molecules like cytokines or damage-associated molecular patterns (DAMPs) that are released during the infection can trigger cell death. Since viruses are strongly depending on a living host cell to fulfill their replication cycle, many viruses evolved mechanisms to inhibit cell death (reviewed in [52]). For example, Epstein-Barr virus encodes the LMP1 protein (latent membrane protein 1) targeting the receptor-interacting protein kinases RIPK1 and RIPK3, both mediators of necroptosis, for endosomal degradation, thereby inhibiting necroptotic cell death [53]. Similarly, rhinoviruses encode the viral protease 3C to directly cleave RIPK1 [54]. CMV is a master of cell death inhibition and encodes multiple proteins to inhibit not only necroptosis but also apoptosis and pyroptosis.

3.2.2 Inhibition of apoptosis by cytomegalovirus

Apoptosis, the first PCD pathway that was described, is characterized by chromatin condensation, shrinkage of the cell, and membrane “blebbing” leading to the formation of apoptotic vesicles [55]. Apoptotic vesicles expose phosphatidylserine on the outside of their membrane, which functions as an “eat me” signal for phagocytes [56]. As a consequence, phagocytes take up and degrade apoptotic vesicles. Since the plasma membrane stays intact throughout the whole process of apoptosis, it has been believed for a long time that apoptosis is a non-inflammatory pathway of PCD. However, recent data showed that apoptosis can be immunogenic and that DAMPs

are released by apoptotic cells [57]. Still, the exact mechanism of DAMP release and its consequence during apoptosis need further investigation.

Apoptosis can be stimulated extrinsically and intrinsically. The extrinsic pathway is also called the death-receptor-induced pathway, since it is activated upon ligand binding to so-called “death receptors” like the Fas receptor or tumor necrosis factor (TNF) receptor (TNFR) [58]. Ligand binding leads to the activation of caspase-8, which in turn activates the final effector caspases, i.e. caspase-3 and 7 (Figure 5). During infection, CMV can be sensed by mechanisms of innate immunity leading to increased expression of death receptors or the release of their ligands (e.g. TNF), thereby activating extrinsic apoptosis. Both MCMV and HCMV are able to prevent cell death with the proteins M36 and UL36, respectively. These so-called viral inhibitors of caspase-8 activation (vICA) bind to pro-caspase-8 preventing its cleavage and activation [59, 60].

Intrinsic apoptosis, in contrast to the extrinsic pathway, is triggered by cellular stress caused, for instance, by DNA damage and stress of the endoplasmic reticulum (ER). Stress responses promote the activation of pro-apoptotic proteins while anti-apoptotic proteins are inhibited. This imbalance causes activation of the pore-forming proteins, the Bcl-2 Associated X protein (BAX) and the Bcl-2 Antagonist Killer (BAK). Subsequently, BAX and BAK form large complexes in the outer membrane of mitochondria causing mitochondrial outer membrane permeabilization (MOMP) and release of cytochrome c [61]. A downstream consequence of cytochrome c release is the cleavage and activation of caspase-9, which similarly to caspase-8 in the extrinsic pathway activates the effector caspases-3 and 7 (Figure 5) [62]. During the replication of CMV cellular stress responses are very common. Increased protein synthesis can lead to unfolded-protein responses and ER stress while viral genome replication and processing triggers DNA damage responses [63, 64]. To counteract the resulting activation of intrinsic apoptosis, CMV encodes proteins to inhibit MOMP. In the case of HCMV, this protein is encoded by UL37 exon 1 (UL37x1), which inhibits BAX [65]. In contrast, MCMV encodes two separate proteins, m38.5 and m41.1, that inhibit the complex formation of BAX and BAK and the following cytochrome c release [66].

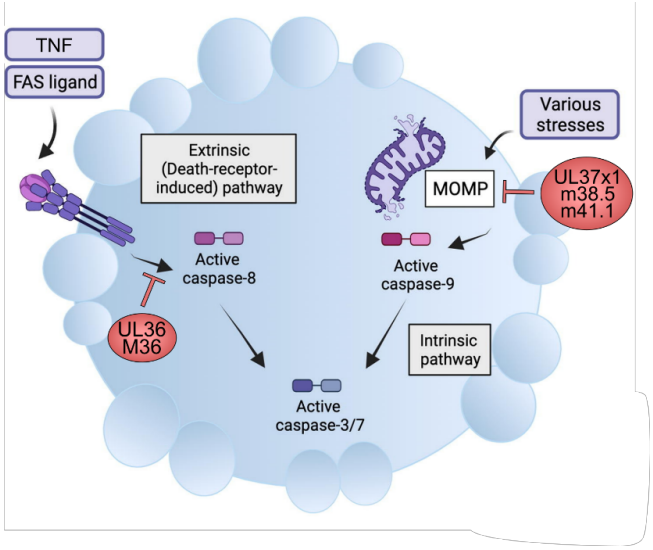

Figure 5: Inhibition of apoptotic cell death by cytomegalovirus
CMV inhibits extrinsic as well as intrinsic apoptosis by distinct viral proteins. UL36 and M36 of HCMV and MCMV, respectively, inhibit the activation of caspase-8 during extrinsically induced apoptosis. The prevention of mitochondrial outer membrane permeabilization (MOMP) by HCMV UL37x1 and MCMV m38.1 as well as m41.1 inhibit intrinsic apoptosis. The figure is adapted from Ketelut-Carneiro *et al.*, J Mol Biol. 2022 [67]

3.2.3 Inhibition of pyroptosis by cytomegalovirus

Like apoptosis, pyroptosis is one of the caspase-dependent types of PCD. However, the caspases involved in pyroptosis differ fundamentally from those activated during apoptosis. In addition, there are further characteristics that clearly separate these two types of cell death. While apoptosis is universal, mediators of the pyroptosis pathway are cell type-specific and are mainly expressed in myeloid cells [68]. Moreover, pyroptosis is characterized by the rapid formation of pores in the plasma membrane that allows the secretion of molecules like cytokines (e.g. interleukin (IL)-1β, IL-18) or DAMPs (Figure 6). In addition, these pores allow ions and water to enter the cell causing swelling and osmotic lysis [69]. With this, additional inflammatory factors are released, classifying pyroptosis as an inflammatory PCD in contrast to apoptosis.

The pyroptotic pathway is induced by the formation of the inflammasome, which occurs when cytosolic sensors (e.g. absent in melanoma 2 [AIM2], NLR family pyrin domain-containing 3 [NLRP3]) detect pathogen-associated molecular pattern molecules (PAMPs) or DAMPs. Upon recognition, the sensors oligomerize with the adapter protein ASC (apoptosis-associated speck-like protein containing a CARD) forming ASC specks that recruit pro-caspase-1 to form the mature inflammasome enabling the cleavage of pro-caspase-1. The activated caspase-1 then cleaves gasdermin D (GSDMD) allowing the N-terminus to oligomerize and integrate into the

cell membrane to form GSDMD pores, which are a specific hallmark of pyroptosis [70]. Furthermore, active caspase-1 cleaves pro-IL-1β and pro-IL-18 into their mature and active forms before they are released through the GSDMD pores [71].

The cytosolic sensors AIM2 and NLRP3 are crucial for detecting viral DNA and initiating antiviral responses via the inflammasome. While the herpesvirus varicella-zoster virus is sensed via NLRP3, CMV has been shown to trigger inflammasome formation and pyroptosis via AIM2 (reviewed in [72]). Recently, the M84 protein of MCMV has been identified as a viral inhibitor of pyroptosis. M84 can interact with AIM2 and ASC preventing downstream events of inflammasome formation as well as caspase-1 activation and GSDMD pore formation [73] (Figure 6).

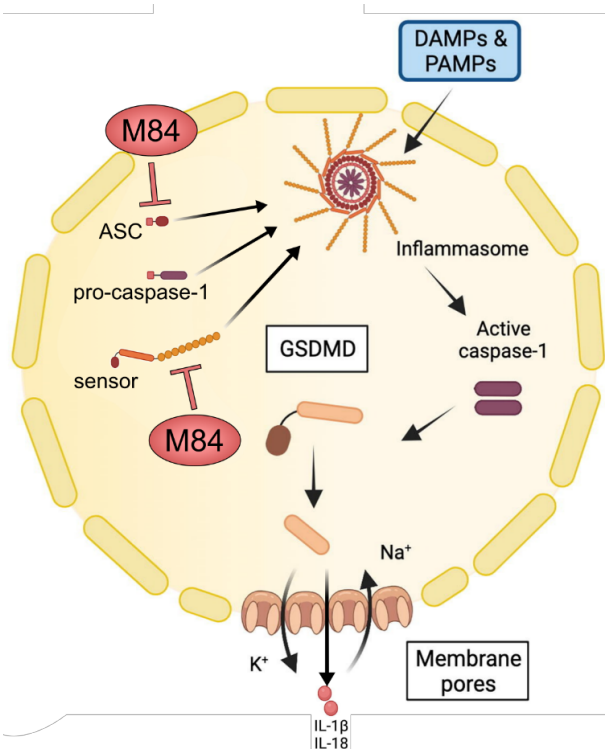

Figure 6: Inhibition of pyroptotic cell death by cytomegalovirus.
MCMV M84 can bind to the cytosolic DNA-sensor (AIM2) and the adapter protein ASC, thereby preventing assembly of the inflammasome and downstream events leading to pyroptotic cell death. The figure is adapted from Ketelut-Carneiro *et al.*, J Mol Biol. 2022 [67]

3.2.4 Inhibition of necroptosis by cytomegalovirus

The last of the three main forms of PCD is necroptosis. Like pyroptosis, necroptosis belongs to the inflammatory forms of cell death. However, induction of necroptosis is independent of caspase activities and therefore unique in this group (reviewed in [67]). Interestingly, the initial steps of necroptosis are very similar to the ones of the extrinsic apoptosis. After binding of TNF to its receptor, a protein complex including

receptor-interacting serine/threonine-protein kinase 1 (RIPK1) is formed at the cytosolic domain of the TNF.

This complex will activate caspase-8 resulting in apoptosis. However, in absence or inhibition of caspase-8, RIPK1 binds to RIPK3 and initiates necroptosis [74]. Interaction of RIPK1 with RIPK3 induces autophosphorylation of RIPK3, which subsequently phosphorylates mixed lineage kinase domain-like (MLKL). Next, MLKL undergoes conformational changes that allow its oligomerization and integration into the plasma membrane. This finally disrupts membrane integrity resulting in osmotic cell lysis and release of cellular material such as cytokines or DAMPs [75] (Figure 7).

Interestingly, it has been shown that RIPK1 is not essential for RIPK3 activation. Via alternative stimuli RIPK3 can be activated in absence of RIPK1 [76]. RIKP3 contains a RIP homotypic interacting motif (RHIM) enabling the assembly of large amyloid-like oligomers, the necrosome. Other cellular RHIM-containing proteins (e.g. TRIF, ZBP1) can interact with RIPK3 leading to subsequent activation and necroptosis [77]. Interestingly, MCMV encodes a protein, M45, which contains a RHIM. M45 has been shown to inhibit necroptosis by preventing RHIM-dependent activation of RIPK3 [77-79] (Figure 7). Additionally, HCMV UL36, also known as viral inhibitor of caspase-8 and therefore an apoptosis inhibitor (described in 3.2.2), is able to target MLKL for degradation and provides a mechanism of necroptosis inhibition in HCMV infection [80].

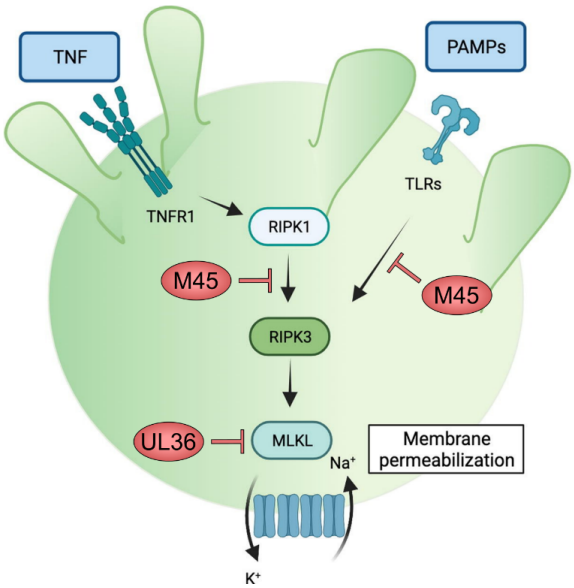

Figure 7: Inhibition of necroptotic cell death by cytomegalovirus.
MCMV M45 contains a RIP homotypic interaction motif (RHIM), which is able to inhibit RHIM-dependent activation of RIPK3. HCMV UL36 is able to target MLKL for degradation preventing incorporation of MLKL into the plasma membrane. The figure is adapted from Ketelut-Carneiro *et al.*, J Mol Biol. 2022 [67]

3.3 High-mobility group box 1 protein (HMGB1)

3.3.1 HMG protein class

In 1973, Ernest Johns and colleagues were the first ones to isolate and describe a group of proteins from calf thymus chromatin that rapidly migrate in a polyacrylamide gel electrophoresis. Therefore, they later called this group of proteins “high-mobility proteins” (HMGs) [81]. Today we know that HMG proteins are the most abundant non-histone nuclear proteins in mammals interacting with chromosomal DNA, thereby, taking part in many DNA-related processes (e.g. transcription, DNA repair). In addition, many HMG proteins are involved in cell proliferation, differentiation, and migration as well as tissue damage signaling and tissue repair when they occur extracellularly. In 2001, Michael Bustin categorized the class of HMG proteins into new superfamilies clustering HMGs according to their functional motif [82]. Since then, three different protein families, i.e. HMGN, HMGA, and HMGB are known. While HMGN proteins are characterized by a nucleosomal binding domain, HMGA proteins carry an AT-hook motif preferable binding to A/T-rich DNA regions. All HMGB proteins share an HMG-box motif [83]. Due to their different functional motifs, HMGN, HMGA, and HMGB bind different DNA structures. However, canonical HMG proteins all have in common that they interact with DNA in a sequence-independent manner [83].

The most abundant family, the HMG-box family, is further organized into two groups based on the function, DNA specificity, and abundance of the proteins [84-86]. While the second group consists mostly of less abundant, non-canonical proteins containing only a single HMG-box domain binding DNA in a sequence-specific fashion, HMGB proteins of the first group are highly abundant and contain two or more HMG-box motifs binding independently of the DNA sequence. Among the first group, the mammalian proteins HMGB1-4 are evolutionary highly conserved and share high amino acid sequence identity (~80 %). Despite their great similarity, the functions and expression profiles of these HMGB proteins differ considerably [87]. While HMGB3 is mainly expressed during embryonic development, HMGB2 and HMGB4 are mainly expressed in the lymphoid organs and testes of adults. In contrast, HMGB1 is expressed at all times and in almost every nucleated cell, and is also functionally the most versatile of the HMGB proteins [87].

3.3.2 HMGB1 structure

The non-histone DNA-binding protein HMGB1 (formerly HMG-1) is not only the most abundant HMG protein, but also one of the most abundant nuclear proteins besides histones [88]. HMGB1 is broadly expressed in most mammalian cells and highly conserved between species. As such, mouse and human HMGB1 share 99 % amino acid sequence identity, while HMGB1 of mouse and rat are 100 % identical [89-91]. Expression of HMGB1 can vary between different cell types and tissues [92]. For instance, it has been shown that HMGB1 expression in the spleen and thymus is usually the highest, and that myeloid cells express more HMGB1 than lymphoid cells [93]. HMGB1 is a highly dynamic protein within the nucleus that can also shuttle to the cytosol, thereby exerting various functions due to its multiple interactions with cytoplasmic and nuclear proteins or chromosal DNA [94, 95].

The structure of HMGB1 reflects the typical organization of an HMG protein. The *Hmgb1* gene contains five exons and multiple introns encoding the 215 amino acids (aa) large HMGB1 protein [96] (Figure 8 A). HMGB1 consist of two HMG-box domains called A- and B-box and an acidic tail at the C-terminus (Figure 8 B). The A- and B-box facilitate DNA binding without sequence specificity and mediate the nuclear export of HMGB1 mediated by nuclear export signals (NES) [97]. Besides this, two nuclear localization signals (i.e. NLS1 aa27-43, NLS2 aa179-185) ensure the steady nuclear localization of HMGB1 [98]. Both HMG boxes are structurally similar and fold into a DNA-binding domain containing three α-helices and two loops in an L-shape arrangement (Figure 8 C) [99-103]. A short flexible region links both domains. The C-terminal acidic tail is unstructured and has recently been described to function as an IDR [104] (Figure 8 D). In addition, the C-terminus can interact with the HMG domains and maintain their tertiary structure [105, 106]. Importantly, HMGB1 contains three cysteine residues (i.e. Cysy23, Cys45, and Cys106), which form intramolecular disulfide bonds under oxidative conditions, which alters the structure, localization, and function of HMGB1 depending on the redox state of the cell [107, 108].

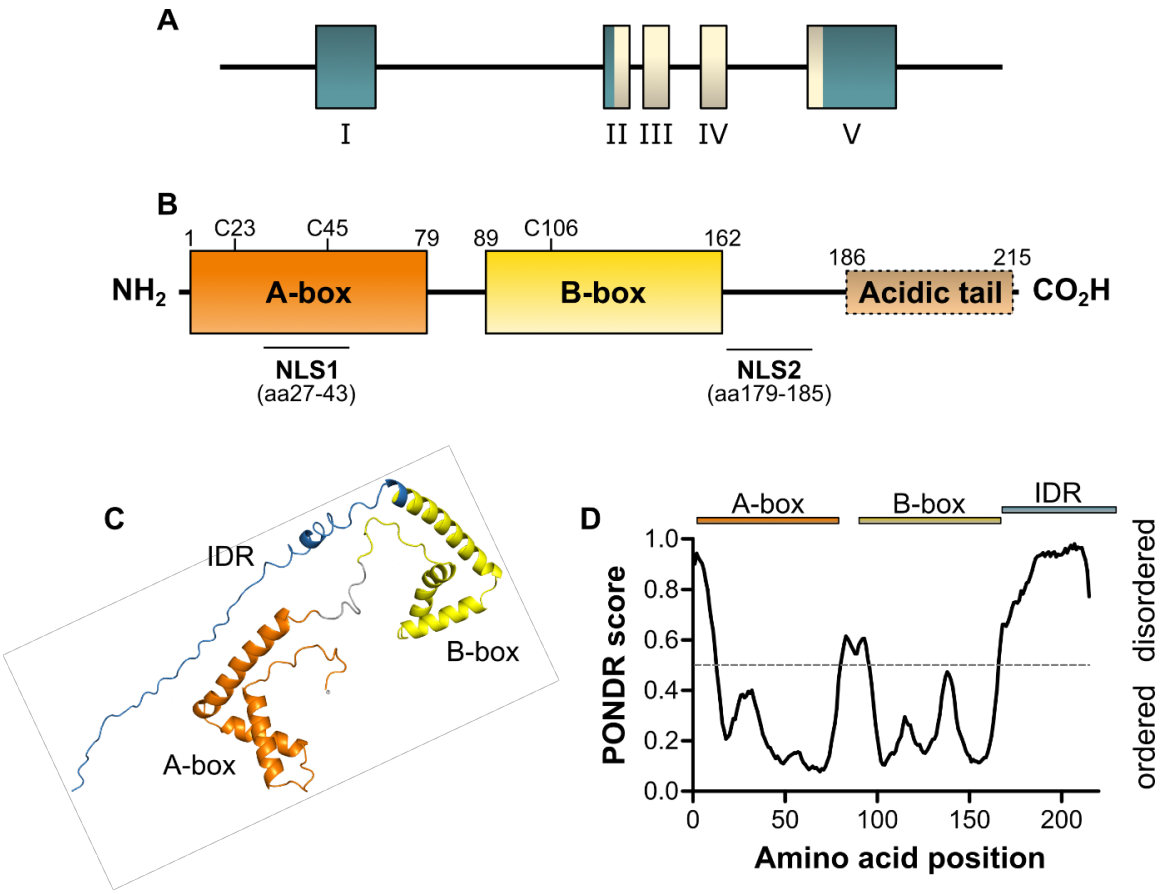

Figure 8: Structure of high-mobility group box 1 protein.
A) Schematic representation of the Hmgb1 gene with its five exons (blue: non-coding; white: coding regions). Adapted from Ferrari et al. [96] **B)** The HMGB1 protein contains two DNA-binding domains (A- and B-box) and a C-terminal acidic tail. Adapted from He et al. [109] **C)** Structure prediction of HMGB1 using AlphaFold2. **D)** Graph plotting the intrinsic disorder of HMGB1 predicted by metapredict. The boxes above highlight the positions of the A- and B-box as well as the IDR.

3.3.3 HMGB1 localization and release

HMGB1 is highly concentrated in the nucleus of mammalian cells, where it can bind DNA and regulate multiple processes. However, due to its NES and NLS sequences, a constant shuttling of HMGB1 between the nucleus and the cytoplasm is taking place [110]. In addition, several stimuli, such as oxidative stress or infection, can disrupt the balance in HMGB1 shuttling and lead to translocation of HMGB1 into the cytoplasm or even its release into the extracellular milieu [111, 112]. Depending on its localization, HMGB1 exerts different functions. Several studies have shown that the translocation and active release of HMGB1 are regulated by various posttranslational modifications (PTMs) as well as the redox state of HMGB1. For instance, acetylation and phosphorylation of either lysine or serine residues within the NLS regulate nucleocytoplasmic shuttling and translocation [98, 113-117], while methylation (Lys42), N-glycosylation (Asn37, Asn134 and Asn135) and redox

modulation (Cys23, Cys45 and Cys106) alter the conformation of HMGB1, thereby reducing its DNA-binding affinity and promoting translocation and release [118-123].

Extracellular HMGB1 is known to be a potent DAMP, signaling cell damage to surrounding cells. HMGB1 release occurs via either active secretion or passive release. Both are highly regulated by various factors including PTMs as well as interactions with proteins of multiple inflammatory and cell death pathways. Already in 1999, Wang and colleagues showed that the endotoxin lipopolysaccharide (LPS) induces secretion of HMGB1 from macrophages *in vitro* and *in vivo* [124]. Since then, multiple sterile and pathogen-related stimuli (e.g. extra- and intracellular pathogen-derived molecules as well as cellular stress responses) have been identified to trigger the active secretion of HMGB1 from different cells such as immune cells, fibroblasts, and epithelial cells. Although various studies have proven active HMGB1 secretion, the exact mechanisms remains mostly unsolved. Since HMGB1 lacks the leader sequence targeting proteins for the conventional ER-Golgi secretory pathway [125, 126], alternative secretion pathways must be in place. Therefore, the current model of active HMGB1 secretion hypothesizes that HMGB1, once it accumulates in the cytoplasm, is packaged into secretory lysosomes, autophagosomes, or other intracellular vesicles and is released by subsequent fusion with the plasma membrane. This process seems to be highly complex and regulated by a variety of factors. For instance, the cellular stress response-induced reactive oxygen species (ROS) are known to mediate HMGB1 secretion by nuclear factor kappa B (NF-κB) and MAPK (mitogen-activated protein kinase) pathways [123, 127]. NF-κB and MAPK pathways, in turn, have been shown to be involved in HMGB1 secretion in sterile tissue damage as well as in the context of infection [128-132]. However, the exact mechanisms how these pathways contribute to HMGB1 secretion are still unknown.

Passive HMGB1 release takes place whenever a cell is dying. Cell death, however, can either occur through mechanical rupture of a cell or by activation of PCD like apoptosis, necroptosis, or pyroptosis. It has been shown that HMGB1 is released during each of these forms of cell death. However, while apoptotic cells usually release only small amounts, HMGB1 is released in large quantities during pyroptosis and necroptosis. Interestingly, HMGB1 is released upon the disruption of the plasma membrane and cell lysis, but not necessarily via the generated membrane pores [133]. Therefore, inhibition of mediators of PCD like RIPK3 (necroptosis) or caspase-

1 (pyroptosis) can attenuate the release of HMGB1 and subsequent effects [134, 135]. In contrast to pyroptosis and necroptosis, apoptosis is characterized as non-inflammatory cell death and an intact cell membrane. Therefore, it was believed that apoptotic cells do not release DAMPs like HMGB1 but rather sequester them in apoptotic vesicles. Indeed, HMGB1 can be found within those vesicles [136], however, if phagocytic clearance of apoptotic vesicles is impaired HMGB1 release can be observed [137]. Finally, extracellular HMGB1, in turn, can activate PCD, creating a positive feedback cascade leading to even more HMGB1 release and cell death.

In general, PTMs that promote HMGB1 translocation into the cytoplasm are required for the secretion of HMGB1, while cell death results in the release of unmodified or differently modified forms of HMGB1. Based on its modifications and redox state extracellular HMGB1 interacts with different receptors resulting in various effects on neighboring cells ranging from chemoattractive and pro-inflammatory effects to immune tolerance (reviewed in [125, 138]).

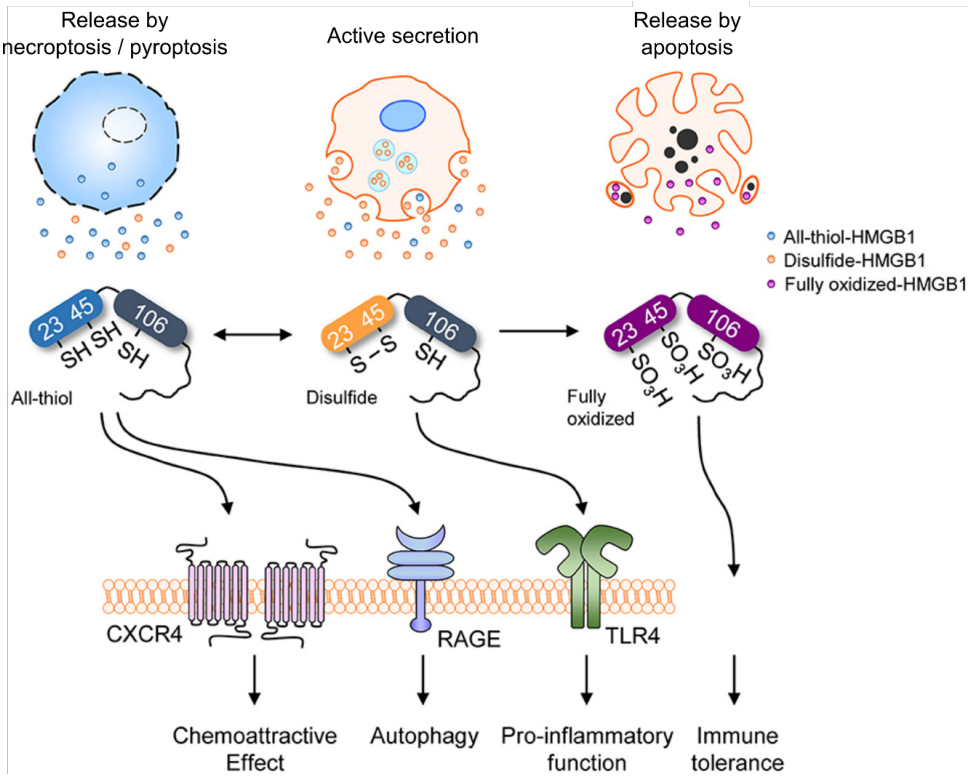

Figure 9: Active secretion and passive release of HMGB1.
Upon multiple stimuli, HMGB1 can be either actively secreted by distinct cell types or passively released during cell death and lysis. Different redox states of HMGB1 are linked with specific mechanisms of HMGB1 release as well as individual immunological functions. The figure is adapted from Kwak *et al.*, Front Immunol. 2020 [125]

3.4 Functions of HMGB1

As indicated before, HMGB1 is highly interactive and multifunctional. Its function is thereby largely depending on its PTM, redox state as well as localization. External or internal stimuli can affect HMGB1 modification and localization leading to a change of function. HMGB1 is involved in many important biological processes and cell survival. However, it is not only involved in intended inflammation but also in many pathological processes like chronic and autoimmune diseases as well as cancer. Interestingly, HMGB1 can perform completely opposite functions depending on its localization and the context.

3.4.1 Functions of nuclear HMGB1

Under physiological conditions, HMGB1 is most abundant in the cell nucleus, binding to DNA in a structure-specific but sequence-unspecific manner. Due to its DNA binding as well as DNA bending activities, HMGB1 is characterized as a DNA chaperone. As such, HMGB1 is an important factor for genome chromatinization and contributes to nucleosome maintenance by additionally interacting with linker and core histones [139-142]. Furthermore, HMGB1 can relax the nucleosome structure, thereby enabling other proteins or complexes to access the DNA [143]. Due to its versatile DNA and protein interactions HMGB1 is involved in many key processes within the nucleus like DNA transcription, replication as well as repair.

Cellular transcription can be affected by HMGB1 through several mechanisms. Due to its DNA-bending activity, HMGB1 can compact or loop DNA. While compacting DNA limits transcription rates, HMGB1-induced loops can serve as transcription initiation sites [144, 145]. Furthermore, HMGB1 bends promoter regions increasing the binding affinity of transcription factors to regulatory elements. For example, HMGB1 promotes the binding of TBP (TATA-binding protein) to the TATA box. In addition, subsequent recruitment of further transcription factors as well as the RNA polymerase II are more efficient in presence of HMGB1. By interfering with transcription factors, such as Sox9 or p53 [146, 147], HMGB1 is not only able to activate or enhance but also to repress transcription.

Apart from transcription, HMGB1 is also involved in DNA replication and repair. HMGB1 binds and unwinds DNA [144] thereby destabilizing the DNA helix. This can initiate recruitment of the DNA polymerase and further factors necessary for DNA

replication of genomic DNA as well as closed circular DNA such as the viral episome. Additionally, different HMGB1 modifications have been shown to either positively or negatively regulate the activity of the DNA polymerase. While phosphorylated HMGB1 reduces the HMGB1-mediated polymerizing activity of the DNA polymerase, acetylation of HMGB1 stimulates polymerase activity [87].

DNA replication can always lead to DNA damage, which is repaired by different mechanisms: mismatch repair, base excision, and ligation of DNA strand breaks. HMGB1 is involved in all these processes. Mediated by its high affinity to distorted and damaged DNA HMGB1 identifies damaged regions and recruits proteins of the repair machinery [148, 149]. In addition, HMGB1 has the ability to enhance the activity of involved enzymes, like ligases, enhancing the DNA repair efficiency [150, 151]. Therefore, a loss of HMGB1 often results in lower DNA repair efficiency, more DNA damage, and subsequent cell death.

3.4.2 Functions of cytosolic HMGB1

Oxidative stress, hypoxia, heat, and inflammatory stimuli induced by cytokines and chemokines can trigger the translocation of HMGB1 from the nucleus into the cytoplasm. The normal ratio of 30:1 (nuclear:cytoplasmic) [152] is disrupted, and HMGB1 is present in large amounts in the cytoplasm. The functions of cytosolic HMGB1, however, are less explored than the ones of nuclear or extracellular HMGB1. One major role of cytosolic HMGB1 is the regulation of autophagy. Autophagy is a conserved mechanism to degrade cellular protein aggregates or damaged organelles via intracellular lysosomal pathways. Autophagy maintains intracellular homeostasis, thereby preventing e.g. apoptosis. Cytosolic HMGB1 interacts with Beclin-1, a central regulator of autophagy, and release it from the anti-apoptotic factor Bcl-2. With this HMGB1 promotes autophagy and inhibits apoptosis at the same time [153]. Furthermore, HMGB1 protects Beclin-1 as well as another autophagy factor, ATG5, from cleavage during inflammation to keep the cell in a pro-autophagic and anti-apoptotic state [154].

3.4.3 Functions of extracellular HMGB1

Extracellular HMGB1 is a prototypic DAMP having multiple roles in inflammation and immunity, as well as in cell migration, proliferation and differentiation, wound healing and pathogen defense. Different intracellular signaling pathways are induced when HMGB1 binds to its main receptors: the receptor for advanced glycation endproducts (RAGE), and toll-like receptors 2 and 4 (TLR2, TLR4). In addition, extracellular HMGB1 is a “sticky” protein interacting with a variety of DAMPS, PAMPs, chemokines, and cytokines (e.g. histones, LPS, CXCL12, IL-1β). Bound to these molecules, HMGB1 can synergistically amplify their pro-inflammatory potential [155-158]. Therefore, HMGB1-dependent signaling was also reported for several other receptors like TLR9, chemokine receptor CXCR4, and IL-1R (interleukin-1 receptor).

Whether HMGB1 comes alone or bound, as dimer or multimer, in high or low concentration, oxidized, reduced, or modified; all these variables can affect and regulate HMGB1 receptor binding and signaling. For example, oxidized HMGB1 released by apoptotic cells stimulates immune tolerance, while other redox forms induce pro-inflammatory responses [125, 159] (Figure 9). In addition, active caspase-1 is able to cleave HMGB1, which generates a pro-inflammatory peptide reversing the immune tolerance mediated by the full-length HMGB1 [160]. Since extracellular HMGB1 is extremely versatile, a tight regulation of the different functions is crucial. In addition to redox changes and PTMs, which modulate the different functions of HMGB1, negative regulators such as thrombomodulin are known to inhibit HMGB1 signaling. Thrombomodulin has been identified to bind extracellular HMGB1, which on the one hand inhibits HMGB1-receptor interaction and on the other hand leads to degradation of HMGB1 into less inflammatory peptides [161, 162].

HMGB1 released upon sterile or infectious stimuli can activate a broad range of cell types (e.g. innate immune cells, epithelial cells, fibroblasts), which results in cytokine release and a pro-inflammatory environment. HMGB1 further shapes immune responses by triggering chemokine release and subsequent recruitment, activation, and proliferation of immune cells (e.g. macrophages, natural killer cells, T-cells) (reviewed in [87]). In contrast, high concentrations of extracellular HMGB1 are cytotoxic and induce cell death (e.g. apoptosis, necroptosis) [163]. Extracellular HMGB1 has also been shown to induce pyroptosis in macrophages via an endocytosis-dependent mechanism [164]. HMGB1-induced cell death can lead to

further release of HMGB1 creating a positive feedback loop and, if not well regulated, inducing massive tissue damage.

In order to counteract tissue damage, extracellular HMGB1 additionally induces multiple mechanisms of tissue repair and wound healing. For example, HMGB1 recruits epithelial progenitor cells and stem cells to the site of tissue damage to promote regeneration [165-167]. Furthermore, migration and sprouting of endothelial cells are regulated by HMGB1 during angiogenesis, the formation of new blood vessels, while extracellular HMGB1 triggers cytoskeletal reorganization in keratinocytes to close scratch wounds [168, 169].

3.5 Functions of HMGB1 in infection

3.5.1 Role of HMGB1 in bacterial infections

HMGB1 is known to be a double-edged sword in many acute infections but also chronic and sterile inflammatory conditions. HMGB1 derived from adenoid glands, for example, has shown high antibacterial effects against several bacteria including *E. coli*. Interestingly, HMGB1 was not found in the glandular secretions, leading to the hypothesis that intracellular HMGB1 might mediate these antibacterial effects [170]. Consistent with this, it has been demonstrated that intracellular HMGB1 promotes macrophage autophagy and limits cell death during bacterial infection, thereby protecting the host from endotoxic shock [171]. Furthermore, HMGB1 can limit bacterial dissemination throughout the host [172] and promotes the formation of neutrophil extracellular traps, which can further capture bacteria and inhibit spreading [173]. Especially leukocyte-derived HMGB1 was shown to be crucial for early recruitment of inflammatory immune cells and pathogen clearance in listeriosis [172]. Overall, low levels of HMGB1 often contribute to a rapid and efficient immune response to clear bacterial infections. However, high HMGB1 levels or prolonged exposures to HMGB1 are associated with poor disease outcomes and a higher risk for chronic inflammation, tissue fibrosis, or persistent bacterial infections [174]. Furthermore, HMGB1-driven immune activation and tissue damage can promote the breakdown of epithelial barriers, organ failure, and even death [175].

3.5.2 Role of HMGB1 in viral infections

Although the different functions of HMGB1 in the context of viral infections are less studied, it already has become clear that HMGB1 is highly versatile affecting different aspects of viral life cycles, showing both proviral as well as antiviral effects depending on its localization and modifications as well as on the virus studied. Several studies demonstrated that viral infections trigger the release of HMGB1 from infected cells by both active secretion and cell death-driven passive release. PTMs, such as acetylation, and the accumulation of ROS have been shown to drive HMGB1 translocation and release from cells infected with e.g. dengue virus (DENV), respiratory syncytial virus (RSV), or hepatitis C virus (HCV) [119, 176]. On the one hand, extracellular HMGB1 shows antiviral activities and limits virus production and spread during DENV and HCV infection [176, 177]. Mechanistically, HCV infection is restricted by HMGB1 signaling through TLR4 and subsequent interferon-β production [176]. On the other hand, multiple studies confirmed that high levels of extracellular HMGB1 contribute to overshooting immune reactions and cytokine storms as well as virus-related tumorigenesis [178]. For example, HMGB1 drives severe pneumonia and encephalopathy, two severe pathologies of influenza A infection [179, 180]. Furthermore, HMGB1 potentiates pro-inflammatory signaling during SARS-CoV2 infections, thereby promoting inflammatory cell death, cytokine storm, and severe COVID-19 outcome (reviewed in [181]). Serum levels of HMGB1 often directly correlate with disease progression and severity in patients and can be meaningful clinical indicators [175, 179, 180, 182]. In many cases, reduction of HMGB1 release or inhibition of extracellular HMGB1 using neutralizing antibodies resulted in attenuated organ pathology, reduced disease severity, and even lower mortality in cases of influenza A, RSV, murine hepatitis virus as well as Newcastle disease virus [183-187].

Not only extracellular but also intracellular HMGB1 has been shown to affect viral replication cycles. While cytosolic HMGB1 can promote translation and replication of HCV RNA genomes by interacting with the 5’ untranslated region (UTR) [188], nuclear HMGB1 binds to the nucleoprotein NP of influenza viruses maintaining the activity of the viral polymerase, facilitating genome replication [189]. In contrast to these proviral effects of intracellular HMGB1 on viral replication, HMGB1 has been demonstrated to act also in an antiviral manner. Nuclear HMGB1 positively regulates the expression of antiviral genes such as interferon-stimulated genes, which is

detrimental to DENV replication [190]. Therefore, treatment with resveratrol or glycyrrhizin, which inhibit HMGB1 translocation into the cytoplasm forcing it to remain in the nucleus, negatively affects DENV infection. With this, previous research highlights the fine balance between proviral and antiviral properties of HMGB1 during viral infections.

3.5.3 Role of HMGB1 in herpesvirus infections

As demonstrated before, fast-replicating RNA viruses are often associated with strong inflammatory responses and severe pathologies. HMGB1 is an important driver of this virus-induced inflammation. However, contrary to RNA viruses, fewer studies were done to establish the role of HMGB1 during DNA virus infection, especially herpesvirus infection. As they encode more proteins that allow complex interactions and strong adaptation to their host, they could potentially have evolved strategies to better control HMGB1-mediated inflammation or on the contrary, developed more mechanisms to exploit HMGB1 for their benefit.

HMGB1 has been shown to be released by herpesvirus-infected cells. However, the release is often dependent on cell death and not active secretion. The alpha herpesvirus HSV-2 induces apoptosis and sequestration of HMGB1 within the nucleus. Only in later stages necrosis occurs, which causes HMGB1 release [191]. Similarly, the release of HMGB1 from cells infected with pseudorabies virus, a close relative to HSV, can be observed [192]. Besides, infections with the beta herpesvirus HHV6A and the gamma herpesvirus Epstein-Barr virus (EBV) trigger the release of HMGB1 [193, 194]. Extracellular HMGB1 can limit virus spread, alter immune responses, and increase cell migration and proliferation, which is associated e.g. with the progression of virus-associated carcinomas like EBV-infected nasopharyngeal carcinomas [191-195]. Furthermore, HMGB1-RAGE signaling causes reactivation of the human immunodeficiency virus (HIV-1) in HIV-1/HSV-2 co-infected patients [191].

Independent studies showed that infection by pseudorabies virus or EBV increases the expression of HMGB1, while HSV or KSHV do not affect HMGB1 expression [191, 192, 194, 196]. This may indicate different functions of HMGB1 in infections with the various viruses. HMGB1 has been found to localize in HSV-1 replication compartments, where it interacts with nascent DNA and functions as a cofactor for transcription mediated by the viral protein ICP4 [197, 198]. Furthermore, HMGB1

interacts with the EBV immediate-early transcription factor ZEBRA (BZLF1, Zta, Z, EB1) and RTA (replication and transcription activator) to promote their binding to promoters and enhancer regions thereby regulating viral latency and B-cell immortalization [199, 200]. Consistent with this, HMGB1 stimulates RTA-dependent transcription in cells infected with KSHV or the related murine gammaherpesvirus-68 (MHV-68). Both viruses show reduced lytic viral replication in HMGB1-deficient cells [196, 201], highlighting the proviral effect of intracellular HMGB1 on herpesvirus replication. In addition, HMGB1 interacts with LANA (latency-associated nuclear antigen), the major regulator of KSHV latency, and participates in nucleosomal remodeling during KSHV reactivation [196, 202].

In summary, extracellular HMGB1 has mainly inhibitory activities, while intracellular HMGB1 seems to have proviral functions in the most cases by supporting lytic replication and latency. However, the exact mode of action of HMGB1 appears to be more strictly dependent on which herpesvirus is involved.

While studies mentioned before focused on viruses from the alpha- and gamma-herpesvirus families, the knowledge of how HMGB1 affects infections with beta-herpesviruses, such as CMV, is very limited. In 2012, Kagele *et al.* identified proteins that interact with the oriLyt of the HCMV genome and contribute to viral DNA replication initiation. In this study they identified HMGB1 as a potential interactor of this region [203]. However, an independent study, which aimed for the identification of virus and host factors on nascent HCMV DNA, did not recognized HMGB1 as such a factor [204].

The exact role of HMGB1 during herpesvirus infection remains to be further investigated. Especially its role in CMV infection is of further interest since there is very limited knowledge in this field, although HCMV is an opportunistic pathogen causing severe burdens in the health care systems worldwide.

4. Aim of the study

CMV is a significant human pathogen that can cause severe disease in immunocompromised individuals and congenital infections. Understanding the host factors that influence CMV infection is crucial for developing novel therapeutic strategies. High Mobility Group Box 1 (HMGB1) is a pivotal host factor involved in various cellular processes, including immune responses and inflammation. HMGB1 has also been shown to be highly versatile during viral infections. It affects the replication of different RNA and DNA viruses in multiple ways in a proviral as well as antiviral manner. While extracellular HMGB1 has been shown to inhibit virus replication and spread via different mechanisms, intracellular HMGB1 has versatile functions and can either support or reduce viral replication depending on the virus. However, the knowledge about the role of HMGB1 in herpesvirus infection, especially with beta-herpeviruses is extremely limited.

Therefore, the aim of this study is to investigate the role of HMGB1 in the context of CMV infection. In order to evaluate if HMGB1 is a relevant host factor for CMV, its expression, localization, and release from different infected cell lines was investigated. Indeed, any changes in these parameters could indicate that CMV has evolved strategies to hijack or evade functions of HMGB1 in order to optimize its replication. In addition, knockdown and knock-in cell culture systems were used in order to decipher the proviral or antiviral roles of HMGB1in the context of CMV infection. Finally, this study aimed to provide insights into the role of HMGB1 in CMV infection and pathogenesis *in vivo* using a conditional HMGB1-knockout mouse model for the first time in the context of viral infections. Due to the high species specificity of CMV the study was performed using murine cytomegalovirus (MCMV) as a model. By elucidating the interplay between HMGB1 and CMV, this research could provide insights into potential therapeutic targets for managing CMV infections.

5. Results

5.1 Endogenous expression of HMGB1 in murine cell lines

To study how HMGB1 affects MCMV replication, suitable *in vitro* systems are needed. Since MCMV has a broad cell tropism, various well-established murine cell lines can be used for infection studies. In addition, HMGB1 is described to be present and functional in various cell types, however with varying protein levels. Therefore, multiple commonly used immortalized mouse cell lines were tested for their HMGB1 expression and suitability for infection studies. HMGB1 protein and mRNA levels were evaluated using immunoblot and RT-qPCR approaches, respectively. Endothelial cells (SVEC4-10), fibroblasts (NIH-3T3, 10.1) as well as bone marrow stromal cells (M2-10B4) displayed comparable HMGB1 protein levels in immunoblot, while HMGB1 seemed to be expressed to lower levels in immortalized bone marrow-derived macrophages (iBMDM) (Figure 10 A, B). Hepatocytes (Hepa1-6) showed the highest protein levels of HMGB1 (Figure 10 A, B) among these cell lines. The mRNA levels mostly reflected the amounts of HMGB1 protein in the individual cell line (Figure 10 C). However, 10.1, iBMDMs, and M2-10B4 cells showed slightly higher mRNA levels than expected from their HMGB1 protein levels. Taken together, all commonly used murine cell lines showed robust HMGB1 expression and were suitable for following *in vitro* investigations. Amongst these different cell types SVEC4-10, NIH-3T3, Hepa1-6, and iBMDMs were chosen for subsequent investigations to elucidate the role of HMGB1 during MCMV infection in a cell type-dependent manner.

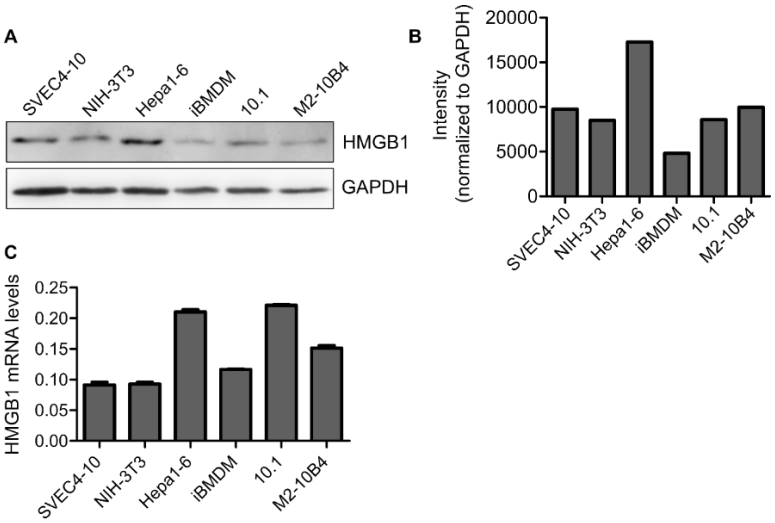

Figure 10: HMGB1 is broadly expressed in murine cell lines.

A) Murine cells were lysed and analyzed by immunoblot for HMGB1 expression. GAPDH was stained as loading control. **B)** Quantification of band intensities detected by immunoblot (panel A). Quantifications were performed using Fiji and HMGB1 values were normalized to GAPDH. **C)** Total RNA was isolated and analyzed for HMGB1 mRNA expression using RT-qPCR. Values were normalized to β-actin.

5.2 Regulation of HMGB1 expression by MCMV

Many viruses developed mechanisms to regulate expression of host proteins to create an environment favorable for viral propagation. The way the expression of a host factor is modified during the infection, can give indications about its function during viral replication. Therefore, HMGB1 expression in MCMV-infected cells was analyzed. First, all four cell types mentioned above were infected with MCMV wild-type (WT) at a high MOI (MOI 5) in order to have all cells infected. At indicated time points, infected cells were lysed and protein or RNA was extracted to quantify the amounts of HMGB1 at the protein or mRNA level, respectively.

In NIH-3T3 fibroblasts and SVEC4-10 endothelial cells similar phenotypes could be observed, with a more pronounced phenotype in the endothelial cells. Indeed, during early infection (2-8 hpi) the mRNA levels of HMGB1 seemed to be stable but increased at 24 hpi (1.7-fold in NIH-3T3 and up to 3-fold for SVEC4-10 cells at 72 hpi, Figure 11 A, B). These changes in mRNA levels were reflected at the protein level for NIH-3T3 (Figure 11 C) but not for SVEC4-10 cells, in which protein levels of HMGB1 were stable throughout the different time points (Figure 11 D). A similar phenotype could be observed in the Hepa1-6 cells, however with an upregulation of mRNA level of HMGB1 occurring already at 4 hpi and increasing progressively until 72 hpi (Figure 11 E). These changes could also be observed at the protein level (Figure 11 G). On the contrary, the HGMB1 mRNA and protein levels behaved differently in MCMV-infected iBMDMs. In contrast to the other cells lines, the infection of macrophages resulted in a downregulation of HMGB1 to a minimum of expression at 8 hpi (Figure 11 F, H). At later time points, mRNA and protein levels returned to values similar to non-infected cells, and an upregulation of the protein level of HGMB1 could even be detected from 24 hpi.

In conclusion, HMGB1 levels are altered upon MCMV infection. Whereas the mRNA level showed an increase in fibroblasts, endothelial cells and hepatocytes at early time points, the infected iBMDMs behaved differently with a decrease in HMGB1 expression. This mRNA changes, however, did not directly translate into the same

modifications of HMGB1 protein amounts. In all cell line, except SVEC4-10 cells, protein amounts increased especially to late time points of infection.

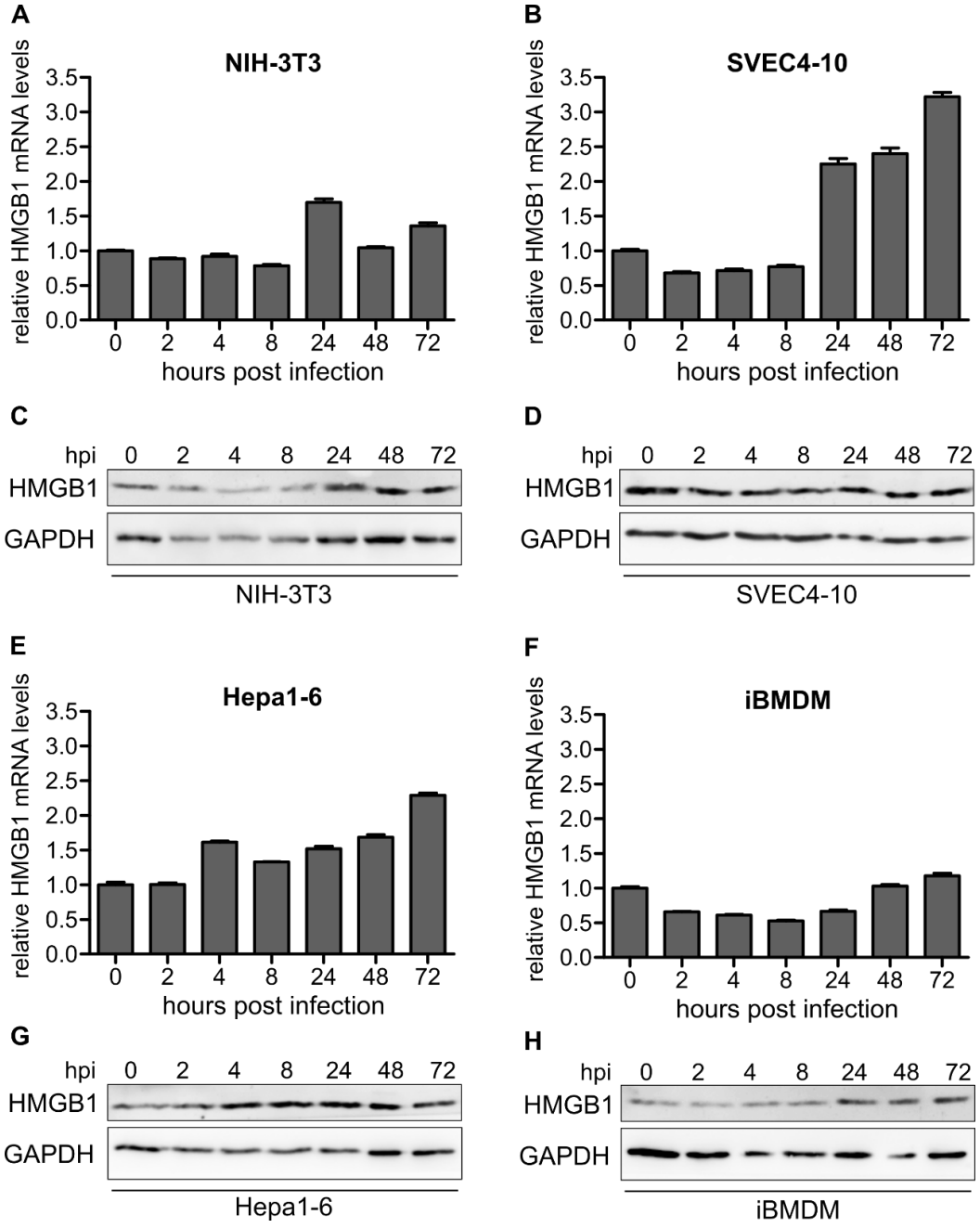

Figure 11: HMGB1 expression varies upon MCMV infection.
NIH-3T3 fibroblasts **(A)**, SVEC4-10 endothelial cells **(B)**, Hepa1-6 hepatocytes **(E)**, and iBMDM macrophages **(F)** were infected with MCMV WT at an MOI of 5. At the indicated time points, total RNA was isolated and HMGB1 mRNA levels were quantified using RT-qPCR. Values are normalized to β-actin. NIH-3T3 fibroblasts **(C)**, SVEC4-10 endothelial cells **(D)**, Hepa1-6 hepatocytes **(G)**, and iBMDM macrophages **(H)** were infected with MCMV WT at an MOI of 5 and lysed at indicated time points. HMGB1 protein expression was analyzed by immunoblot. GAPDH served as loading control. Shown are representative results from three independent replicates.

5.3 Effects of a HMGB1 overexpression on MCMV replication *in vitro*

Previous results demonstrated that MCMV-infection induced an upregulation of HMGB1 expression. In order to mimic this upregulation and its effect on MCMV replication, HMGB1 overexpressing cells were established. Using lentiviral transduction, HMGB1 was introduced into the four different cell types. For better visualization, HMGB1 was N-terminally tagged with an enhanced green fluorescent protein (EGFP). Since long-term overexpression of HMGB1 could alter cell fitness, a doxycycline-inducible lentiviral expression vector was used to regulate the expression of EGFP-HMGB1. After transduction, the inducible overexpression of HMGB1 was confirmed by fluorescent microscopy and immunoblot.

As shown in Figure 12 A-D, EGFP-HMGB1 expression was visible in all cell types 24 h after addition of 2 µg/ml doxycycline. In addition, EGFP-HMGB1 could be detected in the nucleus, similar to what is known for endogenous HMGB1 [205]. The majority of NIH-3T3 and Hepa1-6 EGFP-HMGB1 bulk cultures were efficiently expressing EGFP-HMGB1 (Figure 12 A, C). However, the induction of EGFP-HMGB1 expression in SVEC4-10 and iBMDM bulk cultures seemed to be less efficient with about 50 % of cells responding to the doxycycline treatment (Figure 12 B, D).

In order to adjust the expression of HMGB1, the optimal dosage of doxycycline for each cell type needed to be tested. To do so, different concentration of doxycycline were applied to the generated cell lines and the expression of EGFP-HMGB1 was analyzed by immunoblot 24 h post induction (Figure 12 E-H). NIH-3T3 and Hepa1-6 EGFP-HMGB1 cells showed a dose-dependent increase of EGFP-HMGB1 with a maximum expression reached with 2.5 µg/ml of doxycycline (Figure 12 E, G). In contrast, even high amounts of doxycycline were not sufficient to induce the expression of EGFP-HMGB1 in SVEC4-10 cells (Figure 12 F). With the support of the immunofluorescence data, it seemed likely that the transduction efficiency of these cells was too low to detect a proper EGFP-HMGB1 expression in the bulk culture. Concerning the last cell type, iBMDM EGFP-HMGB1 cells were very sensitive to doxycycline induction as low concentrations (0.5 µg/ml) induced strong expression of EGFP-HMGB1. In those cells, increasing concentrations of doxycycline did not enhance the expression of HMGB1 (Figure 12 H).

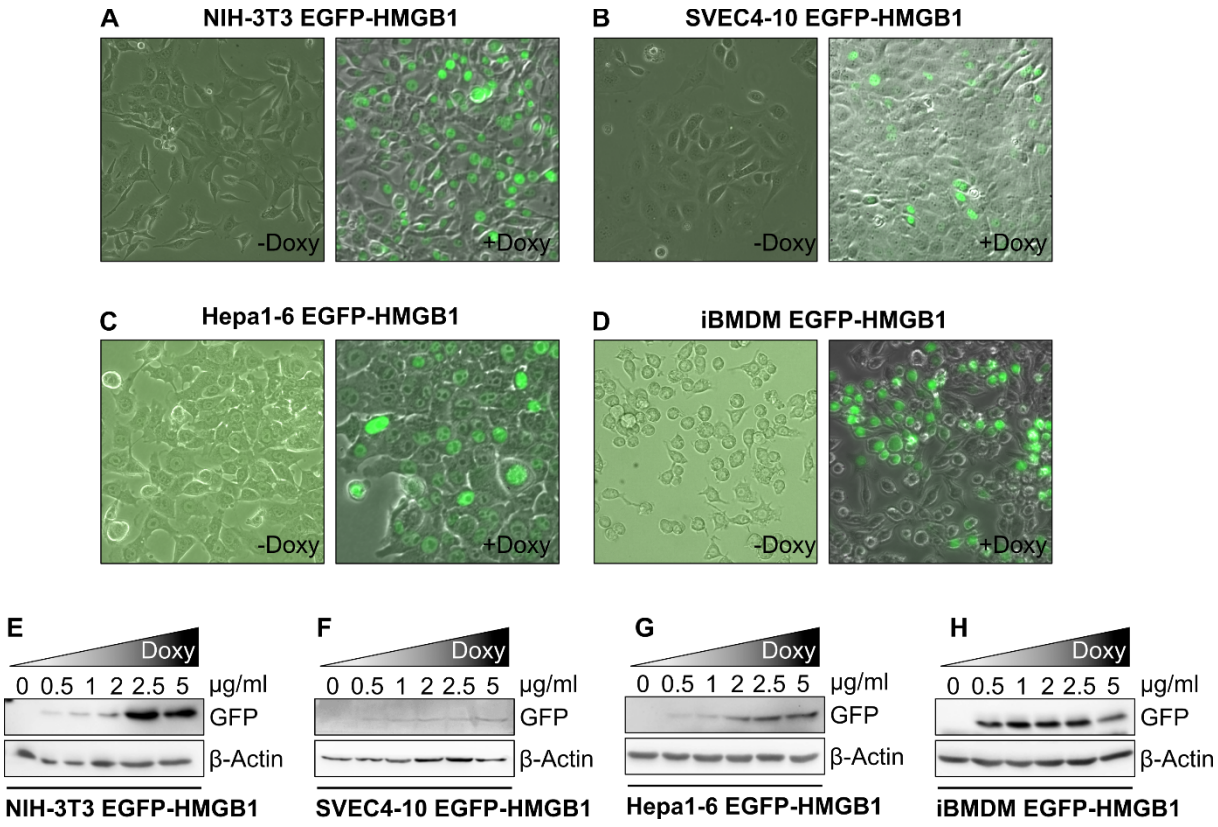

Figure 12: Establishment of inducible EGFP-HMGB1 expression in murine cell lines.
EGFP-HMGB1 transduced NIH-3T3 **(A)**, SVEC4-10 **(B)**, Hepa1-6 **(C)**, or iBMDM **(D)** were treated with either 0 µg/ml (-Doxy) or 2 µg/ml doxycycline (+Doxy) for 24 h. EGFP-HMGB1 expression was detected by fluorescent microscopy. Shown are overlays of green fluorescence signal and bright-field images. **E-H)** Indicated cell lines were induced with an increasing amount of doxycycline for 24 h. Cells were lysed and EGFP-HMGB1 expression was analyzed by immunoblot using a GFP-specific antibody. β-actin was used as loading control.

Once EGFP-HMGB1 overexpression was established in each of the cell types, multistep replication analyses of MCMV were performed in these cells and virus released into the supernatant in presence and absence of doxycycline was titrated. HMGB1 overexpression (+Doxy) did not affect MCMV replication in NIH-3T3, SVE4-10 and Hepa1-6 EGFP-HMGB1 cells as MCMV replicated with the same kinetics and to similar levels in these cell types (Figure 13 A-C). In contrast, MCMV replication in HMGB1-overexpressing iBMDMs was impaired (Figure 13 D). While virus replication in treated (+ Doxy) and untreated (- Doxy) cells was similar in the first 5 dpi, virus titer decreased rapidly 7 dpi when HMGB1 was overexpressed, in contrast to control cells in which virus titer continued to increase.

Taking these results together, overexpression of HMGB1 did not affect MCMV replication in fibroblasts, endothelial cells, and hepatocytes. As endogenous HMGB1 is upregulated upon MCMV infection in these cells (Figure 11), this could indicate that the virus requires the protein for its replication. However, since the

overexpression of HMGB1 did not enhance viral replication, this could indicate that the endogenous level of HMGB1 is sufficient to support MCMV replication. In contrast, the overexpression of HMGB1 in iBMDMs had a severe impact on the replication of the virus, suggesting that HMGB1 has an antiviral role in macrophages.

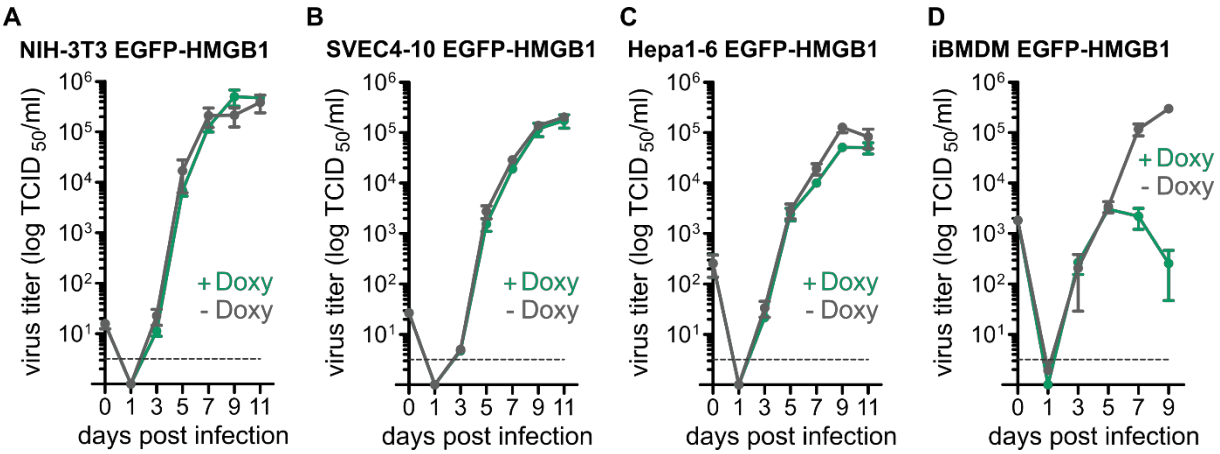

Figure 13: HMGB1 overexpression impairs MCMV replication in macrophages but not in other cell types. Multistep replication kinetics of MCMV WT in EGFP-HMGB1 overexpressing NIH-3T3 fibroblasts **(A)**, SVEC4-10 endothelial cells **(B)**, Hepa1-6 hepatocytes **(C)**, and iBMDM macrophages **(D)**. SVEC4-10 and NIH-3T3 were infected at an MOI of 0.01, Hepa1-6 at an MOI of 0.02, and iBMDMs at an MOI of 0.025. Cells were kept either in normal cell culture medium (-Doxy) or medium containing 2 µg/ml doxycycline (+Doxy). Viral titers are shown as mean ± SEM of three biological replicates.

5.4 HMGB1 release from MCMV-infected cells

As previous studies have shown that especially extracellular HMGB1 has antiviral effects on viral replication and spread, the release of HMGB1 from MCMV-infected cells was determined. HMGB1 is known to be released from cells by cell death-dependent and independent mechanisms. In order to investigate HMGB1 release from MCMV-infected cells in the context of different cell death modalities, not only MCMV WT, which is able to suppress cell death, but also different MCMV mutants lacking the ability to inhibit either apoptosis (MCMV m38.5stop), necroptosis (MCMV M45mutRHIM), or pyroptosis (MCMV M84stop) were used. In addition, a luciferase-based HMGB1-release assay was established allowing the detection and quantification of HMGB1 in cell culture supernatants. For this, an HMGB1-GLuc fusion protein, in which HMGB1 was linked to a secretion-deficient Gaussia luciferase [206], was PCR-amplified and cloned into a lentiviral vector. Subsequently, the four different cell types were transduced with this construct and single clone-selected for the expression of the fusion protein. In parallel to the quantification of HMGB1 in cell culture supernatants, cell viability was monitored using an adenosine

triphosphate (ATP) assay. Both, HMGB1 release and cell viability, were analyzed 2, 4, 8, 24, 48 and 72 hpi for each virus and cell type. A decrease of minimum 10 % of cell viability was considered as cell death and marked with a grey background (Figure 14).

NIH-3T3 cells infected with MCMV WT only released HMGB1 at late time points after infection. An increase of extracellular HMGB1 (eHMGB1) was first detected 48 hpi, preceding the detection of any cell death (Figure 14 A). However, HMGB1 was mostly released at 72 hpi when infected cells died. Similarly, HMGB1 was released from NIH-3T3 cells infected with the apoptosis-inducing mutant MCMV m38.5stop at 48 and 72 hpi, while cell viability declined. However, no eHMGB1 was detectable before the onset of cell death. MCMV M45mutRHIM-infected NIH-3T3 cells only released HMGB1 at 72 hpi, while MCMV M84stop-infected cells released HMGB1 starting at 48 hpi. Interestingly, reduction in cell viability was not detected within the first 72 h after infection with MCMV M45mutRHIM or M84stop. As fibroblasts are susceptible to necroptosis induced by MCMV M45mutRHIM, more severe cell death was expected. However, during necroptosis, molecules like HMGB1 can be released from the cells before the actual cell death occurs, as pores are embedded in the plasma membrane.

In comparison to fibroblasts, SVEC4-10 cells seemed to be quite resistant to cell death. Neither MCMV WT, nor MCMV m38.5stop, nor MCMV M84stop induced any cell death within 72 h (Figure 14 B). In addition, no eHMGB1 was detectable in the supernatants of SVEC4-10 cells infected with these different MCMV mutants. However, SVEC4-10 cells were sensitive to necroptosis induced by MCMV M45mutRHIM, resulting in reduced cell viability starting between 8 and 24 hpi. Necroptotic cell death of SVEC4-10 cells was accompanied by increasing amounts of eHMGB1, which was detectable 8 hpi and steadily increased until 72 hpi.

In infected Hepa1-6 cells, cell death occurred similarly to what was observed for NIH-3T3 fibroblasts, with a loss of cell viability in MCMV WT-infected cells at 72 hpi, in MCMV m38.5stop-infected cells 48 hpi, and no detected cell death in Hepa1-6 cells infected with either MCMV M45mutRHIM or M84stop (Figure 14 C). In contrast to NIH-3T3 and SVEC4-10 cells, release of HMGB1 was detectable already before cell death occurred, regardless of the MCMV variant used for infection. Indeed,

MCMV WT-infected Hepa1-6 cells started to release HMGB1 already 24 hpi, while cell death occurred only at 72 hpi.

Similarly to Hepa1-6 cells, iBMDMs released HMGB1 independently of cell death in early stages of infection as well as in parallel to cell death (Figure 14 D). MCMV WT-infected iBMDMs started to release HMGB1 24 hpi, while cell viability was decreasing only 72 hpi. However, the amount of HMGB1 released by MCMV WT-infected iBMDMs was relatively low compared to iBMDMs infected with the different MCMV mutants. Both, MCMV m38.5stop and M45mutRHIM-infected iBMDMs released HMGB1 starting at 8 hpi, while a decrease in cell viability was detected starting at 48 hpi. The pyroptosis-inducing MCMV M84stop mutant triggered HMGB1 release (24 hpi) and cell death (72 hpi) in similar kinetics like MCMV WT.

Overall, all four cell types released HMGB1 in a cell death-dependent manner after MCMV infection. In addition, the release of HMGB1 was dependent on the sensitivity of a cell type to a specific type of programmed cell death pathway. Interestingly, Hepa1-6 cells and iBMDMs were able to release HMGB1 already before cell death was detectable, which indicated that these cells might actively secrete HMGB1 upon MCMV infection.

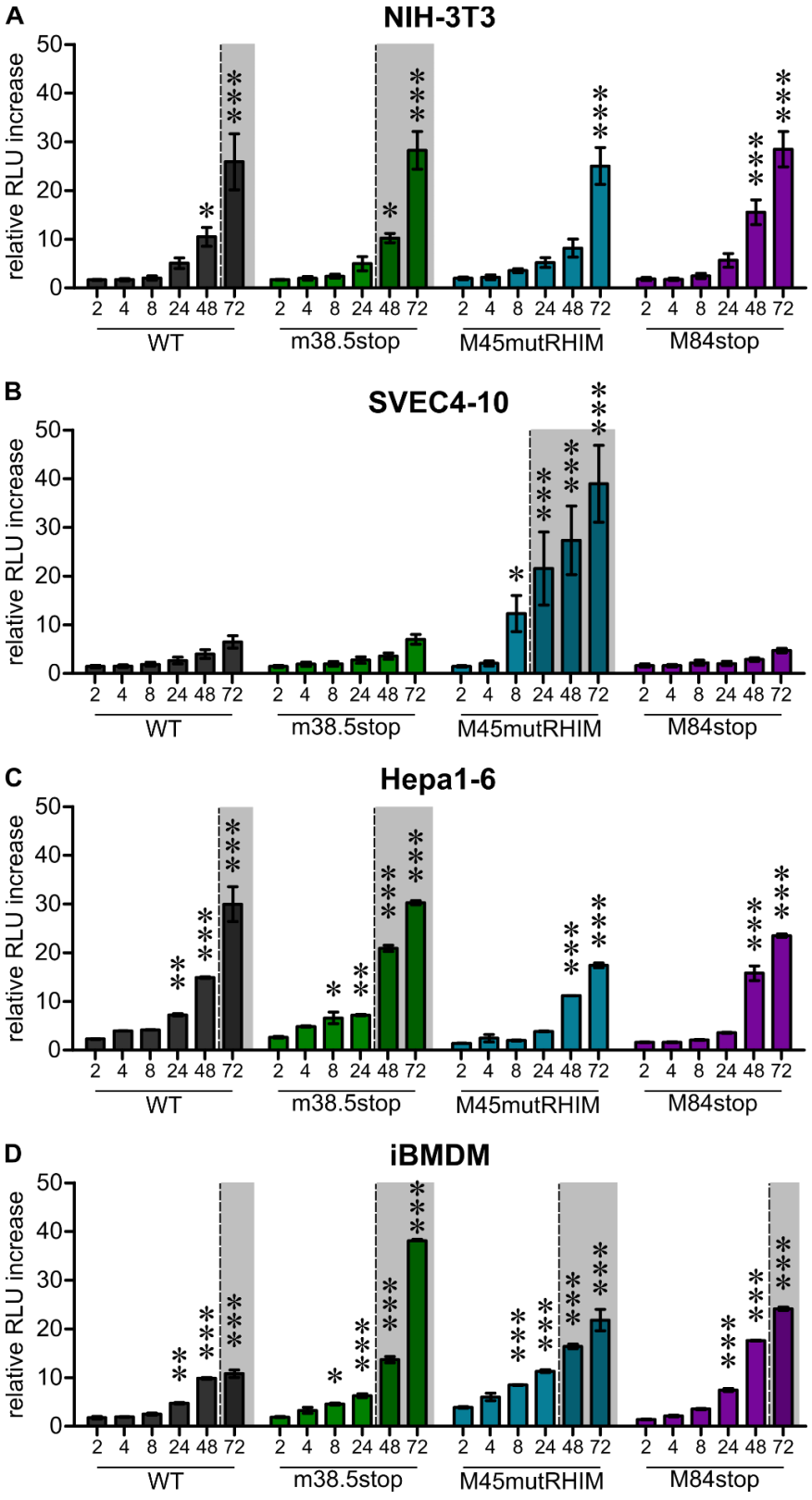

Figure 14: MCMV-infected cells release HMGB1 in a cell type-specific manner.
NIH-3T3 fibroblasts **(A)**, SVEC4-10 endothelial cells **(B)**, Hepa1-6 hepatocytes **(C)**, and iBMDM macrophages **(D)** expressing HMGB1 fused to Gaussia luciferase, were infected with either MCMV WT or indicated MCMV mutants at an MOI of 5. Cell supernatants were harvested at indicated time points and extracellular HMGB1 was quantified by luciferase activities. Shown are the relative increases over background levels of two independent experiments. Each sample was measured in two technical replicates. 2way ANOVA was used for statistical analysis comparing values of each time point to the individual 2 hpi time point. *: $p<0.5$; **: $p<0.01$; ***: $p<0.001$. In parallel, ATP assays were performed for each condition and time points to detect cell viability. Grey areas indicate time points to which cell viability was reduced by at least 10 %.

5.5 The effect of extracellular recombinant HMGB1 on MCMV infection

As HMGB1 seemed to be actively secreted by MCMV-infected iBMDMs, and overexpression of HMGB1 in these cells reduced MCMV replication, possibly due to increased HMGB1 release, the effects of extracellular HMGB1 on MCMV infection in iBMDMs were investigated further. For this purpose, recombinant HMGB1 (rHMGB1) was used at the recommended concentration to mimic extracellular HMGB1, and viral growth kinetics in treated cells were evaluated. As seen in Figure 15, the supplementation of rHMGB1 did not have any effect on MCMV growth in macrophages, as the virus replicated in similar kinetics and to similar titers in the presence and absence of rHMGB1.

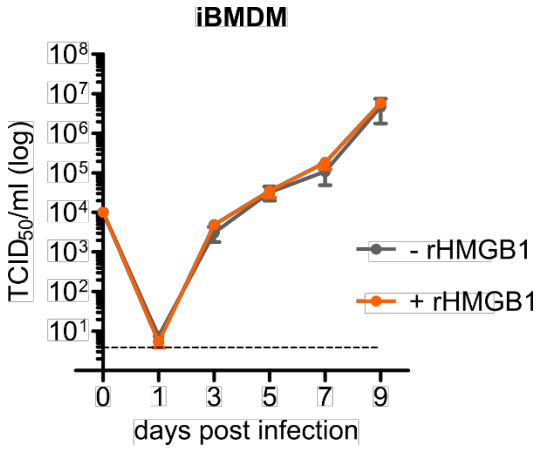

Figure 15: Recombinant extracellular HMGB1 does not affect MCMV growth in macrophages.
Multistep replication kinetics of MCMV WT in iBMDM macrophages. iBMDMs were infected at an MOI of 0.025. Cells were kept in either normal cell culture medium (-rHMGB1) or medium supplemented with 25 ng/ml fully reduced, recombinant HMGB1 (+rHMGB1). Viral titers are shown as mean ± SEM of three biological replicates.

5.6 Effects of HMGB1 knockdown on MCMV replication *in vitro*

The previous results showed that, even if eHMGB1 is described as having an antiviral role against different viruses, it seems that this is not the case against MCMV since rHMGB1 did not affect MCMV replication. In contrast, intracellular HMGB1 has been described to support replication of several viruses e.g. by interacting with viral promoters and transcription initiators, or by directly interacting with the viral genome. In addition, it was speculated that HMGB1 might also increase lytic HCMV replication since it was found to interact with its oriLyt. If this were also the case for MCMV, a knockdown of HMGB1 would be expected to a reduced lytic replication and impaired growth of MCMV. In contrast, HMGB1 overexpression

reduced MCMV growth in macrophages. Consequently, a knockdown of HMGB1 in macrophages could rescue this phenotype and lead to increased MCMV replication. To investigate further the possible involvement of intracellular HMGB1 on MCMV replication, HMGB1 was depleted from the different cell types.

For this, stable shRNA-mediated HMGB1 knockdowns were established in NIH-3T3, SVEC4-10, Hepa1-6, and iBMDM cells using lentiviral vectors. Each cell type was transduced with either a non-targeting scramble (scr) shRNA or shRNAs targeting specific regions of HMGB1 mRNAs (sh1, sh2). While sh1 was complementarily binding within the coding region of HMGB1 mRNAs, sh2 bound within the 3' UTR (Figure 16 A). The efficiency of the knockdown was validated by RT-qPCR and immunoblot. In comparison to the scr controls, the levels of HMGB1 mRNA were significantly reduced in sh1 and sh2 transduced cells of all tested cell types (Figure 16 B-E). The knockdown efficiency of sh2 was at about 80 % mRNA downregulation compared to the scr controls, in contrast to sh1 that enabled a downregulation of up to 99% in all cell types (Figure 16 B-D), except iBMDMs, in which the knockdown efficiency was similar for both shRNAs (i.e. around 80 % of downregulation, Figure 16 E).

Subsequent immunoblots of all cell lines confirmed the results obtained by RT-qPCR. HMGB1 protein levels decreased with both shRNAs (Figure 16 F-I). Both shRNAs were able to reduce HMGB1 protein expression to undetectable levels in NIH-3T3 and SVEC4-10 cells (Figure 16 F, G), whereas in the Hepa1-6 cells the effect of sh2 on the protein level seemed to be less efficient, since a faint band could still be observed (Figure 16 H). In contrast to the other cell types, HMGB1 protein could still be detected in iBMDM sh1 and sh2 cells, however, the signal was strongly decreased compared to the scr control iBMDMs (Figure 16 I).

Taken together, the transduction of two different shRNAs targeting HMGB1 mRNA resulted in the successful establishment of stable HMGB1 knockdowns in different murine cell types. The sh2 targeting the 3' UTR of HMGB1 mRNA was slightly less efficient than the sh1 targeting the coding region.

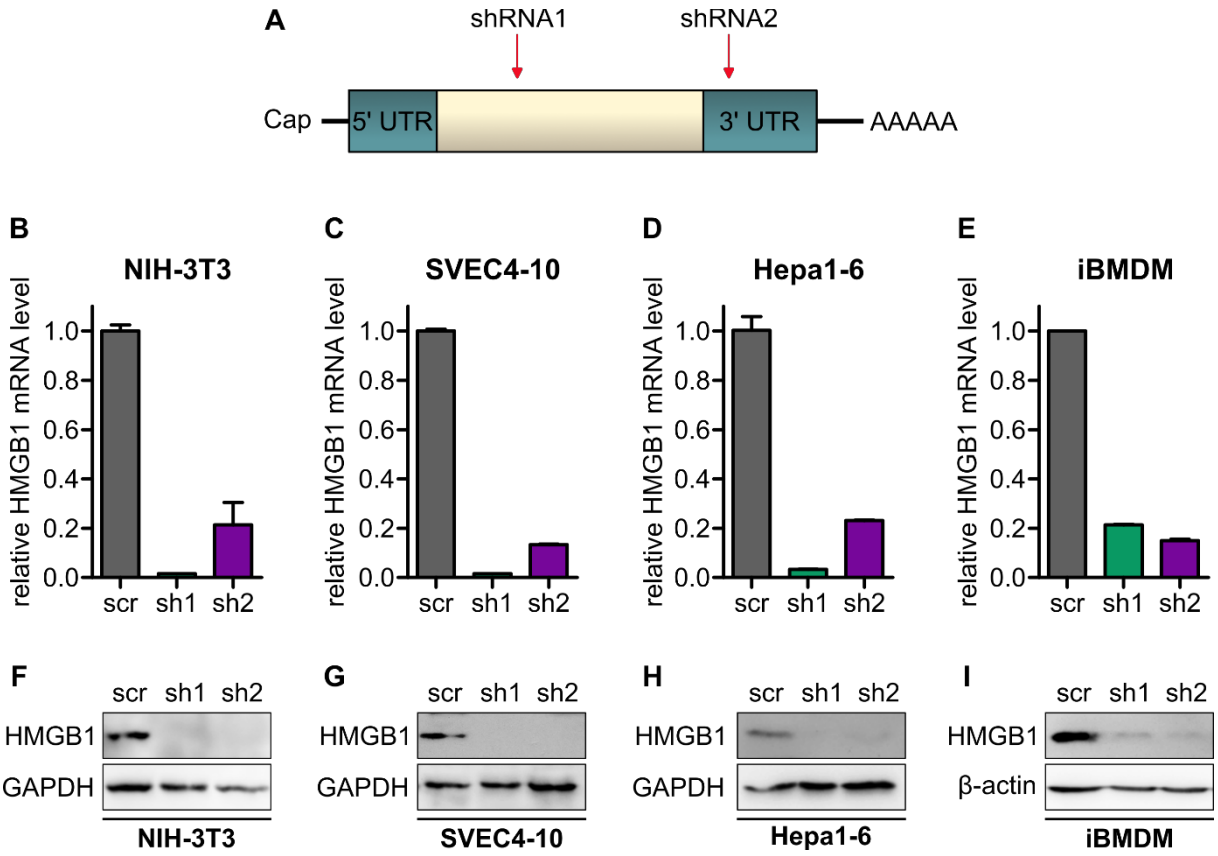

Figure 16: Establishment of murine HMGB1 knockdown cells using shRNAs.
A) Schematic representation of the HMGB1 mRNA with its 5' and 3' untranslated regions (blue) and the coding region (white). The arrows indicate the complementary regions targeted by HMGB1-specific shRNAs. **B-E)** Different murine cell lines (indicated above) were transduced with either a non-targeting scramble (scr) shRNA or shRNAs targeting HMGB1 mRNA (sh1, sh2). Total RNA was isolated from each cell line and levels of HMGB1 mRNA were quantified by RT-qPCR. Obtained values were normalized to β-actin. Shown are representative results from three independent experiments. **F-I)** Transduced cells were lysed and HMGB1 protein expression was analyzed by immunoblot. GAPDH or β-actin were stained as control for equal loading.

These generated cell lines were used to evaluate the impact of intracellular HMGB1 on MCMV infection. For doing this, scr control cells, as well as sh1 and sh2 cells of each cell type, were infected with MCMV WT and virus growth was monitored at the indicated time points by titration. Similar to the results of HMGB1-overexpressing cells, virus growth was not affected in absence of HMGB1 in NIH-3T3 or SVEC4-10 cells (Figure 17 A, B). On the contrary, an effect of HMGB1 downregulation could be observed in Hepa1-6 cells and iBMDMs. In sh1 iBMDMs, MCMV replicated significantly faster and to higher titers compared to the iBMDM scr control cells (Figure 17 D), confirming an antiviral phenotype of HMGB1 in macrophages. In contrast, in Hepa1-6 sh1 cells MCMV replication appeared to be delayed in comparison to the kinetics observed in the Hepa1-6 scr control cells, suggesting a supportive effect of HMGB1 on MCMV replication (Figure 17 C). However, these different phenotypes could not be confirmed in the sh2 cell lines, possibly due to the

higher amount of remaining HMBG1 that could be sufficient for the protein to perform its functions (Figure 16).

In summary, the downregulation of HMGB1 in sh1-transduced cells affected MCMV replication in a cell type-specific manner. HMGB1 seemed not to play a role in MCMV replication in fibroblast and endothelial cells. However, in hepatocytes and macrophages, HMGB1 appeared to be a host factor that significantly influences viral replication. Surprisingly, HMGB1 had a dual role, proviral in hepatocytes and antiviral in macrophages.

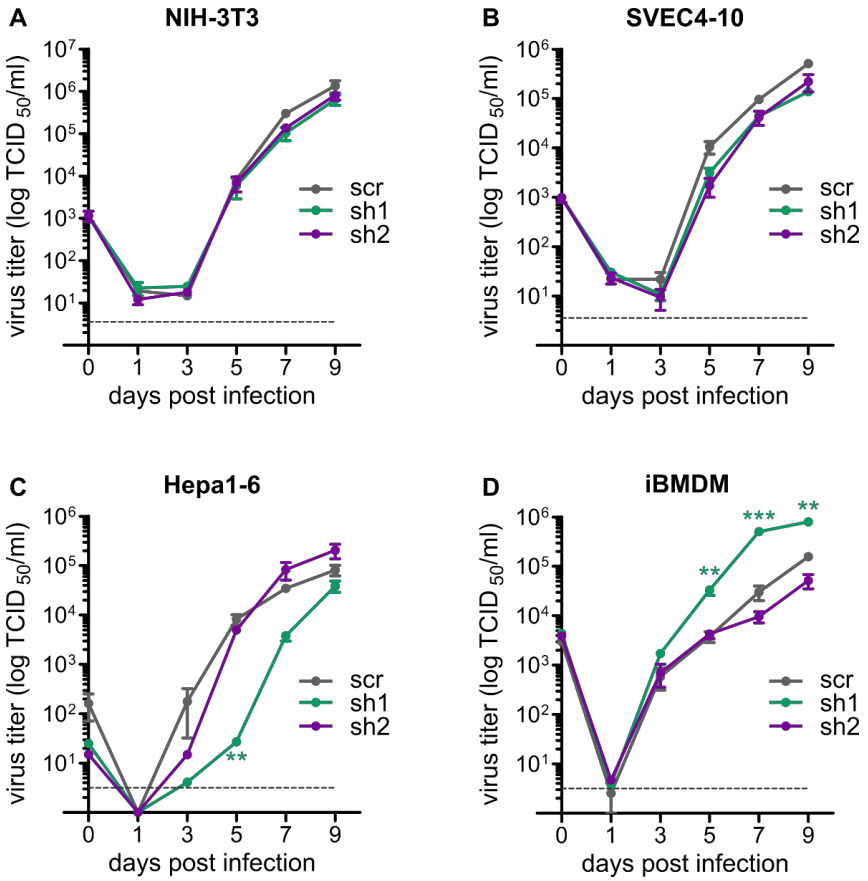

Figure 17: HMGB1 knockdown affects MCMV growth in a cell type-specific manner.
Multistep replication kinetics of MCMV WT in NIH-3T3 fibroblasts **(A)**, SVEC4-10 endothelial cells **(B)**, Hepa1-6 hepatocytes **(C)**, and iBMDM macrophages **(D)**. Each cell type was transduced with either a non-targeting control shRNA (scr) or one of two shRNAs targeting HMGB1 (sh1, sh2). SVEC4-10 and NIH-3T3 were infected at an MOI of 0.01, Hepa1-6 at an MOI of 0.02, and iBMDMs at an MOI of 0.025. Viral titers are shown as mean ± SEM of three biological replicates. Statistical analysis were performed with a 1way ANOVA with Dunnett's Multiple Comparison test; **: $p<0.005$; ***: $p<0.0001$.

5.7 Regulation of viral gene expression by HMGB1

Since HMGB1 showed both, proviral and antiviral properties, depending on the cell lines, a closer look into intracellular processes was needed. Knowing that HMGB1 is a regulator for transcription, the effect of HMGB1 on viral gene expression was

tested. For this, control cells (scr) as well as HMGB1-knockdown cells (sh1, sh2) of each cell type were infected with MCMV WT and lysed at different stages of the MCMV replication cycle. Subsequently, immunoblots were performed to detect viral protein expression. One representative of viral immediate early, early, and late proteins was chosen, namely IE1, E1, and gB. In all cell types alterations of viral protein expression were detectable in HMGB1 knockdown cells compared to their respective scr control cells. It should be noted here, that sh2 knockdown cells showed a less pronounced phenotype than sh1 cells for all cell types. This goes in line with MCMV growth kinetics, where no effects of HMGB1 knockdown were seen in sh2 cells.

In NIH-3T3 and SVEC4-10 sh1 knockdown cells all tested viral proteins showed alteration in their expression (Figure 18 A, B), which was not reflected in the replication kinetics (Figure 17 A, B). In both cell types, a reduction of viral IE1 expression could be detected in sh1 cells as early as 2 hpi compared to the scr cells. Interestingly, this reduction was not a permanent effect as this difference was not detectable anymore starting at 24 hpi. Similar effect could be observed for the E1 protein at early time points (4 or 8 hpi) and for gB at late time points starting 48 hpi.

Surprisingly, viral gene expression was less affected in Hepa1-6 sh1 cells (Figure 18 C), although MCMV growth in these cells was significantly delayed (Figure 17 C). IE1 and E1 expression in Hepa1-6 sh1 and scr cells were comparable throughout the infection, while only the expression of the late protein gB was reduced at 48 hpi in sh1 cells. However, this seemed to be transient, as at 72 hpi the levels of gB evened out and no difference between scr and sh1 cells was detectable anymore. Delayed gB expression in HMGB1 knockout Hepa1-6 cells however could explain the delayed MCMV growth in these cells.

Interestingly, MCMV was able to replicate more efficient in iBMDM sh1 cells (Figure 17 D), while viral gene expression was delayed in those cells compared to iBMDM scr (Figure 18 D). Similar to what was observed in NIH-3T3 sh1 cells, iBMDM sh1 showed reduced levels of IE1 starting 2 hpi, reduced levels of E1 starting at 8 hpi, and less gB expression at 48 hpi and later time points.

In conclusion, knockdown of HMGB1 altered the expression of all tested viral proteins in all cell types, regardless of the effect that HMGB1 knockdown had on the

viral growth in these cells. Since viral protein expression was usually affected only at early stages of expression, HMGB1 might promote transcription initiation.

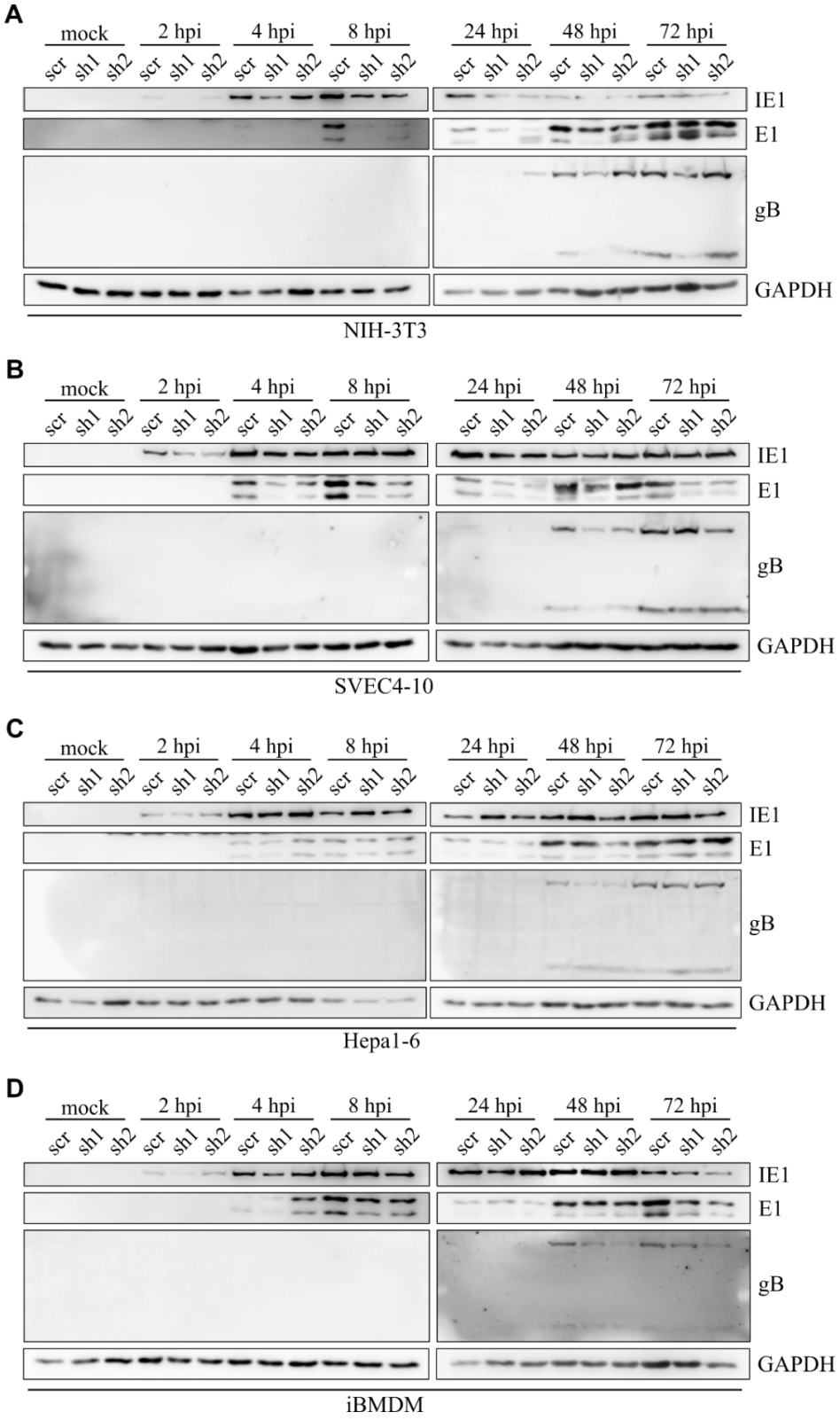

Figure 18: MCMV protein expression is reduced in HMGB1 knockdown cells.
NIH-3T3 fibroblasts **(A)**, SVEC4-10 endothelial cells **(B)**, Hepa1-6 hepatocytes **(C)**, and iBMDM macrophages **(D)** were transduced with either a non-targeting control shRNA (scr) or with one of two shRNAs targeting HMGB1 (sh1, sh2). Each cell lines was infected with MCMV WT at an MOI of 5, cells were lysed at indicated time points and expression of the viral proteins IE1, E1, and gB was detected by immunoblot. GAPDH served as a loading control.

5.8 The opposing functions of HMGB1 in MCMV-infected macrophages

The data generated during this work showed that iBMDMs represent a special cell type as they behave differently from other cell types tested. As previously shown, expression of the viral proteins IE1, E1, and gB were reduced in HMGB1-depleted macrophages (Figure 18) indicating that HMGB1 might support or accelerate MCMV transcription in macrophages. However, MCMV replication was enhanced in HMGB1 knockdown iBMDMs (Figure 17) and reduced when HMGB1 was overexpressed (Figure 13), which is contradictory with the previous observation. Furthermore, initial experiments showed that rHMGB1 did not affect MCMV replication in macrophages, leading to the conclusion that antiviral effects of HMGB1 were not mediated by extracellular HMGB1 (Figure 15). However, the use of the recombinant HMGB1 might not reflect the full functional potential of cell-derived HMGB1, as different post-translational modifications of the protein can occur within the cell. This could have led to wrong conclusion. In addition, eHMGB1 has been described to induce pyroptosis in macrophages [164], which could lead to increased cell death and reduced viral replication.

To verify whether HMGB1-induced pyroptosis might explain the striking phenotype observed in macrophages, previous experiments were repeated with $ASC^{-/-}$ iBMDMs lacking the ability to undergo pyroptosis. First, $ASC^{-/-}$ iBMDMs, which were described previously [73], were transduced with either scr shRNA or the HMGB1-targeting shRNAs, sh1 or sh2. As in wild-type iBMDMs, the expression of HMGB1 was significantly reduced in $ASC^{-/-}$ iBMDM sh1 and sh2 cells compared to $ASC^{-/-}$ iBMDM scr cells. Similarly to previous cell types, sh1 was able to reduce HMGB1 expression levels by more than 80 %, while sh2 was less efficient and reduced mRNA expression by about 60 % (Figure 19 A). In addition, knockout of ASC was confirmed via immunoblot. As expected, wild-type iBMDMs showed ASC expression, while ASC was not detectable in $ASC^{-/-}$ iBMDM scr, sh1, and sh2 cells (Figure 19 B).

Scr control and knockdown cells were then infected with MCMV WT, and multistep replication kinetics were performed. As seen in Figure 19 C, MCMV replication was delayed in $ASC^{-/-}$ iBMDM sh1, and to lesser extent also in sh2 cells as the maximum virus titer was reached 7 dpi in sh1 cells and 5 dpi in scr cells, when MCMV titers in sh1 cells were significantly lower.

In addition, ASC$^{-/-}$ iBMDM scr, sh1 and sh2 cells were infected with MCMV WT and cells were lysed at specific time points to investigate the expression of the viral proteins IE1, E1, and gB. The expression of the early proteins IE1 and E1 seemed not to be altered in HMGB1 knockdown ASC$^{-/-}$ iBMDMs during MCMV infection, while the expression of the late protein gB was reduced in sh1 and sh2 cells at 48 and 72 hpi (Figure 19 D), thus reflecting the data observed in ASC-competent iBMDMs (Figure 18 D).

Taken these results together, ASC$^{-/-}$ iBMDM displayed the same phenotype regarding MCMV growth and protein expression that was seen in Hepa1-6 cells, supporting the hypothesis that intracellular HMGB1 accelerates MCMV replication. In addition, the fact that ASC knockout alone was able to invert the antiviral effect of HMGB1 seen in iBMDMs to a proviral effect supports the hypothesis that extracellular HMGB1 alone suppresses viral replication by triggering pyroptosis. Pyroptotic cell death ultimately leads to less viable cells and lower viral titers.

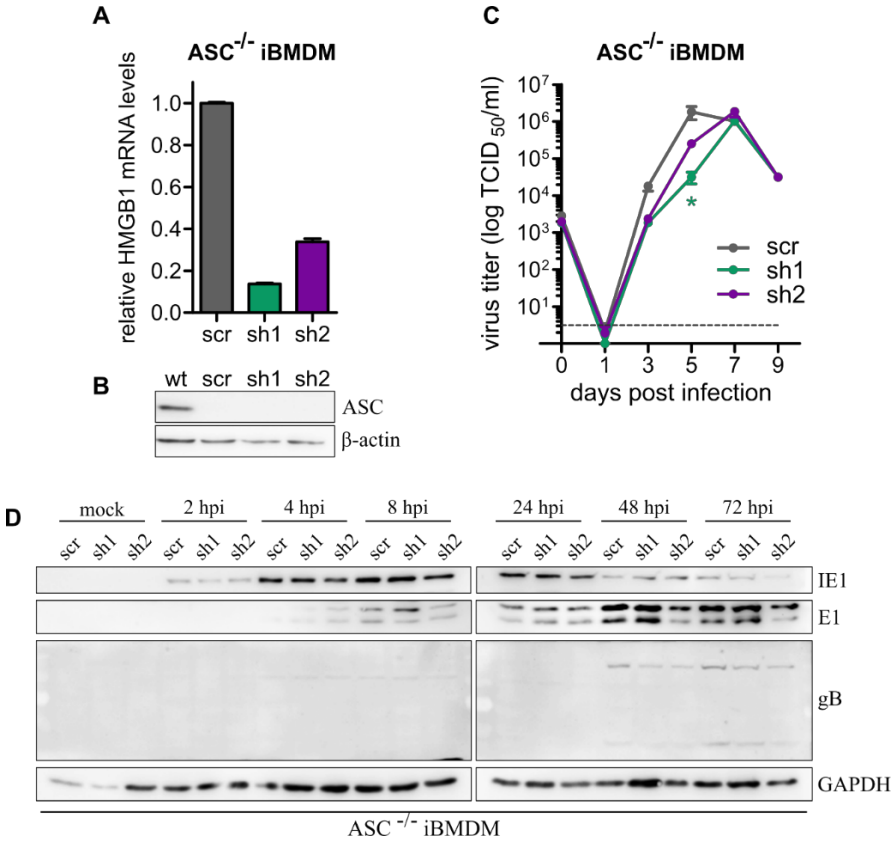

Figure 19: Inhibition of pyroptosis restores proviral phenotype of HMGB1 in macrophages.
A) ASC$^{-/-}$ iBMDMs were transduced with either a non-targeting scramble shRNA (scr) or shRNAs targeting HMGB1 (sh1, sh2). Total RNA was isolated from transduced cells and HMGB1 mRNA levels were quantified by RT-qPCR. Obtained values were normalized to β-actin. Shown are representative results from three independent experiments. **B)** Wild-type iBMDMs and transduced ASC$^{-/-}$ iBMDMs were lysed and ASC protein was detected by immunoblot. β-actin was detected as loading control. Shown are representative results from three independent experiments. **C)** Multistep replication kinetics of MCMV WT in transduced ASC$^{-/-}$ iBMDMs. Cells were infected with MCMV WT at an MOI of 0.025. Shown are mean ± SEM of three biological replicates. Statistical analysis was

performed with a 1way ANOVA with Dunnett's Multiple Comparison test; *: $p<0.05$ **D)** Viral protein expression kinetics in transduced $ASC^{-/-}$ iBMDMs. Cells were infected with MCMV WT at an MOI of 5, lysed at indicated time points and expression of viral proteins IE1, E1 and gB was detected by immunoblot. GAPDH was stained as loading control. Shown are representative results from two independent experiments.

5.9 Intracellular localization of HMGB1 in MCMV-infected cells

As shown before, intracellular HMGB1 supported viral gene expression. To gain first hints on how HMGB1 mediates this effect, localization of HMGB1 in MCMV-infected cells was investigated. For this, inducible HMGB1-overexpressing NIH-3T3, SVEC4-10, Hepa1-6 and iBMDM (see 5.3) were infected with MCMV WT and treated with doxycycline to induce the expression of EGFP-HMGB1. After 24 hpi cells were fixed and EGFP-HMGB1 as well as MCMV E1 were detected by confocal microscopy. Uninfected but doxycycline-induced cells served as control.

As previously described, HMGB1 localized exclusively in the nucleus of uninfected cells (Figure 20). In all cell types, HMGB1 was dispersed within the nucleus but also showed accumulation in some round, nuclear compartments. Upon MCMV infection, HMGB1 remained in the nucleus of infected, E1-positive cells. No translocation into the cytoplasm was visible. Similar to what was observed in uninfected cells, HMGB1 accumulated in nuclear compartments. Interestingly, some of these accumulations co-localized with the MCMV E1 protein (Figure 20). As E1 is the major component of viral replication compartments (RCs), this lead to the conclusion that HMGB1 localized to RCs were viral transcription and replication take place. Importantly, enrichment of HMGB1 was observed in all stages of RC formation. Small spherical early RCs incorporated HMGB1 as well as larger amorphous late RCs.

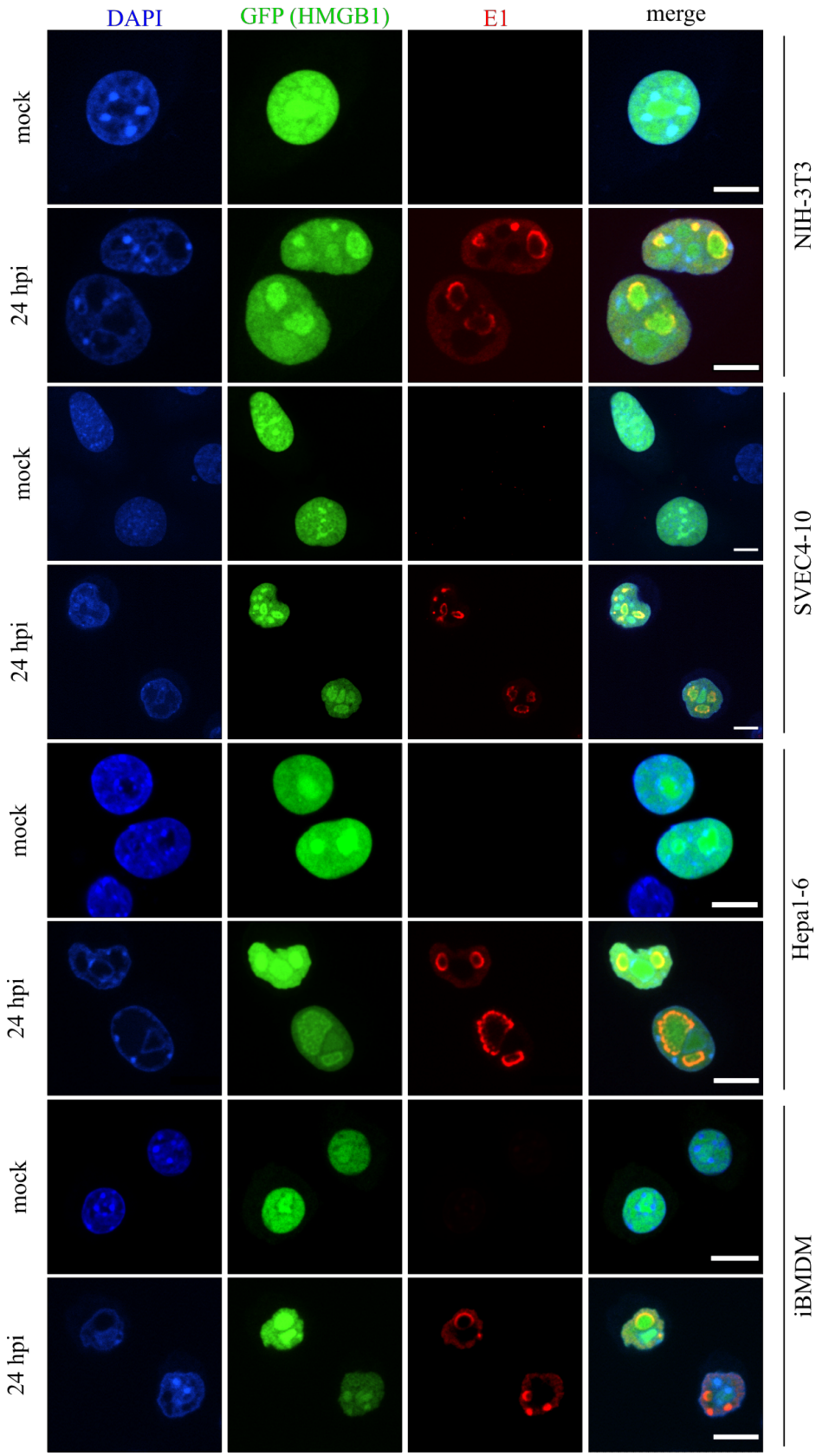

Figure 20: HMGB1 remains in the nucleus of MCMV-infected cells and localizes to viral replication compartments.
NIH-3T3, SVEC4-10, Hepa1-6 and iBMDM EGFP-HMGB1 cells were infected with MCMV WT at an MOI of 3 and EGFP-HMGB1 expression was induced using 1 µg/ml doxycycline. 24 hpi cells were fixed and stained for MCMV E1 and chromatin. EGFP-HMGB1 (green), E1 (red), and chromatin (Dapi, blue) signals were detected using an A1 confocal laser scanning microscope (Nikon). Scale bar: 10 µm.

5.10 Recruitment of HMGB1 to viral replication compartments

It was previously described that the intrinsically disordered region (IDR) of HCMV UL112-113 (E1) drives the formation of viral replication compartments via liquid-liquid phase separation (LLPS). In addition, HMGB1 is known to have a C-terminal IDR facilitating LLPS. Interestingly, alterations of the disordered C-terminal tail of HMGB1 can cause mispartitioning of HMGB1 leading to nucleolar dysfunctions [104]. Since HMGB1 was enriched in viral replication compartments formed by MCMV E1, it was of further interest to investigate the impact of the IDR of HMGB1 on the recruitment of HMGB1 into the RCs.

First, NIH-3T3 were co-transfected with EGFP-HMGB1 and E1 to exclude that other viral components are involved in the recruitment of HMGB1. Subsequent immunofluorescence staining and confocal microscopy showed that the expression of E1 was enough to detect co-localization. In co-transfected NIH-3T3, E1 was forming small dot-like structures as well as bigger, more amorphous structures, highly similar to RCs seen in infected cells (Figure 21 A). Similar to what was observed in MCMV-infected cells, signals of HMGB1 co-localized with these E1-positive nuclear compartments, indicating that indeed no other viral components were needed to recruit HMGB1 to E1-positive compartments. To exclude that the co-localization of these two proteins is due to a direct interaction, HEK293T cells were co-transfected with expression plasmids as before and co-immunoprecipitation with subsequent immunoblot was performed. Next to an untransfected control cells were transfected with either EGFP-HMGB1 and E1, GFP and E1 (negative control), or EGFP-HMGB1 and 3xFlag-TLR4 (positive control). All proteins were well expressed in the cells as shown in the input control (Figure 21 B). After immunoprecipitation of GFP or EGFP-HMGB1, the precipitates were analyzed for E1 as well as Flag-TLR4 by immunoblot. While TLR4, which served as positive control, was detectable in immunoprecipitates of EGFP-HMGB1, E1 was not seen to interact with neither EGFP-HMGB1 nor GFP (negative control) (Figure 21 B).

Finally, different truncation mutants of HMGB1 were generated, which lack either parts of the IDR or the complete IDR. With this, the impact of LLPS on HMGB1 recruitment into E1-positive dots was investigated. The HMGB1 mutants were designed based on previous publications, IDR predictions and locations of NLS sequences. HMGB1$^{(1\text{-}185)}$ represented the longest of the mutants lacking only the acidic tail but still containing the natural NLS2 sequence and almost half of the

predicted IDR (Figure 8 D). NIH-3T3 transfected with EGFP-HMGB1$^{(1-185)}$ only (-E1) showed a similar distribution than full-length HMGB1 i.e. localizing in the nucleus with accumulations in nuclear compartments (Figure 21 C). EGFP-HMGB1$^{(1-185)}$ also accumulated within E1-positive nuclear dots in co-transfected NIH-3T3 cells (+E1, Figure 21 D)

The second mutant EGFP-HMGB1$^{(1-162)}$ encoded a shorter form as it lacked the complete previously predicted IDR as well as the NLS2. Although the NLS2 was missing, EGFP-HMGB1$^{(1-162)}$ localized to the nucleus of transfected NIH-3T3 (-E1, Figure 21 D). However, the nuclear distribution appeared to be more homogenous and EGFP-HMGB1$^{(1-162)}$ did not accumulate in nuclear compartments as observed with full-length HMGB1. In addition, EGFP-HMGB1$^{(1-162)}$ was distributed in the cytoplasm with some punctate accumulations. Co-expressed with E1, nuclear EGFP-HMGB1$^{(1-162)}$ co-localized with E1-positive dots (+E1, Figure 21 D). Interestingly, EGFP-HMGB1$^{(1-162)}$ was also enriched in E1-negative nuclear compartments, even though this was not observed in cells that did not express E1.

Similarly to the HMGB1 mutant “Del IDR” from Mensah et al. [104] the last mutant was constructed. EGFP-HMGB1$^{(1-134)}$ lacks not only the complete C-terminal tail but also a part of the DNA-binding B-box. To enhance nuclear localization of this mutant the sequence of the NLS2 was re-introduced at the C-terminus. EGFP-HMGB1$^{(1-134)}$ transfected NIH-3T3 showed mostly cytoplasmic but also nuclear localization (-E1, Figure 21 E). Very prominent aggregations of EGFP-HMGB1$^{(1-134)}$ could be observed in the cytoplasm. Within the nucleus, EGFP-HMGB1$^{(1-134)}$ was mostly evenly distributed but excluded from nuclear compartments, which differentiated it from the other mutants as well as full-length HMGB1. When EGFP-HMGB1$^{(1-134)}$ and E1 were co-expressed, no co-localization was detected. Instead, EGFP-HMGB1$^{(1-134)}$ was fully excluded from E1-positive structures (+E1, Figure 21 E).

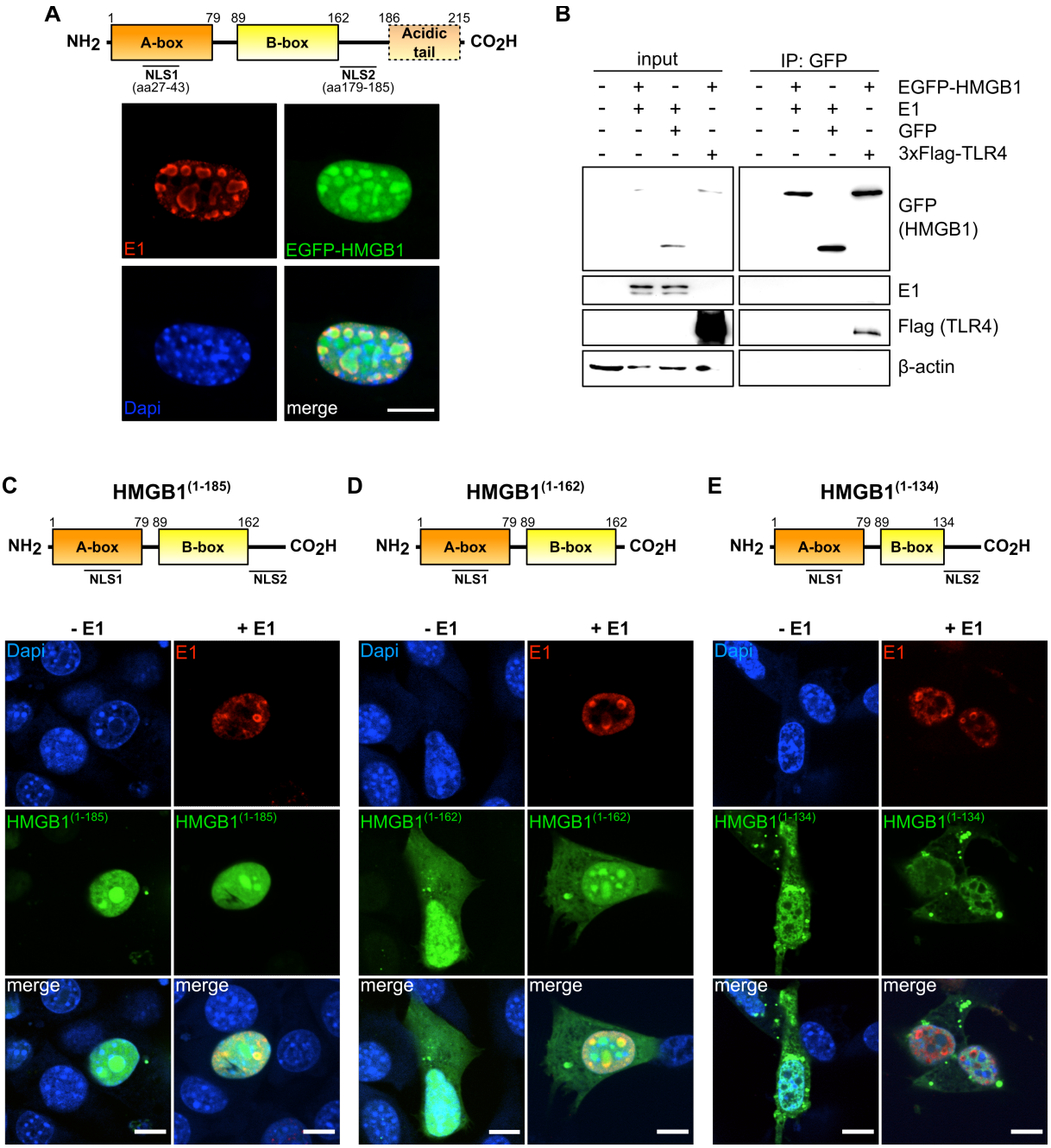

Figure 21: HMGB1 might be recruited to MCMV replication compartments by liquid-liquid phase separation rather than direct protein interaction.
A) NIH-3T3 cells were co-transfected with plasmids encoding MCMV E1 and EGFP-HMGB1 (full-length, schematic representation above). 48 h post-transfection cells were fixed and localization of E1 (red) and HMGB1 (green) was detected using a confocal spinning disk microscope (Nikon). The nucleus was identified using Dapi staining. Scale bar: 10 µm. **B)** HEK-293T cells were co-transfected with plasmids encoding either EGFP-HMGB1 and E1, GFP and E1, or EGFP-HMGB1 and 3xFlag-TLR4. Cells were lysed 24 hpi and EGFP/GFP was immunoprecipitated from the lysate. GFP/EGFP-HMGB1, E1 and Flag-TLR4 were detected in the whole cell lysate (input) as well as in the immunoprecipitate by immunoblot. **C-E)** NIH-3T3 cells were either singly transfected (-E1) with plasmids encoding different C-terminal truncated mutants of EGFP-HMGB1 (schematic representation above) or co-transfected with plasmids encoding EGFP-HMGB1 mutants as well as MCMV E1 (+E1). 48 h post-transfection cells were fixed and localization of E1 (red) and HMGB1 (green) was detected using a confocal spinning disk microscope (Nikon). Nuclei were identified by Dapi staining. Scale bar: 10 µm.

5.11 The impact of HMGB1 on MCMV infection *in vivo*

To evaluate the effect that HMGB1 has on the MCMV infection *in vivo*, infection experiments using HMGB1 knockout-mice were performed. Since embryonic HMGB1 knockout is lethal, a tamoxifen-inducible Cre-loxP system was used to generate conditional whole-body knockouts in adult mice. For this, *Hmgb1*$^{fl/fl}$ animals (gene encoding HMGB1 flanked by loxP sites) were crossbred with UBC-CreERT2 mice (ubiquitin C promoter-regulated expression of tamoxifen-inducible CreERT2 recombinase). UBC-CreERT2 positive animals resulting from these breedings as well as UBC-Cre negative *Hmgb1*$^{fl/fl}$ mice (control group) were treated for 5 days with tamoxifen intraperitonal (i.p.). This activated the CreERT2 recombinase, if present, and lead to the excision of the *Hmgb1* gene, thereby generating Δ*Hmgb1*^{UBC} mice with a whole-body HMGB1 knockout. Deletion efficiency 7-8 weeks after tamoxifen induction was confirmed by immunoblot. Spleen, liver and lung were homogenized, lysed and HMGB1 expression was detected. As shown in Figure 22 A, the expression of HMGB1 in the spleen of Δ*Hmgb1*^{UBC} mice was strongly reduced. However, some remaining HMGB1 was detectable. In contrast, in the liver (Figure 22 B) and lung (Figure 22 C) of Δ*Hmgb1*^{UBC} mice a complete knockout was achieved, since no HMGB1 was detectable anymore.

Finally, 7-8 weeks post-induction, mice were infected with MCMV WT, sacrificed either 3 or 7 days post-infection, and organs were collected for subsequent analysis. Since acute early MCMV replication mainly takes place in spleen and liver after i.p. application, viral loads in these organs 3 dpi were titrated by plaque assay. As seen in Figure 22 D and E, MCMV titers were reduced in both the spleen and liver of Δ*Hmgb1*^{UBC} mice compared to *Hmgb1*$^{fl/fl}$ control mice 3 dpi. In the liver, while in two Δ*Hmgb1*^{UBC} mice viral titers were comparable to *Hmgb1*$^{fl/fl}$ control mice, in three Δ*Hmgb1*^{UBC} mice, MCMV was not detectable (Figure 22 E). Later during infection, MCMV usually spreads from the peritoneum towards other organs such as the lung. Interestingly, viral loads 7 dpi seemed higher in lungs of Δ*Hmgb1*^{UBC} mice compared to *Hmgb1*$^{fl/fl}$ control mice (Figure 22 F).

In conclusion, HMGB1 knockout animals showed reduced titers early in MCMV infection. In the liver, titers showed a stronger reduction than in the spleen. This effect could be the results of a less efficient HMGB1 knockout in the spleen of Δ*Hmgb1*^{UBC} mice. Later in infection (7 dpi), the phenotype changes and HMGB1

knockout seemed to be beneficial for MCMV. Higher titers in the lung 7 dpi could indicate that HMGB1 reduces MCMV spread and/or replication in the lung.

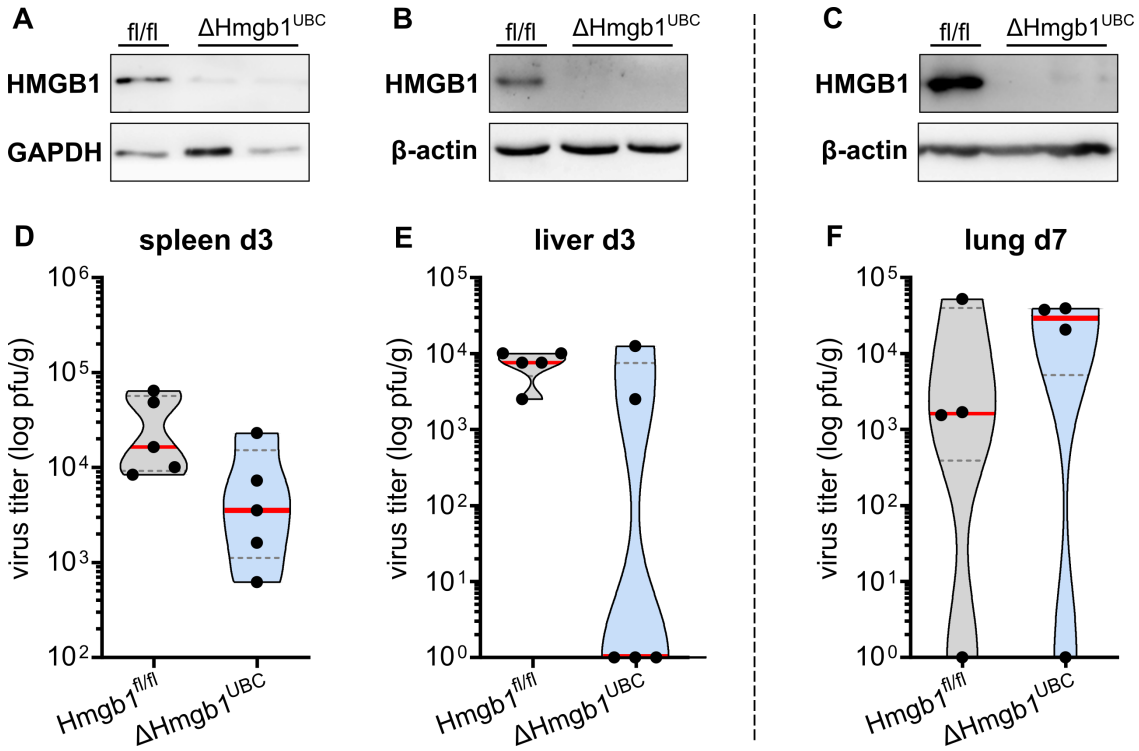

Figure 22: HMGB1 supports early MCMV replication *in vivo*.
Eight weeks-old Hmgb1$^{fl/fl}$ and ΔHmgb1^{UBC} mice were i.p. injected with 75 mg/kg tamoxifen for 5 days. 7-8 weeks later mice were infected with 2x10^5 pfu MCMV WT (i.p.). Mice were sacrificed on day 3 or 7 post-infection (as indicated) and organs were collected. Viral loads in spleen **(A)**, liver **(B)** or lung **(C)** were analyzed by plaque assay and are shown as violin plot showing each animal as individual dot, the median as red line, and the 25th and 75th percentiles are indicates as dashed lines. HMGB1 expression was detected by immunoblot for spleen **(D)**, liver **(E)** and lung **(F)**. GAPDH or β-actin were used as loading controls.

5.12 The effect of anti-HMGB1 neutralizing antibodies on MCMV replication *in vivo*

As previously mentioned, release of HMGB1 can affect the behavior of responding cells and with this affect viral spread and survival. Even though *in vitro* experiments showed only an effect of extracellular HMGB1 on MCMV-infected macrophages, the impact of extracellular HMGB1 *in vivo* could be amplified due to more cell types responding to it. In addition, the previous *in vitro* experiments showed that HMGB1 can be actively but also passively secreted by different cell types upon MCMV infection. To verify that a similar mechanism exists also at the level of the whole organism, WT mice were infected i.p. with MCMV WT and serum levels of HMGB1 were measured 3 dpi by ELISA. As shown if Figure 23 A, the HMGB1 serum level is

increased in infected mice compared to uninfected control animals, raising the question of the role of the extracellular HMGB1 on MCMV replication *in vivo*.

Neutralizing monoclonal antibodies (mAb) against HMGB1 already served as therapeutic agent to limit inflammation and lower disease severity upon sterile tissue damage or infection. Moreover, they are a powerful tool to separate the effects of intracellular and extracellular HMGB1, as mAb only target the extracellular form of the protein that can be release after MCMV infection. Thus, MCMV-infected WT mice were randomly assigned into two groups, one group treated with an IgG control antibody (ctrlAb), whereas the second group was treated with the anti-HMGB1 mAb. The antibodies were injected i.p. every 24 h throughout the infection starting 1 hpi. At day three post-infection animals were sacrificed and organs were collected. No differences in the viral titers could be observed between the mice treated with the control IgG or the anti-HMGB1 mAb in spleen (Figure 23 B), liver (Figure 23 C), or lung (Figure 23 D).

These data suggest that antibody-mediated neutralization of extracellular HMGB1 has no effect on early MCMV replication *in vivo* or that the level of extracellular HMGB1 was too low at the time point tested to have a detectable effect on MCMV replication *in vivo.*

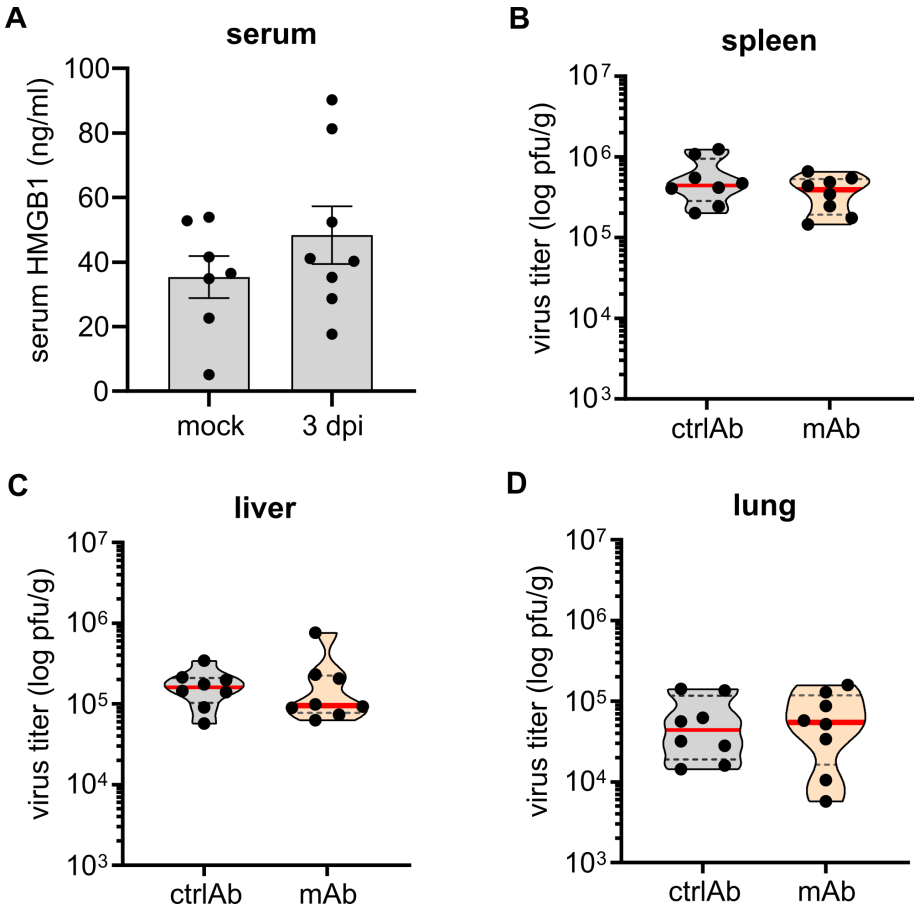

Figure 23: Anti-HMGB1 neutralizing antibodies do not affect *in vivo* MCMV infection.
Eight weeks-old wild-type C57BL/6J mice were infected with MCMV WT (10^6 pfu, i.p.). Mice were randomly assigned to two groups. Each group was injected with antibodies every 24 h. The group of nAb animals were treated with anti-HMGB1 monoclonal antibodies, while the group ctrlAb was treated with a control IgG. Mice were sacrificed 3 d post-infection, organs were collected and viral loads in spleen **(A)**, liver **(B)**, and lung **(C)** were determined by plaque assay. Viral titers are shown as violin plot showing each animal as individual dot, the median as red line, and the 25th and 75th percentiles are indicates as dashed lines **D)** Eight weeks-old wild-type C57BL/6J mice were either infected with MCMV WT (3 dpi) or injected with PBS (mock). 3 dpi animals were sacrificed, serum was collected, and HMGB1 levels were detected by ELISA.

5.13 The importance of myeloid cell-derived HMGB1 in MCMV infection *in vivo*

MCMV replication in HMGB1 whole-body knockout mice was negatively affected during early infection and positively affected to later time points (Figure 22), suggesting a dual role of HGMB1 *in vivo*. Such dual role was also observed in iBMDMs *in vitro*, which raised the question of the interaction of HMGB1 with these specific cells *in vivo* upon MCMV infection. To study this aspect, Δ*Hmgb1*^{LysM} mice were used. These mice lack HMGB1 only in cells of the myeloid lineage (e.g. macrophages, dendritic cells) as shown in Figure 24 A, where HMGB1 expression was absent in BMDMs isolated from Δ*Hmgb1*^{LysM} mice, while HMGB1 expression in the spleen composed of different cell types was not affected (Figure 24 B). As

performed previously, Δ*Hmgb1*^{LysM} mice and *Hmgb1*$^{fl/fl}$ control mice were infected with MCMV WT and organs were collected either 3 or 7 d later. Similar to Δ*Hmgb1*^{UBC} mice, MCMV titers in the spleen 3 dpi were reduced in Δ*Hmgb1*^{LysM} mice compared to *Hmgb1*$^{fl/fl}$ control mice (Figure 24 C). In contrast, viral loads in the liver 3 dpi appeared to be slightly higher in Δ*Hmgb1*^{LysM} mice (Figure 24 D). Additionally, MCMV titers in the lung 7 dpi were not affected by myeloid HMGB1 knockout (Figure 24 E).

In summary, these results indicate that HMGB1 derived from myeloid cell could have different functions during MCMV replication *in vivo*. On the one hand, myeloid-HMGB1 seemed to support MCMV replication in the spleen, which is rich in myeloid cells. This proviral effect of HMGB1 in macrophages was also observed *in vitro*, however, strictly with intracellular HMGB1. On the other hand, in organs where mainly non-myeloid cells are responsible for the release of new MCMV particles (i.e. liver), the effect of myeloid-derived HMGB1 seemed to be masked.

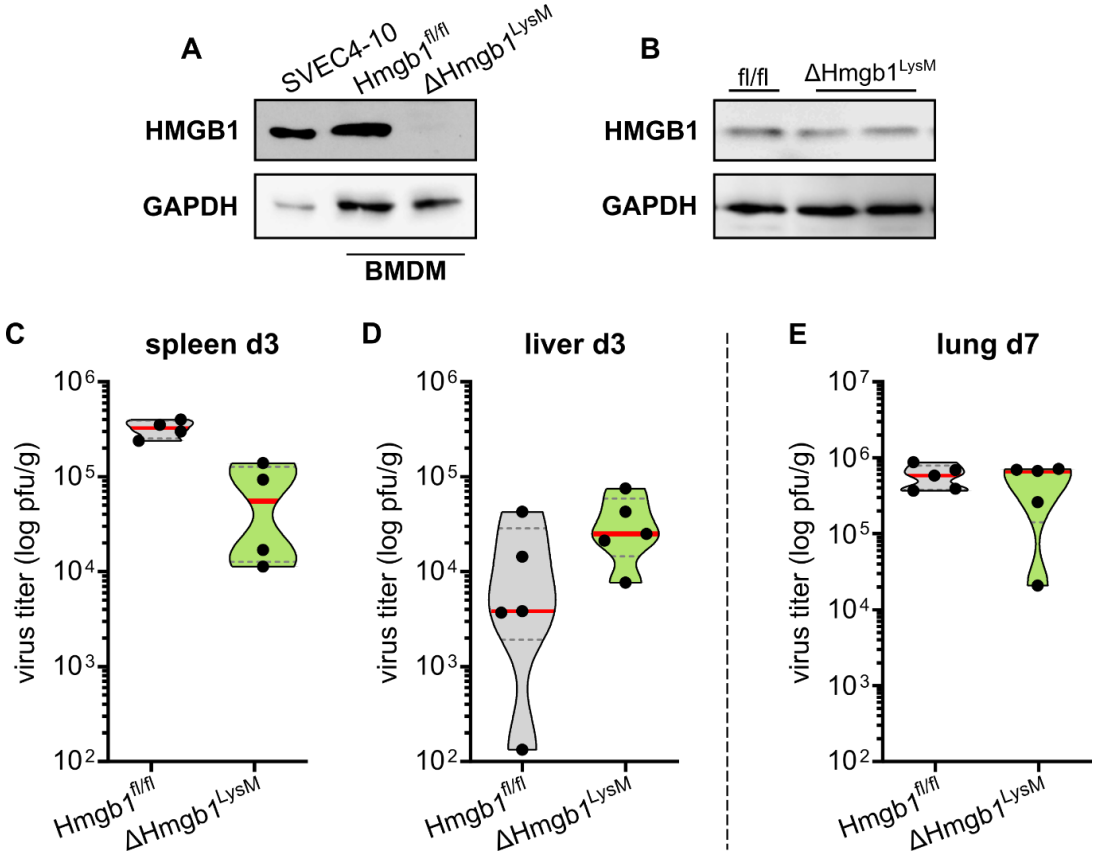

Figure 24: Myeloid cell-derived HMGB1 supports early MCMV replication in the spleen but not in other organs.
A) Bone marrow-derived macrophages (BMDM) were isolated from Hmgb1$^{fl/fl}$ and ΔHmgb1^{LysM} mice. BMDMs were lysed and HMGB1 expression was detected by immunoblot. SVEC4-10 lysate was used as positive control and GAPDH was used as loading control. **B)** Spleen isolated from Hmgb1$^{fl/fl}$ and ΔHmgb1^{LysM} mice was lysed and HMGB1 expression was detected by immunoblot. GAPDH was stained as loading control. **C-E)** Eight weeks-old Hmgb1$^{fl/fl}$ and ΔHmgb1^{LysM} mice were infected with 2x10^5 pfu of MCMV WT (i.p.). Mice were sacrificed on day 3

or 7 post-infection (as indicated) and organs were collected. Viral loads in spleen **(B)**, liver **(C)** or lung **(D)** were titrated by plaque assay. Viral titers are shown as violin plot showing each animal as individual dot, the median as red line, and the 25th and 75th percentiles are indicates as dashed lines.

6. Discussion

6.1 HMGB1 expression in MCMV infection

Previous studies investigating the role of HMGB1 during different virus infections, demonstrated that HMGB1 is highly versatile and can have proviral as well as antiviral functions, thereby promoting or inhibiting viral replication and spread. However, most of the studies describing these antagonistic functions of HMGB1 were performed during RNA virus infection, but little is known if and how HMGB1 affects the replication of herpesviruses, like CMV. Therefore, this study investigated whether and how HMGB1 is involved in the regulation of CMV replication, using both *in vitro* and *in vivo* approaches. As CMV is highly species-specific, mouse CMV was used as a model to allow *in vivo* work.

To first evaluate the function of HMGB1 *in vitro*, its basal expression and regulation upon MCMV infection was investigated in different cell types, all showing a relatively high expression of the protein on a basal level, with some discrepancies between the mRNA and protein level (Figure 10). These differences in the basal levels of HMGB1 could be the result of a different half-life or stability of the protein depending on the cell type. Since HMGB1 is known to be widely expressed in nucleated mammalian cells [87], a broad range of HMGB1-expressing cell lines was expected. Following MCMV infection, HMGB1 upregulation was observed in all cell types except macrophages at later time points (Figure 11). Independent studies have shown that certain herpesviruses, such as pseudorabies virus and EBV, also upregulate HMGB1 expression, while others, including KSHV and HSV, do not [191, 192, 194, 196]. Notably, the regulation of HMGB1 expression appears to be independent of the viral subfamily, indicating a more complex, virus-specific interaction. Similarly, increased levels of HMGB1 mRNA has been reported in cells infected with bovine herpesvirus 1 (BoHV-1), where HMGB1 was identified as a proviral factor facilitating viral gene transcription [207]. Given these parallels, it is possible that MCMV induces HMGB1 expression to exploit its potential proviral effects, similar to what has been observed in BoHV-1 infections.

6.2 The impact of HMGB1 overexpression on MCMV replication

In order to emphasize potential proviral functions of HMGB1, an inducible system overexpressing HMGB1 was established in different cell types. Whereas the generation of transduced cells was successful for all cell types, with a proper nuclear localization of HMGB1 upon induction, endothelial cells showed low expression of the transduced EGFP-HMGB1 (Figure 12). Despite an antibiotic selection, which excludes the possibility of low transduction efficiency, SVEC4-10 endothelial cells only expressed low amounts of EGFP-HMGB1, suggesting that high amounts of the protein might be detrimental for this specific cell type. A single clone selection for cells showing strong EGFP signals could help to identify the reason for the low expression of HMGB1 in those cells (i.e. spontaneous antibiotic resistance of non-transduced cells, low sensitivity to doxycycline induction, toxicity of high HMGB1 expression).

Nevertheless, these cells were used for subsequent experiments, taking into account that the phenotype that could be observed needs to be analyzed cautiously, and indeed, no effect on viral growth could be observed in those cells (Figure 13 B), confirming that the expression of HMGB1 was most likely too low to affect viral growth. However, a similar phenotype (i.e. no changes in the viral replication kinetics upon HMGB1 overexpression) was observed in fibroblasts and hepatocytes (Figure 13 A, C) and neither a proviral nor an antiviral effect of HMGB1 could be detected under these conditions. This indicates either that HMGB1 does not affect viral replication, like it was shown in fibroblasts infected with the Newcastle disease virus [186]. However, MCMV is well adapted to its host, which may allow it to achieve optimal replication with endogenous levels of HMGB1. Assuming this, only a small amount of the protein is sufficient to fully support viral replication and any increase of HMGB1 expression would not additionally benefit the virus.

Still, an increase of endogenous HMBG1 could be observed after MCMV infection, supporting the idea that more HMGB1 is beneficial for the virus (Figure 11). It has to be taken into account that the experiment performed in Figure 11 and Figure 13 did not use the same conditions. While replication kinetics were performed at low MOI, the levels of endogenous HMGB1 during MCMV infection were determined at high MOI. Consequently, the levels of HMGB1 could be differently affected, especially the low MOI infection reflects only the effect on a small proportion of infected cells, while

the uninfected neighboring cells could react differently and mask the effect of HMGB1 overexpression on MCMV replication.

Surprisingly, MCMV growth was strongly limited in macrophages overexpressing HMGB1 (Figure 13 D). Contrary to the initial hypothesis that HMGB1 is a proviral factor for MCMV, this result clearly showed that high concentrations of HMGB1 are detrimental for MCMV replication in macrophages. It could be possible that in this cell type, in which the endogenous level of HMGB1 was the lowest (Figure 10), the overexpression has a stronger effect, compared to cells with a high endogenous level of HMGB1. This could explain why HMGB1-mediated alterations of the MCMV replication were only detectable in macrophages. It must also be considered that macrophages, in contrast to the other cell types, are specialized immune cells whose gene expression and cellular machineries are optimized to limit the spread of pathogens. This may be another reason why MCMV-infected macrophages respond differently to HMGB1 overexpression than other cell types.

Interestingly, MCMV grew identically in wild-type and HMGB1-overexpressing macrophages within the first 5 d of infection. It was only at later times that MCMV titers decreased rapidly in HMGB1-overexpressing macrophages (Figure 13 D). This timing could correlate with the period when cell death starts to occur, which leads to HMGB1 release into the extracellular space, where it is known to act as cytokine and chemokine. Extracellular HMGB1 is therefore described to act antiviral and often limits virus replication and spread [176, 195]. One could hypothesize that this antiviral mechanism of extracellular HMGB1 exist in macrophages, and that overexpression of HMGB1 leads to more extracellular HGMB1 when infected cells die, resulting in an inhibition of viral growth, which explains the growth defect of MCMV in Figure 13 D.

6.3 The importance of extracellular HMGB1 in MCMV replication

To assess the possible antiviral role of extracellular HMGB1, recombinant HMGB1 was added in the supernatant of MCMV-infected macrophages (Figure 15), but this could not reproduce the data obtained with HMGB1-overexpressing macrophages (i.e. less viral replication, Figure 13 D), suggesting that extracellular HMGB1 does not mediate antiviral effects in macrophages. However, the recombinant HMGB1 used in the experiment was fully reduced, as described for HMGB1 passively released from cells, which might not reflect the full functional potential of cell-derived HMGB1 as its

diversity of PTMs, such as acetylation, is not represented [125]. In addition, MCMV-induced pyroptosis in macrophages activates caspase-1, which is able to cleave intracellular HMGB1, but not extracellular recombinant HMGB1, into a pro-inflammatory peptide [160]. As PTMs and other modifications can significantly alter the function of HMGB1, this can explain the absence of a phenotype with the recombinant HMGB1. Moreover, the dosage of the protein might have been too low compared to endogenous levels to have a significant effect, although recommended concentrations of recombinant HMGB1 were used. By measuring the concentration of HMGB1 released by MCMV-infected cells by an enzyme-linked immunosorbent assay (ELISA), the dosage of recombinant HMGB1 could be optimized.

Nevertheless, an antiviral role of extracellular HMGB1 cannot be excluded, as the protein is actively secreted by macrophages and hepatocytes, whereas it is only passively released by the other cell types after cell death (Figure 14). This actively secreted HMGB1 is known to exhibit strong cytokine activity due to its modifications [125], which could result in the growth defect of MCMV in the HMGB1-overexpressing macrophages. However, hepatocytes also seemed to actively release HMGB1, although HMGB1 overexpression did not result in a phenotype, unlike in macrophages (Figure 13). Possible explanations for this discrepancy could be that HMGB1 released from hepatocytes carries different PTMs, thus modifying the function of extracellular HMGB1, or hepatocytes could respond differently to extracellular HGMB1 based on responding receptor.

Similar to hepatocytes, HMGB1 overexpression did not result in alterations of MCMV replication in fibroblasts (Figure 13 A), which can be explained by the absence of active HMGB1 release and varying sensitivities to different cell death pathways in fibroblast compared to hepatocytes and macrophages (Figure 14). Active release of HMGB1 requires dissociation from genomic DNA and export into the cytoplasm, which is regulated by different PTMs such as acetylation, phosphorylation, or methylation [125, 208]. In addition, the mode of cell death significantly influences PTMs and the redox state of HMGB1 and, consequently, its function. For example, apoptosis typically releases oxidized HMGB1, which promotes immune tolerance, whereas necroptosis and pyroptosis release reduced HMGB1, which has higher affinities for the RAGE receptor and certain chemokine receptors [125] triggering individual responses such as NF-κB activation and subsequent gene expression resulting in cell survival and regulation of inflammatory responses [209, 210].

Interestingly, fibroblasts were described to actively secrete HMGB1 [211], however this could not be observed in MCMV WT-infected cells but only upon infection with the MCMV M45mutRHIM and MCMV M84stop mutant. As the major difference between these mutants and the WT is the type of PCD that is engaged, i.e. necroptosis or pyroptosis, it cannot be excluded that the active secretion that is observed is just an artifact due to the method of detection used. Indeed, the detection of cell death relied on the measurement of ATP, which only quantifies the number of living cells but does not directly detect the number of dead cells or cells that have already lost membrane integrity, leaking HMGB1 into the extracellular space due to pore formation like it is the case during necroptosis and pyroptosis [67]. Thus, distinguishing between active secretion and passive release of HMGB1 in this context is extremely challenging, and additional test, such as a lactate-dehydrogenase (LDH) release assay, could be performed to differentiate between active and passive secretion.

Despite the difficulties encountered to evaluate the mode of release of HGMB1, it seemed that only hepatocytes and macrophages are able to actively secrete HMGB1 before cell death occurred. However, this observation needs to be further confirmed and additional studies are needed to clarify whether and how the mode and kinetics of HMGB1 release by these cells as well as the PTMs of HMGB1 influence MCMV replication.

Moreover, although active release could be detected, no translocation of HMGB1 from the nucleus to the cytoplasm could be observed in MCMV-infected cells (Figure 20). HGMB1 translocation and secretion, however, could be a highly dynamic and rapid process, making it challenging to capture with conventional static imaging techniques. To address this, live-cell imaging could provide valuable insights into the real-time dynamics of HMGB1 during MCMV infection. In contrast, HMGB1 release has been observed to occur also in a cell death-dependent manner from MCMV-infected cells, where it can be released directly from the nucleus when the nuclear membrane breaks down. This mechanism would not require prior translocation to the cytoplasm, aligning with the observations made during MCMV infection.

6.4 The impact of intracellular HMGB1 on MCMV infection

In contrast to HMGB1 overexpression, which negatively affected the viral replication in macrophages (Figure 13 D), the downregulation of HMGB1 by shRNAs in these cells lead to a reversed phenotype, i.e. an enhanced growth of MCMV (Figure 17 D). These results strongly support the conclusion that HMGB1 exerts an antiviral effect on MCMV replication in macrophages.

Moreover, as sh1 and sh2 behave differently and as it seems that sh1 have a coherent phenotype with previous experiments, it is most likely that sh1 targets HMGB1 efficiently, while the knockdown with sh2 was probably insufficient to result in a phenotype, which is supported by the higher remaining HMGB1 expression in sh2 cells (Figure 16). However, it cannot be excluded that the phenotype observed in sh1 cells is the result of an off-target effect of this shRNA.

Surprisingly, in hepatocytes, a different phenotype was observed: sh1-mediated HMGB1-knockdown revealed a proviral effect, since already early MCMV replication was delayed in these cells (Figure 17 C). Moreover, the reduced viral gene expression observed in the different knockdown cell lines also point towards a proviral role of HMGB1 (Figure 18). This goes in line with studies showing that some gammaherpesviruses, such as KSHV, show reduced lytic viral replication in HMGB1-deficient cells [196, 201]. However, during MCMV infection the absence of HMGB1 seemed to have a dual effect: while it impairs MCMV replication in hepatocytes, it enhances it in macrophages. These opposing effects could be explained by taking into account that the knockdown reduces both, intra- and extracellular HMGB1.

Taking a closer look into the delayed viral gene expression observed in HMGB1-knockdown cells, it seems plausible that HMGB1 interacts with the MCMV genomes to promote viral gene expression, which is consistent with the fact that HMGB1 binds to cellular DNA and regulates replication and transcription processes [87] as well as with the fact that HMGB1 is known to stimulate viral gene expression during the infection with several gammaherpesviruses [196, 201]. As the phenotype observed in MCMV-infected cells is more pronounced at early expression time points, this could imply that HMGB1 is more critical for the initiation of transcription rather than for the entire transcription process. In addition, given that HMGB1 binds to DNA in a structure-specific rather than sequence-specific manner [87], it is likely that HMGB1 influences the expression of all viral genes similarly rather than binding to particular

promoters. Consistent with this, proteins of each stage of infection (i.e. immediate early, early, and late) are affected equally (Figure 18). However, as HMGB1-knockdown cells still express HMGB1 to some extent, which could be sufficient to support MCMV gene expression, a complete deletion of HMGB1 would be necessary to determine whether HMGB1 is an essential factor for MCMV gene expression.

In conclusion, these findings highlight the significant role of intracellular HMGB1 in the transcription of MCMV genes. Future studies further dissecting the mechanisms of HMGB1's interaction with the MCMV genome will be crucial for fully understanding this interaction.

6.5 The opposing functions of HMGB1 in MCMV-infected macrophages

As discussed previously, it is evident that HMGB1 influences the transcription of MCMV genes. This effect is particularly interesting in macrophages, where HMGB1 appears to restrict MCMV growth (Figure 13 D). In the absence of HMGB1, MCMV grows more efficiently (Figure 17 D), even though viral protein expression is reduced (Figure 18 D). These contradictory findings could be reconciled, if intracellular and extracellular HMGB1 functions are taken into account. Indeed, it can be hypothesized that early in infection, intracellular HMGB1 promotes MCMV replication, as indicated by reduced viral gene expression (Figure 18). Later on, infected cells release HMGB1 (Figure 14). The extracellular HMGB1 then limits MCMV replication in macrophages (Figure 13).

As the role of extracellular HMGB1 could not be confirmed by the addition of recombinant HMGB1, pyroptosis-deficient macrophages were used to confirm this hypothesis. Indeed, in ASC-deficient macrophages with HMGB1 knockdown, MCMV growth, as well as viral protein expression, was delayed compared to control cells (Figure 19), similar to what was observed in the other cell lines. This could be explained by the fact that HMGB1 triggers pyroptosis in macrophages by binding to RAGE. This interaction facilitates the endocytosis of HMGB1 and subsequently induces the formation of ASC specks, leading to inflammasome activation and pyroptotic cell death [212]. Thus, the inhibition of HMGB1-induced pyroptosis in these macrophages results in studying the function of the intracellular HMGB1 only, which appears similar in all cell lines testes, i.e. a proviral role of the protein. As

macrophages are particularly prone to undergo pyroptosis, the antiviral phenotype of HMGB1 was specifically observed in macrophages and no other cell line.

Nevertheless, it cannot be excluded that extracellular HMGB1 may exert antiviral effects through other mechanisms in different cellular contexts. While these results provide evidence that the antiviral activity of HMGB1 in macrophages is primarily mediated by extracellular HMGB1 activating cell death by pyroptosis, further research is needed to identify other potential antiviral mechanisms of extracellular HMGB1 and to understand its impact on MCMV infections across different cell types.

6.6 HMGB1 localization and recruitment to E1-positive nuclear compartments

As seen previously, HMGB1 enhances MCMV viral gene expression, most likely by a direct interaction with viral genomes due to its DNA-binding activity. Previous studies reported that HMGB1 often translocates from the nucleus to the cytoplasm upon RNA virus infection in order to regulate the viral replication that occurs in the cytoplasm for these viruses [177, 188]. However, MCMV, a large DNA virus, replicates and transcribes its genome within specialized viral replication compartments (RCs) located within the host cell nucleus. Consistent with observations made in HSV-infected cells [197, 198], HMGB1 remained nuclear during MCMV infection and partially relocalized into viral RCs identified by staining of the viral E1 protein, the major marker of RCs (Figure 20). This enrichment occurred already at early time points, as HMGB1 could be detected in the small spherical structures, as well as in large amorphous RCs, which occur later during infection. This aligns with previous findings that HMGB1 affects early as well as late gene expression (Figure 18). Furthermore, HMGB1 was enriched in specific E1-negative nuclear compartments both in non-infected and MCMV-infected cells. Nuclear staining (DAPI) suggested that these compartments could be nucleoli. However, this requires further validation through staining of nucleolin, for example.

It was recently shown that proteins encoded by HCMV UL112-113, also known as E1, play a crucial role in the formation of RCs and the recruitment of additional proteins through LLPS. Moreover, the IDR of E1 has been identified as a key feature facilitating this process [31]. In addition, HMGB1 was also described to contain an IDR and to undergo LLPS [104], which could explain the recruitment of HGMB1 to

the viral RCs in MCMV-infected cells. Preliminary experiments indicate that LLPS is a significant, though not sole, factor for the recruitment of HMGB1 into viral RCs, as MCMV E1 was sufficient to recruit HMGB1 without direct protein-protein interaction (Figure 21 A, B), however the exact mechanism as well as a defined domain in HMGB1 necessary for this recruitment need further investigations.

To gain first insights into the role of the IDR in HMGB1's recruitment, truncated mutants of HMGB1 lacking the entire IDR or part of it were used. The longest of the mutants (i.e. HMGB1$^{(1\text{-}185)}$), lacking only the C-terminal acidic tail but still containing parts of the IDR, showed co-localization with E1 dots (Figure 21 C), suggesting that the acidic tail is not critical for recruitment. However, the remaining amino acids of the IDR are probably sufficient for LLPS functionality. Interestingly, this mutant was enriched in nuclear compartments even when E1 was not transfected. This was not the case for the same mutant of human HMGB1, as shown by Mensah *et al.* [104], indicating that human and mouse HMGB1 might behave differently in the cellular context, although they share high sequence similarity (99 %) [89-91].

The most striking phenotype observed was with the use of the HMGB1$^{(1\text{-}162)}$ mutant, which localized in both, the nucleus and in the cytoplasm, but not in any specific compartments such as the nucleolus, possibly indicating disrupted LLPS (Figure 21 D). Yet, co-localization with E1 was still observed (Figure 21 D), raising the possibility that the IDR and LLPS may not be the sole drivers of HMGB1 recruitment to viral RCs.

An additional observation that was made with all the IDR-mutants of HMGB1 is the apparent reduced number and size of E1-positive structures formed after co-transfection of the two proteins (Figure 21 C-E). This could indicate the possibility that HMGB1 and E1 influence each other and that the functionality of both the HMGB1 and E1 IDR is necessary for RCs to be formed optimally. This contribution could eventually be evaluated in HMGB1-knockdown cell lines in order to see if a similar interconnection exists and smaller RCs are formed also during infection. Indeed, such mechanism could explain the reduction in MCMV transcription observed in HMGB1-knockdown cells; RCs form less or slower in absence of HMGB1 and MCMV transcription appears delayed.

These findings highlight the complexity of HMGB1 recruitment to viral RCs and suggest that while the IDR and LLPS are important, other factors may also play a

role. Repetition of experiments and additional studies are required to draw definitive conclusions about the mechanisms driving HMGB1 recruitment to RCs and the role of LLPS in this process.

6.7 Role of HMGB1 in MCMV infection *in vivo*

Despite the high species specificity of CMV, the use of the MCMV model allows to study the role of HMGB1 at the level of the whole organism, in order to support the data obtained *in vitro*. Most of the previous studies analyzing the role of HMGB1 in multiple *in vivo* scenarios reaching from sterile tissue damage to bacterial and viral infections used neutralizing antibodies to evaluate the pathogenic potential of HMGB1. Similarly, this was also tested in the present study, however, no differences in MCMV titers in the different organs tested 3 dpi were detected under treatment with anti-HMGB1 neutralizing antibodies (Figure 23 B-D). However, neutralizing antibodies only affect extracellular HMGB1, and as already seen *in vitro*, extracellular HMGB1 seemed to play only a role at late time points and only in specific cell types (i.e macrophages). Thus, 3 dpi is probably too early to observe a phenotype. In addition, cells that do not respond to extracellular HMGB1 could mask its effect. Another explanation for the lack of a phenotype is the low amount of HMGB1 detected in the serum 3 d after MCMV infection (Figure 23 A), as only extracellular HMGB1 can be targeted by the neutralizing antibodies. In comparison, cotton rats infected with influenza B show a significant increase in serum HMGB1 as early as 2 dpi, with levels rising even higher by 4 dpi [213]. However, influenza B replicates remarkably faster than MCMV, which could explain the earlier increase in serum HMGB1 levels in this case.

Nevertheless, it is likely that extracellular HMGB1 levels rise throughout the MCMV infection, potentiating its effect on different cell types, thereby affecting MCMV replication and dissemination. To investigate this further, determining serum HMGB1 levels at later time points and assessing the impact of anti-HMGB1 mAb at later stages of MCMV infection would be necessary.

After intraperitoneal infection, MCMV first infects peritoneal macrophages or directly enters the bloodstream to infect circulating monocytes [214]. The first organs to be productively infected with MCMV are the spleen and liver. Replication in these organs is crucial for MCMV virulence since it determines the course of the secondary

viremia and the dissemination to other organs like the lung [215-217]. Moreover, as shown in this study, myeloid cells, and more particularly macrophages, which are crucial for MCMV dissemination, display a different sensitivity to HMGB1 functions compared to other cells types.

As already discussed, extracellular HMBG1 probably does not occur at the onset of infection and therefore does not play an important role, so that only the proviral impact of intracellular HMGB1 affects MCMV replication at this time point. Already *in vitro*, reduced viral replication was observed in $ASC^{-/-}$ macrophages in the absence of HMGB1, which was reflected by the phenotype observed 3 dpi in the spleen of $\Delta Hmgb1^{LysM}$ mice (Figure 24 C), lacking HMGB1 in myeloid cells, indicating that also *in vivo* intracellular HMGB1 supports MCMV replication in macrophages.

However, the lower replication of MCMV observed at early time point in the spleen could not be detected in the liver of $\Delta Hmgb1^{LysM}$ mice (Figure 24 D), which can be explained by the different cellular composition of these organs. While macrophages are the main producers of viral progeny in the spleen, as the most abundant cell types (i.e. T- and B-cells) do not support MCMV lytic replication [218], this is not the case in other organs such as the liver and lung, as hepatocytes or epithelial cells are the main producers of MCMV particles, respectively.

Although this partially explains the absence of a phenotype in the lungs of $\Delta Hmgb1^{LysM}$ mice (Figure 24 E), additional factors need to be considered here as MCMV titers in the lung to a late time point (i.e. 7 dpi) reflect not only the replication efficiency of MCMV in this organ, but also the dissemination efficiency. As mentioned before, macrophages are important for MCMV dissemination *in vivo* and a severe growth defect of MCMV in macrophages could limit dissemination. However, as MCMV replication in HMGB1-knockdown $ASC^{-/-}$ macrophages *in vitro* showed more a delay than a reduction (Figure 19 C), it seems unlikely that a knockout of myeloid HMGB1 strongly affects MCMV dissemination *in vivo*.

While a cell type-specific knockout can help to increase the understanding of the involvement of individual cell types, it also carries the risk that other important information remain hidden. Indeed, myeloid cells seemed to have play a role early during infection, however, the $\Delta Hmgb1^{LysM}$ model only affect the expression of HMGB1 in myeloid cells, while they can still respond to HMGB1 released by other

cells, particularly hepatocytes. Therefore, the ΔHmgb1^{UBC} mouse model was used for the first time in a viral context to try to elucidate the function of HMGB1 against MCMV infection. Since embryonic HMGB1 knockout causes lethal hypoglycemia in newborn mice [219], HMGB1 knockout was only generated in adult mice using a tamoxifen-inducible system. However, the knockout was incomplete, as HMGB1 protein could still be detected in the different organs, especially the spleen (Figure 22 D-F), which makes the analysis difficult and could explain why the observed phenotype (i.e. less viral replication in ΔHmgb1^{UBC} mice in early infection) was stronger in the liver compared to the spleen (Figure 22 A-B). Nevertheless, this phenotype indicates a proviral phenotype in early *in vivo* MCMV infection, which is supported by previous *in vitro* data showing less MCMV replication in HMGB1-knockdown hepatocytes (Figure 17 C) and ASC$^{-/-}$ macrophages (Figure 19 C).

Later in infection (i.e. 7 dpi) ΔHmgb1^{UBC} animals showed slightly higher viral titers in the lung (Figure 22 C). As for the ΔHmgb1^{LysM} model, viral titers in the lung at this stage reflect not only the efficiency of replication in the lung but also the dissemination of the virus, making it more complicated to draw definite conclusions. Assuming that HMGB1 is released at higher quantities in late infection stages, HMGB1 could reduce the spread of MCMV to the lungs, as extracellular HMGB1 induces pyroptosis in macrophages, which are important for viral dissemination and spread. Its absence in knockout mice would allow more viral particles to reach and replicate in the lung. Given that extracellular HMGB1 is known to inhibit viral spread in the context of HSV infections, it seems plausible to conclude that HMGB1, released during infection, limits MCMV spread to the lung.

6.8 Summary

This study investigated the role of HMGB1 (High Mobility Group Box 1) in cytomegalovirus infection using the murine MCMV as a model virus. It revealed the complex involvement of HMGB1 in viral transcription and replication. HMGB1 is a highly versatile protein with both, proviral and antiviral functions, depending on the context of the viral infection.

This study demonstrated that HMGB1 was expressed and similarly regulated in different MCMV-infected cell types, yet viral growth was affected by HMGB1 in a cell type-dependent manner. In all cell types, HMGB1 supported MCMV transcription as a proviral factor, though the exact mechanism remains to be elucidated. The cell type-dependent differences in viral growth despite the proviral role of intracellular HMGB1 could potentially be explained by varying endogenous expression levels or differential sensitivities to, and effects of, extracellular HMGB1.

The functions of extracellular HMGB1 are influenced by numerous factors, including the kinetics and mode (active or passive) of its release, posttranslational modifications, the availability of binding partners and receptors, and counteractions by MCMV. Although the area of extracellular HMGB1 is highly complex, this study demonstrated that extracellular HMGB1 exerts antiviral functions, such as inducing cell death in macrophages, which are primary MCMV target cells.

Furthermore, in vivo data revealed that HMGB1 had beneficial effects during early MCMV infection, but this was not observed in later stages, likely due to HMGB1 release limiting viral replication and/or dissemination. Despite many unanswered questions, this study provides the first evidence that HMGB1 is a significant host factor for cytomegalovirus.

7. Materials

7.1 Cells

Name	Description	Reference
10.1	Spontaneously immortalized murine embryonic fibroblasts isolated from BALB/c mice	[220]
iBMDM	immortalized murine bone marrow-derived macrophage	NIAID NIH (NR9456)
iBMDM scr	iBMDM stably expressing scramble shRNA	This study
iBMDM sh1/2	iBMDM stably expressing shRNA1 or shRNA2 targeting HMGB1	This study
iBMDM EGFP-HMGB1	iBMDM expressing HMGB1 N-terminally tagged with EGFP upon doxycycline induction	This study
iBMDM HGLuc	iBMDM stably expressing HMGB1 coupled with Gaussia Luciferase	This study
ASC $^{-/-}$ iBMDM	ASC knockout in iBMDMs generated using CRISPR/Cas9	[73]
ASC $^{-/-}$ iBMDM scr	ASC knockout iBMDMs stably expressing scramble shRNA	This study
ASC $^{-/-}$ iBMDM sh1/2	ASC knockout iBMDMs stably expressing shRNA1 or shRNA2 targeting HMGB1	This study
HEK-293T	Human embryonic kidney epithelial cells transformed with large T antigen	ATCC (CL-11268)
Hepa1-6	Murine hepatocytes	[221]
Hepa1-6 scr	Hepa1-6 stably expressing scramble shRNA	This study
Hepa1-6 sh1/2	Hepa1-6 stably expressing shRNA1 or shRNA2 targeting HMGB1	This study
Hepa1-6 EGFP-HMGB1	Hepa1-6 expressing HMGB1 N-	This study

	terminally tagged with EGFP upon doxycycline induction	
Hepa1-6 HGLuc	Hepa1-6 stably expressing HMGB1 coupled with Gaussia Luciferase	This study
M2-10B4	Murine bone marrow stromal cells	ATCC (CRL-1972)
NIH-3T3	Murine embryonic spontaneously immortalized fibroblasts, isolated from NIH/Swiss mice	ATCC (CRL-1658)
NIH-3T3 scr	NIH-3T3 stably expressing scramble shRNA	This study
NIH-3T3 sh1/2	NIH-3T3 stably expressing shRNA1 or shRNA2 targeting HMGB1	This study
NIH-3T3 EGFP-HMGB1	NIH-3T3 expressing HMGB1 N-terminally tagged with EGFP upon doxycycline induction	This study
NIH-3T3 HGLuc	NIH-3T3 stably expressing HMGB1 coupled with Gaussia Luciferase	This study
SVEC4-10	Murine endothelial cells immortalized by SV40 large T antigen	ATCC (CRL-2181)
SVEC4-10 scr	SVEC4-10 stably expressing scramble shRNA	This study
SVEC4-10 sh1/2	SVEC4-10 stably expressing shRNA1 or shRNA2 targeting HMGB1	This study
SVEC4-10 EGFP-HMGB1	SVEC4-10 expressing HMGB1 N-terminally tagged with EGFP upon doxycycline induction	This study
SVEC4-10 HGLuc	SVEC4-10 stably expressing HMGB1 coupled with Gaussia Luciferase	This study

7.2 Viruses

Name	Description	Reference
MCMV WT	MCMV Smith strain pSM3fr-MCK-2fl with deletion of m157	[73]
MCMV M45mutRHIM	MCMV WT with reinserted M45 full length ORF including an C-terminal HA tag and a mutation in the RHIM domain	[222]
MCMV M84stop	MCMV WT with introduction of a C-to-G point mutation at the 183rd nucleotide of the M84 ORF leading to a stop codon	[73]
MCMV m38.5stop	MCMV WT with double point mutation in the initial ATG of m38.5 leading to a stop codon, lacking m157	This study

7.3 Plasmids

Name	Description	Reference
pEPkan-S	Template plasmid for en passant mutagenesis, contains I-Sce-aphA1 cassette, KanR	[223]
pLeGo-iC2 puro	Lentiviral expression vector for transduction of eukaryotic cells, mCherry, AmpR, PuroR	Addgene #27345
pLIX-puro	Lentiviral expression vector, Doxycycline-inducible promoter, PuroR, AmpR,	Addgene #41395
pLKO.1-puro-scr	Lentiviral expression vector encoding non-targeting scramble shRNA, PuroR, AmpR	Addgene #109012
pMDG.2	Lentiviral second-generation packaging plasmid, AmpR	[224]
pCMVR8.91	Lentiviral second-generation packaging plasmid, AmpR	[224]
pcDNA3	Expression vector, AmpR, NeoR	Life

		Technologies
pEGFP C3	EGFP expression plasmid, KanR	Clontech Laboratories
pcDNA-M112/113	Expression vector encoding M112/113 (E1) of MCMV, AmpR	[225]
p3xFlag-mTLR4	Expression vector encoding murine TLR4 tagged with triple Flag tag	Addgene #27148

7.4 Plasmids generated for this work

Name	Description	Cloning approach
pLKO.1-puro-shRNA1/2	Lentiviral expression vector encoding shRNA 1 or 2 targeting HMGB1, PuroR, AmpR	shRNA scr in pLKO.1-puro-scr was replaced with shRNA 1 or 2 using AgeI and EcoRI
pLKO.1-blasti-scr	Lentiviral expression vector encoding non-targeting scramble shRNA, BlastR, AmpR	PuroR of pLKO.1-puro-scr was replaced with BlastR using BamHI and Acc65I
pLKO.1-blasti-shRNA1/2	Lentiviral expression vector encoding shRNA 1 or 2 targeting HMGB1, BlastR, AmpR	PuroR of pLKO.1-puro-shRNA1/2 was replaced with BlastR using BamHI and Acc65I
pEGFP-HMGB1	Expression plasmid encoding EGFP-HMGB1 (N-terminally tagged), KanR	HMGB1 generated by PCR was introduced into pEGFP C3 using HindIII and BamHI
pEGFP-HMGB1$^{(1-134)}$	Expression plasmid encoding EGFP-HMGB1 mutant lacking the IDR (aa135-215) but with restored NLS sequence (aa179-185), KanR	HMGB1 mutant generated by PCR was introduced into pEGFP C3 using HindIII and BamHI
pEGFP-HMGB1$^{(1-185)}$	Expression plasmid encoding EGFP-HMGB1 mutant	HMGB1 mutant generated by PCR was introduced

	lacking the aa186-215, KanR	into pEGFP C3 using HindIII and BamHI
pEGFP-HMGB1$^{(1-162)}$	Expression plasmid encoding EGFP-HMGB1 mutant lacking the aa163-215, KanR	HMGB1 mutant generated by PCR was introduced into pEGFP C3 using HindIII and BamHI
pLIX-puro-EGFP-HMGB1	Lentiviral expression vector encoding EGFP-HMGB1 (N-terminally tagged), Doxycycline-inducible, PuroR, AmpR	EGFP-HMGB1 was introduced into pLIX-puro using EcoRI and SalI
pLeGo-iC2-HGLuc	Lentiviral expression vector encoding HMGB1 coupled with Gaussia luciferase (C-terminally), mCherry, PuroR, AmpR	HMGB1-GLuc was introduced into pLeGo-iC2 puro using EcoRI and NotI

7.5 Bacteria

Name	Description	Reference
E. coli DH10B	*F- mcrA Δ(mrr-hsdRMS-mcrBC) Φ80dlacZΔM15 ΔlacX74 endA1 recA1 deoR Δ(ara,leu)7697 araD139 galU GalK nupG rpsL λ-* Growth at 37°C	Life Technologies
E. coli GS1783 Smith Δm157	DH10B I *cI857Δ(cro-bioA)<>araC-PBADI-sceI* Including BAC encoding for MCMV Smith strain pSM3fr-MCK-2fl with deletion of m157 Growth at 30°C	[73]

7.6 Primers

Name	Sequence	Application
LysM Cre_KI	CCCAGAAATGCCAGATTACG	Genotyping of LysM-Cre mice
LysM Cre_Com	CTTGGGCTGCCAGAATTTCTC	
LysM Cre_WT	TTACAGTCGGCCAGGCTGAC	
UBC cre_F	GACGTCACCCGTTCTGTTG	Genotyping of UBC-Cre mice
UBC cre_R	AGGCAAATTTTGGTGTACGG	
HMGB1_floxed_F	AAAGTTTGATGCGAACACG	Genotyping HMGB1-floxed mice
HMGB1_floxed_R	TGATCTCAAGAGTAGGCACAGG	
mHMGB1_qPCR_F	GCTGACAAGGCTCGTTATGAA	qPCR of murine HMGB1
mHMGB1_qPCR_R	CCTTTGATTTTGGGGCGGTA	
mActin_qPCR_F	AGAGGGAAATCGTGCGTGAC	qPCR of murine β-Actin
mActin_qPCR_R	CAATAGTGATGACCTGGCCGT	
HindIII-HMGB1	TATAAAGCTTATGGGCAAAGGAGATCCTAAA	Cloning of HMGB1 and its mutants into pEGFP C3
HMGB1stop-BamHI	TTAAGGATCCTTATTCATCATCATCATCTTCTTC	
HMGB1$^{(1-134)}$-NLS-BamHI	TTAAGGATCCTTACTTCTTTTTCTTGCTCTTTTCGTTCCACATCTCTCCTAGTTTC	
HMGB1$^{(1-185)}$-BamHI	TTAAGGATCCTTACTTCTTTTTCTTGCTCTTTTCAG	
HMGB1$^{(1-162)}$-BamHI	TTAAGGATCCTTAGTAGGCAGCAATATCCTTCTCATAC	
EcoRI-EGFP	TATAGAATTCATGGTGAGCAAGGGCGAGGAG	Cloning EGFP-HMGB1 into pLIX-puro
HMGB1-SalI	TTAAGTCGACTTATTCATCATCATCATCTTCTTCTT	
BamHI-blastR	ATATAGGATCCATGGCCAAGCCTTTGTCTCAAG	Cloning BlastR into pLKO.1-scr and shRNA 1 and 2
blastR- Acc65I	ATTAAGGTACCTTAGCCCTCCCACACATAACCAGAG	

EcoRI-HMGB1	TATAGAATTCATGGGCAAAGGAGATCCTAAAAA	Cloning HMGB1-GLuc into pcDNA3 and pLeGo-iC2
GLuc-NotI	TTTAAGCGGCCGCCTACTTGTCGTCATCGTCTTTG	
mHmgb1_sh1_F	CCGGTGACAAGGCTCGTTATGAAAGCTCGAGCTTTCATAACGAGCCTTGTCATTTTTG	Cloning of shRNA1 targeting HMGB1 into pLKO.1-puro-scr
mHmgb1_sh1_R	AATTCAAAAATGACAAGGCTCGTTATGAAAGCTCGAGCTTTCATAACGAGCCTTGTCA	
mHmgb1_sh2_F	CCGGATGCAGCTTATACGAAGATAACTCGAGTTATCTTCGTATAAGCTGCATTTTTTG	Cloning of shRNA2 targeting HMGB1 into pLKO.1-puro-scr
mHmgb1_sh2_R	AATTCAAAAAATGCAGCTTATACGAAGATAACTCGAGTTATCTTCGTATAAGCTGCAT	
MCMVm38.5_ATG stop_F	TTCGCTTACAAACCCAAAGAAGGGTCGGCGCACACTCTCCTACGCTGTCCCCTCCACAACTATAGGGATAACAGGGTAATCGATTT	Introducing early stop codon into m38.5 of MCMV
MCMVm38.5_ATG stop_R	GCGGACGGTGCCGCGGGTTGTAGTTGTGGAGGGGACAGCGTAGGAGAGTGTGCGCCGACCCTGCCAGTGTTACAACCAATTAACC	
MCMV_SM3fr (wt)_52164_F	AAGACCGACGTAGACCGCTGAAC	Sequencing of mutated region in MCMV m38.5stop
MCMV_SM3fr (wt)_52531_R	GTCGATGATGGCTGCTACGAGAA	

7.7 Antibodies

7.7.1 Primary antibodies

Antigen	Clone	Species	Application (Dilution)		Source
HMGB1	ab18256	Rabbit	Western blot	1:500	Abcam
MCMV IE1	Croma 101	Mouse	Western blot	1:1000	Stipan Jonjic (University of Rijeka, Rijeka, Croatia)
MCMV E1	Croma103	Mouse	Western blot Immunofluorescence	1:1000 1:300	Stipan Jonjic (University of Rijeka, Rijeka, Croatia)
MCMV M55 (gB)	M55.01	Mouse	Western blot	1:1000	Capri Rijeka
β-actin	AC-74	Mouse	Western blot	1:3000	Sigma
GAPDH	14C10	Rabbit	Western blot	1:1000	Cell signaling
GFP	7.1/13.1	Mouse	Western blot	1:1000	Sigma
Flag	M2	Mouse	Western blot	1:1000	Sigma

7.7.2 Secondary antibodies

Antigen	Conjugate	Species	Application	Dilution	Source
Mouse Ig	HRP	Goat	Western blot	1:5000	Dako Cytomation
Rabbit Ig	HRP	Swine	Western blot	1:5000	Dako Cytomation
Mouse Ig	Alexa 555	Goat	Immunofluorescence	1:1000	Invitrogen

7.8 Chemicals and reagents

7.8.1 Antibiotics

Name	Application	Concentration	Source

Ampicillin	Selection of transformed bacteria	100 µg/ml	Roth
Kanamycin	Selection of transformed bacteria	50 µg/ml	Roth
Chloramphenicol	Selection of transformed bacteria	15 µg/ml	Roth
Penicillin	Cell culture supplement	100 µg/ml	PAA
Streptomycin	Cell culture supplement	100 µg/ml	PAA
Puromycin	Selection of transduced cells	1.5 – 5 µg/ml	Sigma-Aldrich
Blasticidin	Selection of transduced cells	0.5 µg/ml	Invivogen
Doxycycline	Induction of target gene expression in transduced cells	2 µg/ml	Biomol

7.8.2 Enzymes

Name	Source
DreamTaq DNA polymerase and buffers	Thermo Fisher Scientific
Fast Digest restriction enzymes and buffers	Thermo Fisher Scientific
Q5 High-Fidelity DNA polymerase and buffers	New England Biolab
T4 DNA ligase and buffer	Thermo Fisher Scientific

7.8.3 Molecular mass standards

Name	Source
GeneRuler™ DNA Ladder Mix	Thermo Fisher Scientific
PageRuler™ Prestained Protein Ladder	Thermo Fisher Scientific

7.8.4 Other reagents and chemicals

Name	Source
Polyethylenimine (PEI), branched	Sigma-Aldrich
PolyFect Transfection reagent	Qiagen
Polybrene	Millipore
Protease inhibitor cocktail cOmplete™ mini, EDTA free	Roche
ECL Prime Western Blotting Detection Reagent	GE-Healthcare
Lumigen ECL Ultra (TMA-6)	Beckman Coulter

DMSO (dimethyl sulfoxide)	Roth
Methylcellulose (viscosity 4000 cPs)	Sigma-Aldrich
Nitrocellulose membrane (0.2 µm)	GE Healthcare Life Science
Whatman® gel blotting paper, Grade GB003	Sigma-Aldrich
DAPI	Roche
Coelenterazine-h	Synchem
L-(+)-Arabinose	Sigma-Aldrich
Tamoxifen	Sigma-Aldrich
Corn oil	Sigma-Aldrich

7.9 Medium

7.9.1 Cell culture medium

Medium	Component	Source	Amount
Growth medium	Dulbecco's Modified Eagle's Medium (DMEM) with glucose	Pan Biotech	500 ml
	Fetal calf serum (FCS)	Pan Biotech	50 ml (10 %)
	Penicillin/Streptomycin (100x)	Sigma-Aldrich	5 ml
Dulbecco's Phosphate Buffered Saline	Ready to use	Sigma-Aldrich	
Trypsin-EDTA (1×)	Ready to use	Sigma-Aldrich	
Methylcellulose overlay	10x Minimum Essential Medium	Gibco	40 ml
	Methylcellulose 2.5% (m/v)	Sigma-Aldrich	360 ml
	Penicillin/Streptomycin (100x)	Sigma-Aldrich	4 ml
	L-Glutamine	Thermo Fisher Scientific	5 ml
	NaHCO3 (1M)	Roth	15 ml
	Fetal calf serum (FCS)	Pan Biotech	16 ml (4 %)

Sucrose/virus standard buffer	Tris-HCl	Sigma-Aldrich	50 mM
	KCl	Roth	12 mM
	Na_2EDTA	Roth	5 mM
	Sucrose	Roth	15 % (w/v)

7.9.2 Bacteria medium

Medium	Component	Amount	Source
Luria Bertani (LB) liquid medium	LB (Lennox) medium	20 g/l	Roth
Luria Bertani (LB) agar	LB (Lennox) medium	20 g/l	Roth
	Agar-Agar, Kobe I	1.5 %	Roth

7.10 Buffers

7.10.1 Agarose gel electrophoresis buffers

Name	Component	pH
50x TAE buffer stock (working concentration 1x)	2 M Tris-HCl	8.0
	50 mM EDTA	
	5.7 % (v/v) acetic acid	
10x TBE buffer stock (working concentration 0.5x)	1 M Tris-HCl	8.0
	0.02 mM EDTA	
	1M boric acid	

7.10.2 SDS-PAGE and immunoblot buffers and gels

Buffer	Component	pH
4x SDS sample buffer (working concentration 2x)	0.25 M Tris-HCl	6.8
	8 % (v/v) SDS	
	40 % (v/v) Glycerol	
	20 % (v/v) β-Mercaptoethanol	
	Bromophenol blue	
10x SDS running buffer (working concentration 1x)	0.25 M Tris	-
	1.92 M Glycine	

	1 % (w/v) SDS	
1x Transfer buffer (for semi-dry transfer)	50 mM Tris	-
	40 mM Glycine	
	0.04 % (w/v) SDS	
	20 % (v/v) Methanol	
10x TBS-T (working concentration 1x)	0.5 M Tris-HCl	7.5
	1.5 M NaCl	
	1 % (v/v) Tween-20	
RIPA lysis buffer	50 mM Tris	7.2
	150 mM NaCl	
	1 % (v/v) Triton X-100	
	0.1 % (v/v) SDS	
	1 % sodium deoxycholate	

Component	10 % SDS stacking gel	4 % SDS resolving gel
H_2O	3.4 ml	3.7 ml
30 % Acrylamide	750 µl	3 ml
0.5 M Tris-HCl (pH 6.8)	1.4 ml	-
1.5 M Tris-HCl (pH 8.8)	-	2.3 ml
20 % SDS	28 µl	45 µl
10 % APS	75 µl	100 µl
TEMED	7.5 µl	10 µl

7.10.3 Buffers for immunofluorescence

Buffer	Components
Fixation buffer	4 % Paraformaldehyde in PBS
Quenching buffer	50 mM NH_4Cl in PBS
Permeabilization buffer	0.5 % Triton X-100 in PBS
Blocking buffer (TBS-BG)	1x Tris buffered saline (TBS)
	5 % Glycine
	5 % BSA
	0.05 % Tween20

	0.05 % NaN_3

7.10.4 Mini prep buffers

Buffer	Component	pH
S1 buffer	50 mM Tris-HCl 100 µg/ml RNase A 10 mM EDTA	8.0
S2 buffer	200 mM NaOH 1 % (v/v) SDS	-
S3 buffer	2.8 M Calcium acetate	5.2
Tris-HCl	10 mM Tris	8.0

7.11 Kits

Name	Source
innuPREP RNA mini kit	Analytik Jena
TURBO DNA-free	Invitrogen
mi-Plasmid Miniprep	Metabion
NucleoBond Xtra Midi	Macherey-Nagel
NucleoSpin Gel and PCR Clean-up	Macherey-Nagel
HMGB1 Express ELISA	IBL International
ChromoTek GFP-Trap Agarose	Proteintech
Pierce™ BCA Protein Assay	Thermo Scientific
CellTiter-Glo Luminescent Cell Viability Assay	Promega

7.12 Animals

Name	Description	Reference
LysM-Cre	C57BL/6 mice expressing Cre recombinase under control of endogenous lysozyme 2 (*Lyz2*) promoter	Jackson Laboratory
UBC-CreERT2	C57BL/6 mice expressing tamoxifen-inducible Cre-ERT2 recombinase under control of ubiquitin C (UBC) promoter	Jackson Laboratory
Hmgb1$^{fl/fl}$	Transgenic mice with loxP sites flanking exons 2-4 of	[226]

	Hmgb1 gene	
ΔHmgb1^{UBC}	Transgenic mice with loxP sites flanking exons 2-4 of *Hmgb1* gene, expressing tamoxifen-inducible CreERT2 recombinase under control of ubiquitin (UBC) promoter, deletion of *Hmgb1* in all cells upon tamoxifen treatment	generated by cross-breeding
ΔHmgb1^{LysM}	Transgenic mice with loxP sites flanking exons 2-4 of *Hmgb1* gene, expressing Cre recombinase under control of *Lyz2* promoter, *Hmgb1* deletion in myeloid cells	generated by cross-breeding

8. Methods

8.1 Molecular biology methods

8.1.1 Preparation of electrocompetent *E. coli* DH10B and *E. coli* GS1783

10 ml pre-culture of *E. coli* was grown overnight in LB medium without antibiotics (DH10B) or with 15 µg/ml chloramphenicol (GS1783), with continuous shaking at 37°C (DH10B) or 30°C (GS1783). The next day, 5 ml of the pre-culture were inoculated to 200 ml pre-warmed LB medium and cultured with continuous shaking at the respective temperature until bacterial culture reached an OD_{600} value between 0.5 and 0.6. Subsequently, GS1783 were incubated in a water bath shaker for 15 min at 42°C to induce expression of the red recombination system and then cooled on ice for 20 min. DH10B were directly transferred to ice after reaching the correct OD_{600} value. Bacteria were then pelleted at 4°C and 5000 x g for 10 min. The pellet was washed twice with 100 ml ice-cold sterile water and once with ice-cold sterile 10 % glycerol. Finally, the bacteria pellet was dissolved in 1 ml ice-cold sterile 10 % glycerol, immediately aliquoted and then stored at -80°C.

8.1.2 Small-scale plasmid DNA preparation (Mini prep)

A single bacterial colony was picked from a LB agar plate and transferred into 5 ml LB medium containing the required antibiotics. Following an incubation overnight at 37°C (DH10B) or 30°C (GS1783) with continuous shaking, DNA was isolated using alkaline lysis and isopropanol precipitation as described [227]. If highly pure plasmid DNA was required, using the Mi-Plasmid MiniPrep Kit according to the manufacturing protocol. Briefly, 4 ml of bacterial culture were pelleted at 5000 x g for 5 min. For the alkaline lysis supernatants were discarded and pellets were resuspended in 300 µl of S1 buffer and lysed by adding 300 µl of S2 buffer. After 5 min the lysis solution was neutralized by adding 300 µl of S3 buffer. The samples were incubated on ice for 7 minutes until precipitates containing bacterial chromosomal DNA and proteins were visible. In order to remove those precipitates and avoid contaminations, samples were centrifuged for 20 min at 6000 x g and 4°C. The cleared lysates (~ 800 µl) containing plasmid or bacterial artificial chromosome (BAC) DNA were transferred to new tubes and the DNA was precipitated using 640 µl isopropanol and centrifugation at 15000 x g for minimum 30 min. The supernatants were then discarded and the pellets were washed with 500 µl of 70 % ethanol. After another centrifugation

(15000 x g, 5 min), ethanol was removed, pellets were dried at room temperature to remove all traces of ethanol and the DNA was finally resuspended in 50 µl of water or 10 mM Tris-HCl (pH 8.0).

8.1.3 Large-scale plasmid DNA preparation (Midi prep)

Plasmid DNA was prepared using 200 ml of bacterial cultures. The DNA was isolated using the NucleoBond Midi Xtra Kit according to the manufacturing protocol. Depending on the size of the DNA pellet, DNA was dissolved in 200 – 500 µl 10 mM Tris-HCl (pH 8.0).

8.1.4 Polymerase Chain Reaction (PCR)

PCRs were performed using either DreamTaq or Q5 High-Fidelity DNA polymerases according to the manufacture's protocol. DreamTaq polymerase was used for e.g. genotyping of HMGB1 knockout mice, while Q5 polymerase was used for cloning or sequencing that required high-fidelity amplifications since the Q5 polymerase has a proofreading activity.

Reaction Setup:

Q5		**DreamTaq**		
5x Q5 Reaction Buffer	10 µl	10x DreamTaq Green Buffer	5 µl	2.5 µl
10 mM dNTPs	1 µl	10 mM dNTPs	1 µl	0.5 µl
10 µM forward Primer	2 µl	10 µM forward Primer	2 µl	1 µl
10 µM reverse Primer	2 µl	10 µM reverse Primer	2 µl	1 µl
Template DNA (10-100 ng)	X µl	Template DNA (10-100 ng)	X µl	X µl
Q5 High-Fidelity DNA Polymerase	0.5µl	DreamTaq DNA Polymerase	0.25 µl	0.25 µl
H_2O	up to 50 µl	H_2O	up to 50 µl	up to 25 µl

Cycling conditions:

	Q5			DreamTaq		
Cycle Step	Temperature	Time	Cycle(s)	Temperature	Time	Cycle(s)
Initial denaturation	98°C	2 min	1	95°C	2 min	1
Denaturation	98°C	30 s	30-35	95°C	30 s	30-35
Annealing	Tm*-5°C	30 s		Tm*-3°C	30 s	
Extension	72°C	30 s/kb		72°C	1min/kb	
Final extension	72°C	5 min	1	72°C	5 min	1

*Tm was calculated using Tm Calculator (Thermo Fisher)

8.1.5 Restriction digest of DNA

DNA digestion was performed using FastDigest restriction enzymes (Thermo Fisher) according to the manufacturer's instructions.

Reaction setup and digestion conditions:

Plasmid/vector digest		PCR product digest	
10x FastDigest Green Buffer	3 µl	10x FastDigest Green Buffer	5 µl
Plasmid (1 µg)	X µl	PCR product	45 µl
FastDigest restriction enzyme	1 µl/enzyme	FastDigest restriction enzyme	1 µl/enzyme
Fast Alkaline Phosphatase	1 µl	DpnI	1 µl
H_2O	up to 30 µl	H_2O	-
37°C for 30-45 min			

8.1.6 Agarose gel electrophoresis

PCR products or other DNA fragments were analyzed by running through 0.8 – 2 % (w/v) agarose gels, depending on the expected fragment size. Agarose was dissolved in 1x TAE buffer and DNA was visualized by adding 0.5 µg/ml ethidium bromide to the liquid gel solution. In addition to the DNA samples, a size standard (GeneRuler DNA Ladder Mix, Thermo Scientific) was loaded onto the gel. Electrophoresis was performed at 80 -120 V until proper separation of expected

fragments was achieved. DNA bands were visualized using UV illumination in a GelDoc XR+ (BIO-RAD) and analyzed with the Image Lab software. In order to analyze BACs, digested BAC DNA was loaded onto a 0.6 % (w/v) agarose gel in 0.5x TBE containing 0.5 µg/ml ethidium bromide. BAC gels were run overnight at 60 V.

8.1.7 Agarose gel extraction and DNA purification

In order to purify DNA from e.g. buffers, enzymes or other DNA fragments, DNA was separated through an agarose gel as described in 8.1.6. Afterwards, the DNA band with the expected size was cut out from the agarose gel and purified using the NucleoSpin Gel and PCR clean up kit (Macherey-Nagel) according to the manufacturer's instructions. DNA concentrations were determined using a NanoDrop-1000 (Peqlab). DNA was stored at 4°C until further processing.

8.1.8 DNA ligation

Digested and linearized vector as well as digested insert (e.g. gene of interest) were mixed according to the molecular ratio of 1:5 and ligated by using T4-DNA-Ligase.

Reaction setup and ligation conditions:

Component	Amount
10x Ligase Reaction Buffer	2 µl
Vector (linearized, digested)	X µl (100 ng)
Insert (digested)	Y µl
T4 DNA ligase	1 µl
H_2O	up to 20 µl
1 h at 22°C or overnight at 16°C	

8.1.9 Bacterial transformation

Transformation was performed using electroporation of electrocompetent *E. coli* DH10B or GS1783. A 50 µl aliquot of *E. coli* DH10B prepared as described in 8.1.1 was slowly thawed on ice and then mixed with either 1 - 10 ng of plasmid DNA or 4 µl of ligation product. Alternatively, 50 µl *E.coli* GS1783 were thawed on ice and then mixed with 150 ng of a PCR-amplified, linear DNA fragment. The mixture was then

transferred to a 2 mm electroporation cuvette and pulsed using a Gene Pulser XCell (Bio-Rad) with the following settings: 2500 V, 25 µF and 200 Ω. Immediately after pulsing, 1 ml of LB medium (room temperature) was added to the bacteria. DH10B were incubated at 37°C, GS1783 at 30°C for 1 h. Subsequently, the bacteria were centrifuged for 5 min at 2000 x g, the pellet was resuspended in approximately 100 µl LB medium and plated on LB agar plates with the corresponding antibiotics. Plates were incubated overnight at 37°C or 30°C in a bacteria incubator.

8.1.10 DNA sequencing

PCR products and plasmid DNA were sequenced by SEQLAB Sequence Laboratories (Maschmühlenweg 36, 37081, Göttingen, Germany) according to their instructions. MCMV DNA (MCMV m38.5stop) isolated from viral particles was sequenced by the NGS facility of LIV.

8.1.11 *En passant* BAC mutagenesis

In order to mutate BACs containing the viral genome, *en passant* mutagenesis was performed as described by Tischer and colleagues [223]. First, the I-SceI-aphAI-cassette from the pEP-Kan-S plasmid encoding a kanamycin resistance was PCR-amplified using primers containing the necessary homology regions and the point mutation to be introduced into the MCMV genome. To remove template DNA, the PCR product was digested by DpnI and purified via agarose gel electrophoresis and gel extraction using the NucleoSpin Gel and PCR clean up kit. Next, 150 ng purified PCR product were transformed into *E.coli* GS1783 electrocompetent bacteria carrying the MCMV Δm157 BAC. As the bacteria were incubated at 42°C (see 8.1.1), the red recombinases were present to mediate first recombination. By this, the PCR fragments recombined with the BAC using the homology arms incorporating the wanted mutation as well as the kanamycin resistance and *I-Sce-I* restriction site into the BAC. Transformed bacteria were plated on LB agar plates containing chloramphenicol and kanamycin and incubated at 30°C overnight. Resulting single colonies were picked the day after and analyzed by restriction fragment length polymorphism (RFLP). According to the DNA RFLP, 3 positive colonies were used for the secondary recombination procedure. For the second recombination a single colony was inoculated in 2 ml LB- chloramphenicol medium and incubated 2 – 3 h at

30°C with continuous shaking. As soon as the medium turned cloudy, 2 ml pre-warmed LB medium containing 2 % (w/v) L-arabinose were added and the culture was incubated further for 1 h to allow expression of the *I-Sce-I* restriction enzyme and the digest of the BAC DNA. Subsequently, the culture was incubated at 42°C for 15 min with continuous shaking in order to induce expression of the Red recombination system leading to the second recombination and excision of the kanamycin cassette. Finally, bacteria were incubated 2.5 h at 30°C, diluted according to the OD600, plated on LB- chloramphenicol agar plates containing 1 % (w/v) L-arabinose and incubated overnight at 30°C. Single colonies were analyzed by BAC DNA digest and sequencing of the modified region. BAC DNA of at least two selected positive colonies was prepared with Midi-preps for reconstituting the virus in murine fibroblasts.

8.1.12 Extraction of total RNA from cells

Total RNA was isolated from 3-5 x 10^5 eukaryotic cells using the innuPREP RNA Mini Kit (Analytik Jena) according to the manufacturer's instructions. Total RNA was eluted using 35 µl of RNase-free water. To exclude any DNA contaminations, samples were DNaseI treated using the TURBO-DNA-free kit (Fisher Scientific) following the manufacturer's instructions. RNA concentration was determined using a NanoDrop-1000 (Peqlab) photometer. RNA was stored at -80°C.

8.1.13 Complementary DNA (cDNA) synthesis

500 – 1000 ng total RNA were reverse transcribed using RevertAid H Minus Reverse Transcriptase. In order to reverse transcribe mRNA, an oligo$[dT]_{18}$ primer was used. After inactivating the reverse transcriptase in a final heating step at 70°C the synthesized cDNA was either directly used for quantitative PCR or stored at -20°C.

Reaction setup and amplification conditions:

Component	Amount
Total RNA (500 – 1000 ng)	X µl
Oligo[dT]$_{18}$ (100 µM)	1 µl
H_2O	up to 12.5 µl
5 min at 65°C	
1 min on ice	
5x Reaction Buffer	4 µl
RiboLock RNase Inhibitor (Thermo Fisher)	0.5 µl
dNTPs (10 µM each)	2 µl
RevertAis H Minus RT (Thermo Fisher)	1 µl
1 h at 42°C	
10 min at 70°C	

8.1.14 Quantitative polymerase chain reaction (qPCR)

Previous synthesized cDNA (8.1.13) was 1:10 – 1:20 diluted in autoclaved distilled water prior to qPCR. To quantify the amount of a specific mRNA within the sample the PowerTrack SYBR Green Mastermix (Fisher Scientific) was used. Each sample was measured in triplicates in a MicroAmp™ Fast Optical 96-Well Reaction Plate (Thermo Fisher Scientific) with a QuantStudio 3 Real-Time-PCR machine (Thermo Fisher Scientific). Generated data was analyzed using the Design & Analysis Software (Version 2.6.0, ThermoFisher Scientific). Transcripts of interest were normalized to a housekeeping gene (β-actin) and relatively quantified using the ΔΔCt method.

Reaction setup:

Component	Amount
2x PowerTrack SYBR Green Mastermix	5 µl
Primer forward (10 µM)	0.5 µl
Primer reverse (10 µM)	0.5 µl
cDNA (1:10 -1:20 in H_2O)	1 µl
H_2O	3 µl

Cycling conditions:

	Temperature	Time	Cycle(s)
Hot start	50°C	2 min	1
	95°C	10 min	
PCR	95°C	15 s	40
	60°C	30 s	
Melting curve	95°C	15 s	1
	60°C	1 min	
	95°C (0.1°C/s)	15 s	

8.2 Biological and virological methods

8.2.1 Cell culture

All human and murine cells were grown on 10 or 15 cm cell culture dishes and kept at 37°C in a Hera Cell incubator at 5 % CO_2 and 80 % relative humidity. To ensure sterile work conditions, all cell culture work was performed within a Laminar flow hood (HeraSafe, Heraeus). Cells were cultured in complete Dulbecco's modified Eagle medium (DMEM) supplemented with 10% fetal calf serum (FCS) and 100 U/ml penicillin/100 µg/ml streptomycin. At approximately 90 % confluence, cells were washed once with phosphate-buffered saline (PBS) and detached by using 0.25 % Trypsin-EDTA solution at 37°C. After a short incubation the trypsin was neutralized by addition of growth medium containing FCS. Homogenous cell suspension was splitted 1:10. Cell numbers were determined by loading 10 µl of the cell suspension onto a counting slide and counted by a TC20™ Automated Cell Counter (BIO-RAD).

In order to freeze cells, cell suspension was centrifuged for 5 minutes at 250 x g. The cell pellet was resuspended in FCS containing 10 % DMSO. Aliquots of 1 ml were immediately transferred to a freezing device ("CoolCell LX") and stored at -80°C for at least 4 hours. For long term storage cells were kept in liquid nitrogen. To recover cells, aliquots of frozen cells from the liquid nitrogen were transferred into a 37°C water bath and transferred into a tube containing 10 ml regular growth medium. Cells

were pelleted by centrifugation (5 minutes at 250 x g). The cell pellet was then resuspended in 10 ml growth medium and transferred to a 10 cm dish.

8.2.2 Transfection of plasmid DNA

Plasmid DNA was transfected into cells using polyethylenimine (PEI). For this purpose, $3x10^6$ HEK-293T were seeded into a 10 cm dish one day prior transfection. 8 µg total plasmid DNA and 32 µl PEI (4:1 ratio) were diluted in 1 ml OptiMEM or DMEM (without supplements) and incubated 20 minutes at room temperature. During incubation the cell culture medium of the 10 cm dish was reduced to 7 ml. The transfection mix was added dropwise to the cells. Finally, 6 h post transfection the old medium was discarded, cells were washed once in PBS and 8 ml fresh medium was added. Cells were incubated until further use.

8.2.3 Transfection of BAC DNA

MCMV BAC DNA was transfected into 10.1 murine fibroblasts by using Polyfect transfection reagent in order to reconstitute recombinant MCMV viruses. $1.5x10^5$ cells were seeded in a 6-well plate the day before transfection. On the following day, 3 µg of MCMV BAC DNA was diluted in 100 µl of DMEM and 10 µl of Polyfect was diluted to another 100 µl of DMEM. The dilution of BAC DNA and Polyfect were mixed and incubated at room temperature for 20 min. The transfection mix was then added to the cells. The medium was changed 6 h post transfection. As soon as the cells were confluent, they were expanded. The reconstitution of MCMV was monitored by detection of the cytopathic effects. The supernatant from the infected cells was harvested for virus stock production.

8.2.4 Production of lentivirus

Lentiviruses were produced in order to transduce and genetically manipulate target cells. For lentivirus production, HEK-293T cells were co-transfected with 4 µg vector plasmid encoding the gene of interest (i.e. pLKO.1, pLIX, pLeGo), 3 µg packaging plasmid pCMVdR8.91 and 1 µg envelope plasmid pMD2.G as described in 8.2.2. 48 h post transfection cell supernatant was harvested, filtered through a 0.45 µm syringe filter and either used directly for transduction or stored at -80°C. 8 ml of fresh

medium was added to each 10 cm dish for a second harvest the following day (72 h post transfection), which was processed the same way than the supernatant 48 post transfection.

8.2.5 Transduction

In order to transduce target cells using lentiviruses, $3x10^5$ cells were seeded into a 6-well plate one day prior transduction. Virus-containing supernatant produced according to 8.2.4 was mixed 1:2000 with Polybrene (10 mg/ml) and added to the target cell (3.5 ml per well). To enhance the infection efficiency, cells were centrifuged 30 min at 1000 x g and 37°C. Medium was changed 6 hpi. The following day the procedure was repeated with the supernatant harvested 72 h post transfection in the same well. As soon as the cells were confluent, cells were expanded to a 10 cm dish and transduced cells were selected by adding either puromycin or blasticidin to the cell culture medium. A plate of non-transduced cells served as control for successful selection.

8.2.6 Generation of HMGB1-knockdown cell lines

In order to generate murine cell lines with stable knockdown of HMGB1 a lentiviral shRNA system was used. Two shRNAs targeting different positions of HMGB1 (target region of shRNA1: TGA CAA GGC TCG TTA TGA AAG; shRNA2: ATG CAG CTT ATA CGA AGA TAA) were cloned into the lentivirus expression vector pLKO.1 using AgeI and EcoRI restriction enzymes. In addition, pLKO.1-scramble (scr) encoding a non-targeting shRNA (TGC CTA AGG TTA AGT CGC CCT CGA) was used as control. Lentiviruses carrying the respective shRNAs were generated as described in 8.2.4. Subsequently, lentiviruses were used to transduce target cells (8.2.5). Selection of transduced cells was performed with puromycin or, in case of $ASC^{-/-}$ iBMDM, blasticidin. The respective resistance was encoded by the pLKO.1 plasmid.

8.2.7 Generation of inducible EGFP-HMGB1 expressing cell lines

In order to generate stable cell line expressing EGFP-HMGB1 upon Doxycycline induction, murine HMGB1 was first cloned into pEGFP-C3 using HindIII and BamHI

restriction enzymes. The thereby generated pcDNA-EGFP-HMGB1 served as template to clone EGFP-tagged HMGB1 into pLIX-puro. This was done using EcoRI and SalI restriction digest. Lentiviruses encoding EGFP-HMGB1 were generated as described in 8.2.4. Subsequently, lentiviruses were used to transduce target cells (8.2.5). Selection of transduced cells was performed with puromycin. The puromycin resistance was encoded by pLIX-puro.

8.2.8 Generation of HMGB1-GLuc expressing cell lines

Murine cell lines stably expressing Gaussia luciferase-coupled HMGB1 were generated by lentiviral transduction. Therefore, HMGB1 was cloned into pMSCV-puro-iGLuc to replace the encoded pro-IL-1β with HMGB1 using BglII and BamHI restriction enzymes. The resulting pMSCV-puro-HMGB1-GLuc was used as template to PCR-amplify and then clone HMGB1-GLuc into pLeGo-iC2 using EcoRI and NotI restriction digest. Finally, pLeGo-HMGB1-GLuc was used to generate lentiviruses as described in 8.2.4. Transduction of target cells was done as described in 8.2.5 and cells were selected using puromycin. Single-cell clones were obtained by limiting dilutions.

8.2.9 MCMV stock production

$2x10^7$ 10.1 fibroblasts were mixed with virus at a MOI of 0.015-0.025. The cell-virus suspension was distributed to 10x 15 cm dishes. 3 - 4 days post infection virus-containing supernatants were collected and fresh medium was added to the dishes. Supernatants were collected a second time 5 - 6 days post infection. Supernatants were then centrifuged 15 min at 6000 x g and 4°C to remove cell debris. Cleared supernatants were transferred in new centrifugation bottles and centrifuged 3.5 h at 27000 x g and 4°C to pellet viral particles. The virus pellet was resuspended in 0.8 - 1 ml growth medium overnight on ice at 4°C. On the next day, the virus pellet was gently homogenized and remaining cell debris were removed by another centrifugation of 10 min, 6000 x g at 4°C. Afterwards, the virus suspension (2 ml) was loaded on 18 ml of a 15 % sucrose cushion in an ultracentrifuge tube. Ultracentrifugation was performed at 4°C using 72000 x g for 1.5 h in a Optima-L70 Ultracentrifuge (Beckman Coulter). Depending on the pellet size, the virus pellet was resuspended in 200 - 500 µl growth medium (*in vitro* use) or PBS (*in vivo* use)

overnight on ice at 4°C. Finally, the virus pellet was resuspended, aliquoted and stored at -80°C.

8.2.10 Median tissue culture infectious dose ($TCID_{50}$)

Median tissue culture infectious dose ($TCID_{50}$) method was used to determine virus concentrations of MCMV stocks or *in vitro* cell culture samples (e.g. from growth kinetics). In both cases 10.1 murine fibroblasts were seeded into 96-well plates at a concentration of $2.5x10^3$ cells/well one day prior titration. For the titration of MCMV stocks, individual triplicates of serial log_{10} dilutions (from 10^{-3} to 10^{-10}) were prepared in 4 ml growth medium. 100 µl of each dilution was added to an entire row of a 96-well plate (12 wells) in duplicates. While, one plate was simply put back to the incubator, the other plate was centrifuged 30 min at 1000 x g and 37°C to apply the centrifugal enhancement of infection. 7 days post infection, the number of wells showing cytopathic effect in each dilution was counted and the viral titer was calculated applying the Spearman-Kärber method [228]. Since For determining the virus concentration in cell culture samples (i.e. viral growth kinetics), the same procedure as before was used, except that no centrifugal enhancement was used.

8.2.11 Plaque assay

Plaque assay was performed to determine viral loads in mouse organs or the virus concentration of MCMV stocks used for *in vivo* experiments. One day prior titration, $4x10^4$ M2-10B4 cells were seeded in 48-well plates. The following day, for each viral sample individual duplicates or triplicates of serial log_{10} dilutions (from 10^{-1} to 10^{-6} or 10^{-3} to 10^{-8}) were prepared in 1 ml growth medium containing 3 % FCS. Subsequently, 100 µl of each dilution was added to one well of M2-10B4. To prevent viral spreading through the supernatant, 3 h post infection 300 µl of methylcellulose was added to overlay the infected cells. At 7 d post infection, the plaques in each well were counted and the viral titer was calculated as described by Zurbach et.al [229].

8.2.12 Virus infection

In vitro MCMV infection was performed at a specific multiplicity of infection (MOI) according to the $TCID_{50}$ of the respective virus stock. The amount of virus stock needed was calculated as followed:

$$volume\ virus\ stock\ (ml) = \frac{number\ of\ cells \times MOI}{TCID_{50}/ml}$$

The calculated amount of virus was then diluted in the growth medium and the dilution was added to the cells. If necessary, cells were centrifuged for 30 min at 1000 x g for and 37°C to enhance infection efficiency. In order to synchronize the infection, medium was changed 4 h post infection.

8.2.13 Viral growth kinetics

Multistep growth kinetics were started by seeding either $1x10^5$ cells (i.e. Hepa1-6, SVEC4-10, NIH-3T3) or $2x10^5$ cells (i.e. iBMDM) into 6-well plates one day prior infection. The next day, cells were infected using a MOI of 0.01 (SVEC4-10, NIH-3T3), MOI of 0.02 (Hepa1-6) or MOI of 0.025 (iBMDM) as described in 8.2.12. 4 hpi medium was changed. In case of inducible EGFP-HMGB1 expressing cell lines, 4 hpi cells were either incubated in normal cell culture medium or medium containing 2 µg/ml doxycycline. Cell supernatants were collected on days 1, 3, 5, 7 and 9 and titrated on 10.1 cells as described in 8.2.10. After each harvest of the supernatant, cells were washed once with PBS and 3 ml of fresh growth medium (if needed, containing 2 µg/ml doxycycline) was added to each well.

8.2.14 Viral protein expression kinetic

In order to analyze differences in MCMV gene expression in different HMGB1-deficient cells types, HMGB1 knockdown and control cells were first seeded into 6-well plates. Hepa1-6, NIH-3T3 and SVEC4-10 cells were seeded at a concentration of $3x10^5$ cells/well, iBMDMs were seeded at $4x10^5$ cells. The following day, the

seeded cells were infected with MCMV at a MOI of 5. After 4 h the medium was changed. Cells were harvested at 0, 2, 4, 8, 24, 48 and 72 hpi in 2x SDS-PAGE sample buffer as described in 8.3.1. Cell lysates were analysed for viral protein expression of the three most prominent proteins IE1, E1 and gB by immunoblotting as described in 8.3.3.

8.2.15 Cell viability assay

$5x10^3$ cells were seeded in each well of a 96-well plate (black, clear bottom) one day prior infection. The following day, cells were infected with an MOI of 5 of either MCMV WT, MCMV M45mutRHIM, MCMV m38.5stop or MCMV M84stop in 100 µl medium per well. The amount of viable cells at specific time points was determined by measuring intracellular ATP levels using the CellTiter-Glo Luminescent Cell Viability Assay kit (Promega) according to the manufacturer's instructions. Luminescence was measured using a FLUOstar Omega luminometer (BMG Labtech).

8.2.16 HMGB1 release assay

To investigate whether MCMV-infected cells actively or passively release HMGB1 into the extracellular milieu, cells stably expressing HMGB1 coupled with Gaussia Luciferase (HMGB1-GLuc) were used. First, cells were seeded into a 96-well plate at a density of $5x10^3$ cells/well. The day after, cells were infected with MCMV WT, MCMV M45mutRHIM, MCMV m38.5stop or MCMV M84stop at a MOI of 5. Cell supernatants were harvested to specific time points and luciferase activity was measured as described in 8.3.5.

8.3 Biochemical methods

8.3.1 Cell lysis for immunoblotting

To lyse cells for protein detection, cell culture medium was discarded and cells were washed once with PBS. Cells were then either lysed directly in the well by adding 2x SDS-PAGE sample buffer or trypsinized, collected in a tube, pelleted by centrifugation (5 min, 500 x g) and then lysed in RIPA buffer containing protease inhibitors. After 5 min incubation on ice cell debris were removed by centrifugation

(5 min, 16000 x g). Lysates in RIPA buffer were stored at -80°C. Cell lysates in 2x SDS-PAGE sample buffer were boiled 10 min at 95°C and stored at -20°C. The amount of lysis buffer used was in between 100 - 350 µl depending on the cell number.

8.3.2 Protein quantification – Bicinchoninic Acid (BCA) assay

Protein concentrations in cell lysates were measured using BCA Protein assay kit (Thermo Fisher Scientific). Protein lysates were diluted at a ratio 1:4 – 1:10 in PBS in duplicates in a 96-well plate. A standard curve of bovine serum albumin (BSA) was prepared using dilutions of BSA (2.0 mg/ml) in PBS. 100 µl of a 50:1 mix of the BCA solutions A and B were added to each sample and standards. After 20 minutes of incubation at 37 °C, absorbance at 562 nm was measured using FLUOstar Omega reader (BMG Labtech). The BSA standard curve was used to calculate the protein concentration of the sample.

8.3.3 SDS polyacrylamide gel electrophoresis (SDS-PAGE) and immunoblot

Proteins were separated according to their molecular weight by performing gel electrophoresis in a polyacrylamide gel. Prior to separation proteins were denatured using a SDS-PAGE sample buffer containing sodium dodecyl sulfate (SDS) and 2-Mercaptoethanol. Polyacrylamide gels, 1.5 mm thick, were formed by two different phases: The lower resolving or separation gel containing 10-12.5 % acrylamide and the upper stacking gel with 4 % of acrylamide. The fully polymerized gels were mounted in the electrophoresis chamber (Bio-Rad), SDS running buffer was added and samples were loaded on the gels. In addition, 3 µl of a protein standard (PageRuler prestained, Thermo Fisher) was loaded on each gel. Electrophoresis was performed at 70 – 100 V until proper separation was achieved. Subsequently, proteins were transferred to a nitrocellulose membrane by semi-dry blotting. Transfer was performed with 50 mA/gel for 30 – 60 min (depending on protein sizes) in a Trans-Blot Turbo Transfer System (Bio-Rad). Prior to blot assembly, membrane, filter papers and gels were equilibrated in transfer buffer. After completed transfer, membranes were washed briefly with 1x TBS-T and blocked with either 5 % nonfat milk or 5 % BSA diluted in TBS-T for 1 h at room temperature. Membranes were then

incubated with the primary antibody overnight at 4°C. If necessary, membranes were cutted to incubate with different antibodies. The following day, membranes were washed three times with TBS-T for 5 min each. Afterwards, membranes were incubated with horseradish peroxidase (HRP)-coupled secondary antibodies for 1 h in 5 % milk/TBS-T at room temperature. After a final washing (3x 5 min in TBS-T), membranes were briefly incubated with ECL Western Blotting Reagents (Amersham) and chemiluminescence was detected using a Fusion Capture Advance FX7 16.15 camera system (Peqlab). If necessary, intensities were increased using 10 % Lumigen ECL Ultra (Bioquote Limited).

8.3.4 Immunoprecipitation

One day prior to transfection, $3x10^5$ HEK-293T cells were seeded in 6-well format. The following day, HEK293T were transfected with 1 µg plasmid DNA encoding either MCMV E1 (pcDNA-M112/113), pEGFP-HMGB1, pEGFP-C3 or p3xFlag-mTLR4. Transfection was performed using PEI as described in 8.2.2 and medium was changed 6 h post transfection. 24 h post transfection cells of three identical wells were pooled and lysed in 200 µl RIPA buffer. Immunoprecipitation of EGFP or EGFP-HMGB1 was performed using ChromoTek GFP-Trap Agarose according to the manufacturer's instructions. Briefly, cell lysates (diluted in dilution buffer) were incubated with GFP-Agarose beads overnight at 4°C. The next day, beads were pelleted and washed at least three times in wash buffer. In order to elute bound protein complexes, beads were resuspended in 80 µl 2x SDS sample buffer and boiled at 95°C for 5 min. Immunoprecipitated proteins as well as input control, taken from the same sample before incubation with the beads, were analyzed by SDS-PAGE and immunoblotting as described in 8.3.3.

8.3.5 Luciferase assay

Luciferase activity was measured in order to quantify amounts of HMGB1-GLuc in the supernatant of infected cells. 90 µl of cell supernatants were transferred into a black 96-well plate, 10 ml of Coelenterazine-h (1 µg/ml) were added and 10 s later luminescence was measured using a Centro LB 960 XS3 plate reader according to the manufacturer's instructions.

8.4 Immunofluorescence microscopy

8.4.1 Immunostaining of cell culture samples

Cells were seeded on µ-Slide 8 well chamber slides (ibidi) one day prior infection or transfection. The next day, cells were either infected (8.2.12) or transfected (8.2.2) and further incubated for the designated time. In order to prepare cells for immunostaining, cells were briefly washed with PBS and fixed by adding 4 % paraformaldehyde (PFA) for 20 min. Free aldehyde groups were then quenched by incubating cells 20 min in 50 mM NH_4Cl. Permeabilization was performed by incubating cells 10 min in 0.5 % Trition X-100 (in PBS). Lastly, unspecific binding sites were blocked by adding TBS-BG blocking buffer for 1 h at room temperature or overnight at 4°C. In between every step cells were washed three times with PBS.

Prepared cells were then incubated with the respective primary antibodies (diluted in PBS) for 1 h at room temperature, washed three times with PBS and then incubated with fluorophore coupled secondary antibodies and the nuclear dye DAPI for 45 min at room temperature. After final washing steps, cells were overlaid with PBS and stored at 4°C in the dark until analysis. Fluorescence images were acquired using a Nikon A1 confocal laser scanning or spinning disk microscope.

8.5 Animal experiments

All animal experiments were performed according to the recommendations and guidelines of the FELASA (Federation for Laboratory Animal Science Associations) and Society of Laboratory Animals (GV-SOLAS) and approved by the institutional review board and local authorities (Behörde für Gesundheit und Verbraucherschutz, Amt für Verbraucherschutz, Freie und Hansestadt Hamburg, reference number N044/2021). Mice were maintained on a 12-hour dark/12-hour light cycle with free access to food and water.

8.5.1 Genotyping

Tail biopsies of newborn mice were digested at 95°C for 45 min in 100 µl of 50 mM NaOH. After a short cool down 10 µl of 1M Tris/HCl (pH 8.0) were added to neutralize the NaOH. Undigested tissue was pelleted by centrifugation (5 min at

16000 x g). Supernatants were used for PCR reaction as shown below. PCR products were analyzed by agarose gel electrophoresis in a 2 % (w/v) TAE agarose gel.

Reaction setup:

Component	Amount
10x DreamTaq Green Buffer	2.5 µl
dNTPs (10 mM each)	0.5 µl
Primer 1 (10 µM)	1 µl
Primer 2 (10 µM)	1 µl
Primer 3 (10 µM) or H_2O (if only 2 primers)	1 µl
DreamTaq DNA Polymerase	0.25 µl
Template DNA	1 µl
Autoclaved distilled water	up to 25 µl

Cycling conditions:

	DreamTaq		
Cycle Step	Temperature	Time	Cycle(s)
Initial denaturation	95°C	2 min	1
Denaturation	95°C	30 s	30-35
Annealing	Tm-5°C	30 s	
Extension	72°C	1min/kb	
Final extension	72°C	5 min	1

8.5.2 Breeding of transgenic mice

In order to obtain transgenic mice with either inducible whole-body knockout of HMGB1 or embryonic HMGB1 knockout in myeloid cells, Cre-loxP recombination system was used. Therefore, cross breeding of *HMGB1*$^{f/f}$ mice with either LysM-Cre

or UBC-CreERT2 mice was performed. *HMGB1*$^{f/f}$ mice encode loxP sites flanking exons 2 – 4 of the *Hmgb1* gene, thereby providing one essential part of the Cre-loxP recombination system. The Cre recombinase was encoded by the respective breeding partner and expressed either under control of the *Lyz2* promoter (i.e. LysM-Cre) only active in myeloid cells or under control of the ubiquitin 2 (UBC-Cre) promoter active in every cell type. Since embryonic whole-body knockout of HMGB1 is lethal in early life, UBC-CreERT2 mice encode a modified Cre fused to a mutant estrogen ligand-binding domain (ERT2). This allows induction of knockouts in adult mice by tamoxifen treatment and subsequent activation of the CreERT2 recombinase.

Homozygous Hmgb1$^{fl/fl}$ were cross-breed with heterozygous Cre-mice (either UBC- or LysM-Cre) resulting in litters being either *Hmgb1*$^{fl/fl}$ or *Hmgb1*$^{fl/cre}$. In all experiments, *Hmgb1*$^{fl/fl}$ littermates were used as control.

8.5.3 Tamoxifen treatment and infection of mice

In order to induce whole-body knockout of HMGB1 (*ΔHmgb1*^{UBC}) 8-week old mice (knockout and control animals) were injected intraperitoneally 5 days in a row with 75 mg/kg body weight of tamoxifen. Prior to injection tamoxifen was freshly dissolved in corn oil by shaking overnight at 37°C in the dark. Afterwards, tamoxifen-oil solution was stored at 4°C until usage. Seven weeks after tamoxifen treatment mice were infected.

On day 0, mice were infected i.p. with either 1x10^6 pfu or 2x10^5 pfu of MCMV as indicated in a maximum volume of 10 µl/g body weight. Animals of the control groups were injected with the same volume of sterile PBS. After infection, mice were closely monitored for signs of infection until they were sacrificed after indicated time points (e.g. 3 or 7 days).

8.5.4 Organ harvest

Immediately after sacrificing the mice, blood, lung, liver and spleen were harvested from every mouse for further analysis. Blood was collected in a reaction tube containing gel with clotting activator. After minimum 20 min incubation at room temperature, blood samples were centrifuged 15 min at 2000x g to separate the

serum. Serum was aliquoted and stored at -80°C until further analysis. A piece of lung, liver and spleen were either immediately frozen on dry ice, or transferred to a homogenizer tube containing 500 µl of DMEM with 3 % FCS (i.e. for plaque assay).

References

1. Ho, M., *The history of cytomegalovirus and its diseases.* Med Microbiol Immunol, 2008. **197**(2): p. 65-73.
2. Cannon, M.J., D.S. Schmid, and T.B. Hyde, *Review of cytomegalovirus seroprevalence and demographic characteristics associated with infection.* Rev Med Virol, 2010. **20**(4): p. 202-13.
3. Deayton, J.R., et al., *Importance of cytomegalovirus viraemia in risk of disease progression and death in HIV-infected patients receiving highly active antiretroviral therapy.* Lancet, 2004. **363**(9427): p. 2116-21.
4. Lumbreras, C., et al., *Cytomegalovirus infection in solid organ transplant recipients.* Clin Microbiol Infect, 2014. **20 Suppl 7**: p. 19-26.
5. *Babies Born with Congenital CMV*. 2022 27.05.2022 17.04.2024]; Available from: https://www.cdc.gov/cmv/congenital-infection.html.
6. Akpan, U.S. and L.S. Pillarisetty, *Congenital Cytomegalovirus Infection*, in *StatPearls*. 2024: Treasure Island (FL) ineligible companies. Disclosure: Leela Sharath Pillarisetty declares no relevant financial relationships with ineligible companies.
7. Ahmed, A., *Antiviral treatment of cytomegalovirus infection.* Infect Disord Drug Targets, 2011. **11**(5): p. 475-503.
8. El Helou, G. and R.R. Razonable, *Letermovir for the prevention of cytomegalovirus infection and disease in transplant recipients: an evidence-based review.* Infect Drug Resist, 2019. **12**: p. 1481-1491.
9. Tan, B.H., *Cytomegalovirus Treatment.* Curr Treat Options Infect Dis, 2014. **6**(3): p. 256-270.
10. Gibson, W., *Structure and formation of the cytomegalovirus virion.* Curr Top Microbiol Immunol, 2008. **325**: p. 187-204.
11. Brocchieri, L., et al., *Predicting coding potential from genome sequence: application to betaherpesviruses infecting rats and mice.* J Virol, 2005. **79**(12): p. 7570-96.
12. Dolan, A., et al., *Genetic content of wild-type human cytomegalovirus.* J Gen Virol, 2004. **85**(Pt 5): p. 1301-1312.
13. Murphy, E. and T. Shenk, *Human cytomegalovirus genome.* Curr Top Microbiol Immunol, 2008. **325**: p. 1-19.
14. Chen, D.H., et al., *Three-dimensional visualization of tegument/capsid interactions in the intact human cytomegalovirus.* Virology, 1999. **260**(1): p. 10-6.
15. Farrar, G.H. and J.D. Oram, *Characterization of the human cytomegalovirus envelope glycoproteins.* J Gen Virol, 1984. **65 (Pt 11)**: p. 1991-2001.
16. Read, C., P. Walther, and J. von Einem, *Quantitative Electron Microscopy to Study HCMV Morphogenesis.* Methods Mol Biol, 2021. **2244**: p. 265-289.
17. Wu, Y., et al., *Human cytomegalovirus glycoprotein complex gH/gL/gO uses PDGFR-alpha as a key for entry.* PLoS Pathog, 2017. **13**(4): p. e1006281.
18. Martinez-Martin, N., et al., *An Unbiased Screen for Human Cytomegalovirus Identifies Neuropilin-2 as a Central Viral Receptor.* Cell, 2018. **174**(5): p. 1158-1171 e19.
19. Murray, M.J., N.E. Peters, and M.B. Reeves, *Navigating the Host Cell Response during Entry into Sites of Latent Cytomegalovirus Infection.* Pathogens, 2018. **7**(1).

20. Ogawa-Goto, K., et al., *Microtubule network facilitates nuclear targeting of human cytomegalovirus capsid.* J Virol, 2003. **77**(15): p. 8541-7.
21. Fu, Y.Z., et al., *Human Cytomegalovirus Tegument Protein UL82 Inhibits STING-Mediated Signaling to Evade Antiviral Immunity.* Cell Host Microbe, 2017. **21**(2): p. 231-243.
22. Kalejta, R.F., *Functions of human cytomegalovirus tegument proteins prior to immediate early gene expression.* Curr Top Microbiol Immunol, 2008. **325**: p. 101-15.
23. McCormick, A.L., et al., *The human cytomegalovirus UL36 gene controls caspase-dependent and -independent cell death programs activated by infection of monocytes differentiating to macrophages.* J Virol, 2010. **84**(10): p. 5108-23.
24. McSharry, B.P., S. Avdic, and B. Slobedman, *Human cytomegalovirus encoded homologs of cytokines, chemokines and their receptors: roles in immunomodulation.* Viruses, 2012. **4**(11): p. 2448-70.
25. Stinski, M.F., *Sequence of protein synthesis in cells infected by human cytomegalovirus: early and late virus-induced polypeptides.* J Virol, 1978. **26**(3): p. 686-701.
26. Tandon, R., E.S. Mocarski, and J.F. Conway, *The A, B, Cs of herpesvirus capsids.* Viruses, 2015. **7**(3): p. 899-914.
27. Reeves, M. and J. Sinclair, *Aspects of human cytomegalovirus latency and reactivation.* Curr Top Microbiol Immunol, 2008. **325**: p. 297-313.
28. Sinclair, J. and P. Sissons, *Latency and reactivation of human cytomegalovirus.* J Gen Virol, 2006. **87**(Pt 7): p. 1763-1779.
29. Jean Beltran, P.M. and I.M. Cristea, *The life cycle and pathogenesis of human cytomegalovirus infection: lessons from proteomics.* Expert Rev Proteomics, 2014. **11**(6): p. 697-711.
30. Schmid, M., et al., *DNA virus replication compartments.* J Virol, 2014. **88**(3): p. 1404-20.
31. Caragliano, E., et al., *Human cytomegalovirus forms phase-separated compartments at viral genomes to facilitate viral replication.* Cell Rep, 2022. **38**(10): p. 110469.
32. Hyman, A.A., C.A. Weber, and F. Julicher, *Liquid-liquid phase separation in biology.* Annu Rev Cell Dev Biol, 2014. **30**: p. 39-58.
33. Lin, Y., et al., *Formation and Maturation of Phase-Separated Liquid Droplets by RNA-Binding Proteins.* Mol Cell, 2015. **60**(2): p. 208-19.
34. Saar, K.L., et al., *Learning the molecular grammar of protein condensates from sequence determinants and embeddings.* Proc Natl Acad Sci U S A, 2021. **118**(15).
35. Snaar, S.P., M. Vincent, and R.W. Dirks, *RNA polymerase II localizes at sites of human cytomegalovirus immediate-early RNA synthesis and processing.* J Histochem Cytochem, 1999. **47**(2): p. 245-54.
36. Tran, K., J.A. Mahr, and D.H. Spector, *Proteasome subunits relocalize during human cytomegalovirus infection, and proteasome activity is necessary for efficient viral gene transcription.* J Virol, 2010. **84**(6): p. 3079-93.
37. Demogines, A., et al., *Dual host-virus arms races shape an essential housekeeping protein.* PLoS Biol, 2013. **11**(5): p. e1001571.
38. Perot, K., C.M. Walker, and R.R. Spaete, *Primary chimpanzee skin fibroblast cells are fully permissive for human cytomegalovirus replication.* J Gen Virol, 1992. **73 (Pt 12)**: p. 3281-4.

39. Smith, C.B., L.S. Wei, and M. Griffiths, *Mouse cytomegalovirus is infectious for rats and alters lymphocyte subsets and spleen cell proliferation.* Arch Virol, 1986. **90**(3-4): p. 313-23.
40. Lafemina, R.L. and G.S. Hayward, *Differences in cell-type-specific blocks to immediate early gene expression and DNA replication of human, simian and murine cytomegalovirus.* J Gen Virol, 1988. **69 (Pt 2)**: p. 355-74.
41. Walker, D. and J. Hudson, *Analysis of immediate-early and early proteins of murine cytomegalovirus in permissive and nonpermissive cells.* Arch Virol, 1987. **92**(1-2): p. 103-19.
42. Brizic, I., et al., *Mouse Models for Cytomegalovirus Infections in Newborns and Adults.* Curr Protoc, 2022. **2**(9): p. e537.
43. Brune, W., H. Hengel, and U.H. Koszinowski, *A mouse model for cytomegalovirus infection.* Curr Protoc Immunol, 2001. **Chapter 19**: p. Unit 19 7.
44. Reddehase, M.J. and N.A.W. Lemmermann, *Mouse Model of Cytomegalovirus Disease and Immunotherapy in the Immunocompromised Host: Predictions for Medical Translation that Survived the "Test of Time".* Viruses, 2018. **10**(12).
45. Sinzger, C. and G. Jahn, *Human cytomegalovirus cell tropism and pathogenesis.* Intervirology, 1996. **39**(5-6): p. 302-19.
46. Jackson, J.W. and T. Sparer, *There Is Always Another Way! Cytomegalovirus' Multifaceted Dissemination Schemes.* Viruses, 2018. **10**(7).
47. Farrell, H.E., et al., *Alveolar Macrophages Are a Prominent but Nonessential Target for Murine Cytomegalovirus Infecting the Lungs.* J Virol, 2015. **90**(6): p. 2756-66.
48. Schleimer, R.P., et al., *Epithelium: at the interface of innate and adaptive immune responses.* J Allergy Clin Immunol, 2007. **120**(6): p. 1279-84.
49. Bentz, G.L., et al., *Human cytomegalovirus (HCMV) infection of endothelial cells promotes naive monocyte extravasation and transfer of productive virus to enhance hematogenous dissemination of HCMV.* J Virol, 2006. **80**(23): p. 11539-55.
50. Baasch, S., Z. Ruzsics, and P. Henneke, *Cytomegaloviruses and Macrophages-Friends and Foes From Early on?* Front Immunol, 2020. **11**: p. 793.
51. Sacher, T., et al., *The major virus-producing cell type during murine cytomegalovirus infection, the hepatocyte, is not the source of virus dissemination in the host.* Cell Host Microbe, 2008. **3**(4): p. 263-72.
52. Imre, G., *Cell death signalling in virus infection.* Cell Signal, 2020. **76**: p. 109772.
53. Liu, X., et al., *Epstein-Barr virus encoded latent membrane protein 1 suppresses necroptosis through targeting RIPK1/3 ubiquitination.* Cell Death Dis, 2018. **9**(2): p. 53.
54. Croft, S.N., E.J. Walker, and R. Ghildyal, *Human Rhinovirus 3C protease cleaves RIPK1, concurrent with caspase 8 activation.* Sci Rep, 2018. **8**(1): p. 1569.
55. Kerr, J.F., A.H. Wyllie, and A.R. Currie, *Apoptosis: a basic biological phenomenon with wide-ranging implications in tissue kinetics.* Br J Cancer, 1972. **26**(4): p. 239-57.
56. Suzuki, J., et al., *Xk-related protein 8 and CED-8 promote phosphatidylserine exposure in apoptotic cells.* Science, 2013. **341**(6144): p. 403-6.

57. Vandenabeele, P., et al., *Immunogenic Apoptotic Cell Death and Anticancer Immunity.* Adv Exp Med Biol, 2016. **930**: p. 133-49.
58. Elmore, S., *Apoptosis: a review of programmed cell death.* Toxicol Pathol, 2007. **35**(4): p. 495-516.
59. Menard, C., et al., *Role of murine cytomegalovirus US22 gene family members in replication in macrophages.* J Virol, 2003. **77**(10): p. 5557-70.
60. Skaletskaya, A., et al., *A cytomegalovirus-encoded inhibitor of apoptosis that suppresses caspase-8 activation.* Proc Natl Acad Sci U S A, 2001. **98**(14): p. 7829-34.
61. Tait, S.W. and D.R. Green, *Mitochondrial regulation of cell death.* Cold Spring Harb Perspect Biol, 2013. **5**(9).
62. Li, P., et al., *Cytochrome c and dATP-dependent formation of Apaf-1/caspase-9 complex initiates an apoptotic protease cascade.* Cell, 1997. **91**(4): p. 479-89.
63. Gaspar, M. and T. Shenk, *Human cytomegalovirus inhibits a DNA damage response by mislocalizing checkpoint proteins.* Proc Natl Acad Sci U S A, 2006. **103**(8): p. 2821-6.
64. Isler, J.A., A.H. Skalet, and J.C. Alwine, *Human cytomegalovirus infection activates and regulates the unfolded protein response.* J Virol, 2005. **79**(11): p. 6890-9.
65. Goldmacher, V.S., et al., *A cytomegalovirus-encoded mitochondria-localized inhibitor of apoptosis structurally unrelated to Bcl-2.* Proc Natl Acad Sci U S A, 1999. **96**(22): p. 12536-41.
66. Cam, M., et al., *Cytomegaloviruses inhibit Bak- and Bax-mediated apoptosis with two separate viral proteins.* Cell Death Differ, 2010. **17**(4): p. 655-65.
67. Ketelut-Carneiro, N. and K.A. Fitzgerald, *Apoptosis, Pyroptosis, and Necroptosis-Oh My! The Many Ways a Cell Can Die.* J Mol Biol, 2022. **434**(4): p. 167378.
68. Jha, S., W.J. Brickey, and J.P. Ting, *Inflammasomes in Myeloid Cells: Warriors Within.* Microbiol Spectr, 2017. **5**(1).
69. Fink, S.L. and B.T. Cookson, *Caspase-1-dependent pore formation during pyroptosis leads to osmotic lysis of infected host macrophages.* Cell Microbiol, 2006. **8**(11): p. 1812-25.
70. Shi, J., et al., *Cleavage of GSDMD by inflammatory caspases determines pyroptotic cell death.* Nature, 2015. **526**(7575): p. 660-5.
71. Schroder, K. and J. Tschopp, *The inflammasomes.* Cell, 2010. **140**(6): p. 821-32.
72. Kumar, A., G. Stavrakis, and A.H. Karaba, *Herpesviruses and Inflammasomes: One Sensor Does Not Fit All.* mBio, 2022. **13**(1): p. e0173721.
73. Deng, Y., E. Ostermann, and W. Brune, *A cytomegalovirus inflammasome inhibitor reduces proinflammatory cytokine release and pyroptosis.* Nat Commun, 2024. **15**(1): p. 786.
74. Weinlich, R., et al., *Necroptosis in development, inflammation and disease.* Nat Rev Mol Cell Biol, 2017. **18**(2): p. 127-136.
75. Wang, H., et al., *Mixed lineage kinase domain-like protein MLKL causes necrotic membrane disruption upon phosphorylation by RIP3.* Mol Cell, 2014. **54**(1): p. 133-146.
76. Pasparakis, M. and P. Vandenabeele, *Necroptosis and its role in inflammation.* Nature, 2015. **517**(7534): p. 311-20.

77. Upton, J.W., W.J. Kaiser, and E.S. Mocarski, *DAI/ZBP1/DLM-1 complexes with RIP3 to mediate virus-induced programmed necrosis that is targeted by murine cytomegalovirus vIRA.* Cell Host Microbe, 2012. **11**(3): p. 290-7.
78. Upton, J.W., W.J. Kaiser, and E.S. Mocarski, *Cytomegalovirus M45 cell death suppression requires receptor-interacting protein (RIP) homotypic interaction motif (RHIM)-dependent interaction with RIP1.* J Biol Chem, 2008. **283**(25): p. 16966-70.
79. Upton, J.W., W.J. Kaiser, and E.S. Mocarski, *Virus inhibition of RIP3-dependent necrosis.* Cell Host Microbe, 2010. **7**(4): p. 302-313.
80. Fletcher-Etherington, A., et al., *Human cytomegalovirus protein pUL36: A dual cell death pathway inhibitor.* Proc Natl Acad Sci U S A, 2020. **117**(31): p. 18771-18779.
81. Goodwin, G.H. and E.W. Johns, *Isolation and characterisation of two calf-thymus chromatin non-histone proteins with high contents of acidic and basic amino acids.* Eur J Biochem, 1973. **40**(1): p. 215-9.
82. Bustin, M., *Revised nomenclature for high mobility group (HMG) chromosomal proteins.* Trends Biochem Sci, 2001. **26**(3): p. 152-3.
83. Bustin, M., *Regulation of DNA-dependent activities by the functional motifs of the high-mobility-group chromosomal proteins.* Mol Cell Biol, 1999. **19**(8): p. 5237-46.
84. Goodwin, G.H. and E.W. Johns, *Are the high mobility group non-histone chromosomal proteins associated with 'active' chromatin?* Biochim Biophys Acta, 1978. **519**(1): p. 279-84.
85. Griess, E.A., et al., *Phylogenetic relationships of HMG box DNA-binding domains.* J Mol Evol, 1993. **37**(2): p. 204-10.
86. Laudet, V., D. Stehelin, and H. Clevers, *Ancestry and diversity of the HMG box superfamily.* Nucleic Acids Res, 1993. **21**(10): p. 2493-501.
87. Kang, R., et al., *HMGB1 in health and disease.* Mol Aspects Med, 2014. **40**: p. 1-116.
88. Romani, M., et al., *Serological analysis of species specificity in the high mobility group chromosomal proteins.* J Biol Chem, 1979. **254**(8): p. 2918-22.
89. Ferrari, S., et al., *The mouse gene coding for high mobility group 1 protein (HMG1).* J Biol Chem, 1994. **269**(46): p. 28803-8.
90. Gariboldi, M., et al., *Mapping of the Hmg1 gene and of seven related sequences in the mouse.* Mamm Genome, 1995. **6**(9): p. 581-5.
91. Wen, L., et al., *A human placental cDNA clone that encodes nonhistone chromosomal protein HMG-1.* Nucleic Acids Res, 1989. **17**(3): p. 1197-214.
92. Prasad, S. and M.K. Thakur, *Distribution of high mobility group proteins in different tissues of rats during aging.* Biochem Int, 1990. **20**(4): p. 687-95.
93. Cabart, P., et al., *Differential expression of nuclear HMG1, HMG2 proteins and H1(zero) histone in various blood cells.* Cell Biochem Funct, 1995. **13**(2): p. 125-33.
94. Phair, R.D., et al., *Global nature of dynamic protein-chromatin interactions in vivo: three-dimensional genome scanning and dynamic interaction networks of chromatin proteins.* Mol Cell Biol, 2004. **24**(14): p. 6393-402.
95. Sapojnikova, N., et al., *Biochemical observation of the rapid mobility of nuclear HMGB1.* Biochim Biophys Acta, 2005. **1729**(1): p. 57-63.
96. Ferrari, S., et al., *The active gene that encodes human high mobility group 1 protein (HMG1) contains introns and maps to chromosome 13.* Genomics, 1996. **35**(2): p. 367-71.

97. Bianchi, M.E., et al., *The DNA binding site of HMG1 protein is composed of two similar segments (HMG boxes), both of which have counterparts in other eukaryotic regulatory proteins.* EMBO J, 1992. **11**(3): p. 1055-63.
98. Bonaldi, T., et al., *Monocytic cells hyperacetylate chromatin protein HMGB1 to redirect it towards secretion.* EMBO J, 2003. **22**(20): p. 5551-60.
99. Hardman, C.H., et al., *Structure of the A-domain of HMG1 and its interaction with DNA as studied by heteronuclear three- and four-dimensional NMR spectroscopy.* Biochemistry, 1995. **34**(51): p. 16596-607.
100. Ohndorf, U.M., et al., *Basis for recognition of cisplatin-modified DNA by high-mobility-group proteins.* Nature, 1999. **399**(6737): p. 708-12.
101. Stott, K., et al., *Structure of a complex of tandem HMG boxes and DNA.* J Mol Biol, 2006. **360**(1): p. 90-104.
102. Thomas, J.O. and A.A. Travers, *HMG1 and 2, and related 'architectural' DNA-binding proteins.* Trends Biochem Sci, 2001. **26**(3): p. 167-74.
103. Weir, H.M., et al., *Structure of the HMG box motif in the B-domain of HMG1.* EMBO J, 1993. **12**(4): p. 1311-9.
104. Mensah, M.A., et al., *Aberrant phase separation and nucleolar dysfunction in rare genetic diseases.* Nature, 2023. **614**(7948): p. 564-571.
105. Carballo, M., et al., *Interaction between domains in chromosomal protein HMG-1.* EMBO J, 1984. **3**(6): p. 1255-61.
106. Cary, P.D., et al., *Conformation and domain structure of the non-histone chromosomal proteins HMG 1 and 2. Domain interactions.* Eur J Biochem, 1984. **143**(2): p. 323-30.
107. Hoppe, G., et al., *Molecular basis for the redox control of nuclear transport of the structural chromatin protein Hmgb1.* Exp Cell Res, 2006. **312**(18): p. 3526-38.
108. Tang, D., et al., *High-mobility group box 1, oxidative stress, and disease.* Antioxid Redox Signal, 2011. **14**(7): p. 1315-35.
109. He, S.J., et al., *The dual role and therapeutic potential of high-mobility group box 1 in cancer.* Oncotarget, 2017. **8**(38): p. 64534-64550.
110. Isackson, P.J., et al., *High mobility group chromosomal proteins isolated from muclei and cytosol of cultured hepatoma cells are similar.* Biochemistry, 1980. **19**(19): p. 4466-71.
111. Sun, R., et al., *PCV2 Induces Reactive Oxygen Species To Promote Nucleocytoplasmic Translocation of the Viral DNA Binding Protein HMGB1 To Enhance Its Replication.* J Virol, 2020. **94**(13).
112. Wang, B., et al., *Minocycline prevents the depressive-like behavior through inhibiting the release of HMGB1 from microglia and neurons.* Brain Behav Immun, 2020. **88**: p. 132-143.
113. Ge, X., et al., *High mobility group box-1 (HMGB1) participates in the pathogenesis of alcoholic liver disease (ALD).* J Biol Chem, 2014. **289**(33): p. 22672-22691.
114. Oh, Y.J., et al., *HMGB1 is phosphorylated by classical protein kinase C and is secreted by a calcium-dependent mechanism.* J Immunol, 2009. **182**(9): p. 5800-9.
115. Scaffidi, P., T. Misteli, and M.E. Bianchi, *Release of chromatin protein HMGB1 by necrotic cells triggers inflammation.* Nature, 2002. **418**(6894): p. 191-5.
116. Xu, S., et al., *Evidence for SIRT1 Mediated HMGB1 Release From Kidney Cells in the Early Stages of Hemorrhagic Shock.* Front Physiol, 2019. **10**: p. 854.

117. Lu, B., et al., *Molecular mechanism and therapeutic modulation of high mobility group box 1 release and action: an updated review.* Expert Rev Clin Immunol, 2014. **10**(6): p. 713-27.
118. Cui, T., et al., *Oxidative Stress-Induced HMGB1 Release from Melanocytes: A Paracrine Mechanism Underlying the Cutaneous Inflammation in Vitiligo.* J Invest Dermatol, 2019. **139**(10): p. 2174-2184 e4.
119. Hosakote, Y.M., et al., *Respiratory Syncytial Virus Infection Triggers Epithelial HMGB1 Release as a Damage-Associated Molecular Pattern Promoting a Monocytic Inflammatory Response.* J Virol, 2016. **90**(21): p. 9618-9631.
120. Ito, N., et al., *Cytolytic cells induce HMGB1 release from melanoma cell lines.* J Leukoc Biol, 2007. **81**(1): p. 75-83.
121. Kim, Y.H., et al., *N-linked glycosylation plays a crucial role in the secretion of HMGB1.* J Cell Sci, 2016. **129**(1): p. 29-38.
122. Tsung, A., et al., *HMGB1 release induced by liver ischemia involves Toll-like receptor 4 dependent reactive oxygen species production and calcium-mediated signaling.* J Exp Med, 2007. **204**(12): p. 2913-23.
123. Wu, F., et al., *High mobility group box 1 protein is methylated and transported to cytoplasm in clear cell renal cell carcinoma.* Asian Pac J Cancer Prev, 2013. **14**(10): p. 5789-95.
124. Wang, H., et al., *HMG-1 as a late mediator of endotoxin lethality in mice.* Science, 1999. **285**(5425): p. 248-51.
125. Kwak, M.S., et al., *Immunological Significance of HMGB1 Post-Translational Modification and Redox Biology.* Front Immunol, 2020. **11**: p. 1189.
126. Palade, G., *Intracellular aspects of the process of protein synthesis.* Science, 1975. **189**(4206): p. 867.
127. Tang, D., et al., *Hydrogen peroxide stimulates macrophages and monocytes to actively release HMGB1.* J Leukoc Biol, 2007. **81**(3): p. 741-7.
128. Hiramoto, S., et al., *Cystitis-Related Bladder Pain Involves ATP-Dependent HMGB1 Release from Macrophages and Its Downstream H(2)S/Ca(v)3.2 Signaling in Mice.* Cells, 2020. **9**(8).
129. Huang, W., et al., *Heat stress induces RIP1/RIP3-dependent necroptosis through the MAPK, NF-kappaB, and c-Jun signaling pathways in pulmonary vascular endothelial cells.* Biochem Biophys Res Commun, 2020. **528**(1): p. 206-212.
130. Lin, F., et al., *Ox-LDL induces endothelial cell apoptosis and macrophage migration by regulating caveolin-1 phosphorylation.* J Cell Physiol, 2018. **233**(10): p. 6683-6692.
131. Mohanty, S.K., et al., *High Mobility Group Box 1 Release by Cholangiocytes Governs Biliary Atresia Pathogenesis and Correlates With Increases in Afflicted Infants.* Hepatology, 2021. **74**(2): p. 864-878.
132. Wang, C.M., M. Jiang, and H.J. Wang, *Effect of NF□kappaB inhibitor on high□mobility group protein B1 expression in a COPD rat model.* Mol Med Rep, 2013. **7**(2): p. 499-502.
133. Volchuk, A., et al., *Indirect regulation of HMGB1 release by gasdermin D.* Nat Commun, 2020. **11**(1): p. 4561.
134. Khambu, B., et al., *HMGB1 promotes ductular reaction and tumorigenesis in autophagy-deficient livers.* J Clin Invest, 2018. **128**(6): p. 2419-2435.
135. Murakami, Y., et al., *Programmed necrosis, not apoptosis, is a key mediator of cell loss and DAMP-mediated inflammation in dsRNA-induced retinal degeneration.* Cell Death Differ, 2014. **21**(2): p. 270-7.

136. Schiller, M., et al., *During apoptosis HMGB1 is translocated into apoptotic cell-derived membranous vesicles.* Autoimmunity, 2013. **46**(5): p. 342-6.
137. Velegraki, M., et al., *Impaired clearance of apoptotic cells leads to HMGB1 release in the bone marrow of patients with myelodysplastic syndromes and induces TLR4-mediated cytokine production.* Haematologica, 2013. **98**(8): p. 1206-15.
138. Yang, H., et al., *The many faces of HMGB1: molecular structure-functional activity in inflammation, apoptosis, and chemotaxis.* J Leukoc Biol, 2013. **93**(6): p. 865-73.
139. Bernues, J., E. Espel, and E. Querol, *Identification of the core-histone-binding domains of HMG1 and HMG2.* Biochim Biophys Acta, 1986. **866**(4): p. 242-51.
140. Bernues, J., et al., *Detection by chemical cross-linking of interaction between high mobility group protein 1 and histone oligomers in free solution.* J Biol Chem, 1983. **258**(18): p. 11020-4.
141. Celona, B., et al., *Substantial histone reduction modulates genomewide nucleosomal occupancy and global transcriptional output.* PLoS Biol, 2011. **9**(6): p. e1001086.
142. Stros, M. and A. Kolibalova, *Interaction of non-histone proteins HMG1 and HMG2 with core histones in nucleosomes and core particles revealed by chemical cross-linking.* Eur J Biochem, 1987. **162**(1): p. 111-8.
143. Travers, A.A., *Priming the nucleosome: a role for HMGB proteins?* EMBO Rep, 2003. **4**(2): p. 131-6.
144. Javaherian, K., J.F. Liu, and J.C. Wang, *Nonhistone proteins HMG1 and HMG2 change the DNA helical structure.* Science, 1978. **199**(4335): p. 1345-6.
145. Paull, T.T., M.J. Haykinson, and R.C. Johnson, *The nonspecific DNA-binding and -bending proteins HMG1 and HMG2 promote the assembly of complex nucleoprotein structures.* Genes Dev, 1993. **7**(8): p. 1521-34.
146. Banerjee, S. and T.K. Kundu, *The acidic C-terminal domain and A-box of HMGB-1 regulates p53-mediated transcription.* Nucleic Acids Res, 2003. **31**(12): p. 3236-47.
147. Zhang, X.J., Z.G. Luan, and X.C. Ma, *shRNAs targeting high-mobility group box-1 inhibit E-selectin expression via homeobox A9 in human umbilical vein endothelial cells.* Mol Med Rep, 2013. **7**(4): p. 1251-6.
148. Pasheva, E.A., I.G. Pashev, and A. Favre, *Preferential binding of high mobility group 1 protein to UV-damaged DNA. Role of the COOH-terminal domain.* J Biol Chem, 1998. **273**(38): p. 24730-6.
149. Yuan, F., et al., *Evidence for involvement of HMGB1 protein in human DNA mismatch repair.* J Biol Chem, 2004. **279**(20): p. 20935-40.
150. Nagaki, S., et al., *Non-histone chromosomal proteins HMG1 and 2 enhance ligation reaction of DNA double-strand breaks.* Biochem Biophys Res Commun, 1998. **246**(1): p. 137-41.
151. Yumoto, Y., et al., *High mobility group proteins 1 and 2 can function as DNA-binding regulatory components for DNA-dependent protein kinase in vitro.* J Biochem, 1998. **124**(3): p. 519-27.
152. Kuehl, L., B. Salmond, and L. Tran, *Concentrations of high-mobility-group proteins in the nucleus and cytoplasm of several rat tissues.* J Cell Biol, 1984. **99**(2): p. 648-54.
153. Tang, D., et al., *Endogenous HMGB1 regulates autophagy.* J Cell Biol, 2010. **190**(5): p. 881-92.

154. Zhu, X., et al., *Cytosolic HMGB1 controls the cellular autophagy/apoptosis checkpoint during inflammation.* J Clin Invest, 2015. **125**(3): p. 1098-110.
155. Qin, Y., et al., *HMGB1-LPS complex promotes transformation of osteoarthritis synovial fibroblasts to a rheumatoid arthritis synovial fibroblast-like phenotype.* Cell Death Dis, 2014. **5**(2): p. e1077.
156. Urbonaviciute, V., et al., *Induction of inflammatory and immune responses by HMGB1-nucleosome complexes: implications for the pathogenesis of SLE.* J Exp Med, 2008. **205**(13): p. 3007-18.
157. Garcia-Arnandis, I., et al., *High mobility group box 1 potentiates the pro-inflammatory effects of interleukin-1beta in osteoarthritic synoviocytes.* Arthritis Res Ther, 2010. **12**(4): p. R165.
158. Kew, R.R., et al., *The IKKalpha-dependent NF-kappaB p52/RelB noncanonical pathway is essential to sustain a CXCL12 autocrine loop in cells migrating in response to HMGB1.* J Immunol, 2012. **188**(5): p. 2380-6.
159. Watanabe, H. and M. Son, *The Immune Tolerance Role of the HMGB1-RAGE Axis.* Cells, 2021. **10**(3).
160. LeBlanc, P.M., et al., *An immunogenic peptide in the A-box of HMGB1 protein reverses apoptosis-induced tolerance through RAGE receptor.* J Biol Chem, 2014. **289**(11): p. 7777-86.
161. Abeyama, K., et al., *The N-terminal domain of thrombomodulin sequesters high-mobility group-B1 protein, a novel antiinflammatory mechanism.* J Clin Invest, 2005. **115**(5): p. 1267-74.
162. Ito, T., et al., *Proteolytic cleavage of high mobility group box 1 protein by thrombin-thrombomodulin complexes.* Arterioscler Thromb Vasc Biol, 2008. **28**(10): p. 1825-30.
163. Kikuchi, K., et al., *Minocycline attenuates both OGD-induced HMGB1 release and HMGB1-induced cell death in ischemic neuronal injury in PC12 cells.* Biochem Biophys Res Commun, 2009. **385**(2): p. 132-6.
164. Xu, J., et al., *Macrophage endocytosis of high-mobility group box 1 triggers pyroptosis.* Cell Death Differ, 2014. **21**(8): p. 1229-39.
165. Palumbo, R. and M.E. Bianchi, *High mobility group box 1 protein, a cue for stem cell recruitment.* Biochem Pharmacol, 2004. **68**(6): p. 1165-70.
166. Palumbo, R., et al., *Extracellular HMGB1, a signal of tissue damage, induces mesoangioblast migration and proliferation.* J Cell Biol, 2004. **164**(3): p. 441-9.
167. Tamai, K., et al., *PDGFRalpha-positive cells in bone marrow are mobilized by high mobility group box 1 (HMGB1) to regenerate injured epithelia.* Proc Natl Acad Sci U S A, 2011. **108**(16): p. 6609-14.
168. Ranzato, E., et al., *HMGb1 promotes scratch wound closure of HaCaT keratinocytes via ERK1/2 activation.* Mol Cell Biochem, 2009. **332**(1-2): p. 199-205.
169. Schlueter, C., et al., *Angiogenetic signaling through hypoxia: HMGB1: an angiogenetic switch molecule.* Am J Pathol, 2005. **166**(4): p. 1259-63.
170. Zetterstrom, C.K., et al., *High mobility group box chromosomal protein 1 (HMGB1) is an antibacterial factor produced by the human adenoid.* Pediatr Res, 2002. **52**(2): p. 148-54.
171. Yanai, H., et al., *Conditional ablation of HMGB1 in mice reveals its protective function against endotoxemia and bacterial infection.* Proc Natl Acad Sci U S A, 2013. **110**(51): p. 20699-704.
172. Volmari, A., et al., *Leukocyte-Derived High-Mobility Group Box 1 Governs Hepatic Immune Responses to Listeria monocytogenes.* Hepatol Commun, 2021. **5**(12): p. 2104-2120.

173. Tadie, J.M., et al., *HMGB1 promotes neutrophil extracellular trap formation through interactions with Toll-like receptor 4.* Am J Physiol Lung Cell Mol Physiol, 2013. **304**(5): p. L342-9.
174. Venereau, E., C. Ceriotti, and M.E. Bianchi, *DAMPs from Cell Death to New Life.* Front Immunol, 2015. **6**: p. 422.
175. Andersson, U. and K.J. Tracey, *HMGB1 is a therapeutic target for sterile inflammation and infection.* Annu Rev Immunol, 2011. **29**: p. 139-62.
176. Jung, J.H., et al., *Hepatitis C virus infection is blocked by HMGB1 released from virus-infected cells.* J Virol, 2011. **85**(18): p. 9359-68.
177. Kamau, E., et al., *Dengue virus infection promotes translocation of high mobility group box 1 protein from the nucleus to the cytosol in dendritic cells, upregulates cytokine production and modulates virus replication.* J Gen Virol, 2009. **90**(Pt 8): p. 1827-1835.
178. Cheng, B.Q., et al., *Serum high mobility group box chromosomal protein 1 is associated with clinicopathologic features in patients with hepatocellular carcinoma.* Dig Liver Dis, 2008. **40**(6): p. 446-52.
179. Kosai, K., et al., *Elevated levels of high mobility group box chromosomal protein-1 (HMGB-1) in sera from patients with severe bacterial pneumonia coinfected with influenza virus.* Scand J Infect Dis, 2008. **40**(4): p. 338-42.
180. Momonaka, H., et al., *High mobility group box 1 in patients with 2009 pandemic H1N1 influenza-associated encephalopathy.* Brain Dev, 2014. **36**(6): p. 484-8.
181. Wulandari, S., Hartono, and T. Wibawa, *The role of HMGB1 in COVID-19-induced cytokine storm and its potential therapeutic targets: A review.* Immunology, 2023. **169**(2): p. 117-131.
182. Resman Rus, K., et al., *HMGB1 Is a Potential Biomarker for Severe Viral Hemorrhagic Fevers.* PLoS Negl Trop Dis, 2016. **10**(6): p. e0004804.
183. Chen, S., et al., *High-mobility group box-1 protein from CC10(+) club cells promotes type 2 response in the later stage of respiratory syncytial virus infection.* Am J Physiol Lung Cell Mol Physiol, 2019. **316**(1): p. L280-L290.
184. Nosaka, N., et al., *Anti-high mobility group box-1 monoclonal antibody treatment of brain edema induced by influenza infection and lipopolysaccharide.* J Med Virol, 2018. **90**(7): p. 1192-1198.
185. Nosaka, N., et al., *Anti-high mobility group box-1 monoclonal antibody treatment provides protection against influenza A virus (H1N1)-induced pneumonia in mice.* Crit Care, 2015. **19**(1): p. 249.
186. Qu, Y., et al., *Newcastle disease virus infection triggers HMGB1 release to promote the inflammatory response.* Virology, 2018. **525**: p. 19-31.
187. Shi, X., et al., *Glycyrrhetinic acid alleviates hepatic inflammation injury in viral hepatitis disease via a HMGB1-TLR4 signaling pathway.* Int Immunopharmacol, 2020. **84**: p. 106578.
188. Yu, R., et al., *HMGB1 Promotes Hepatitis C Virus Replication by Interaction with Stem-Loop 4 in the Viral 5' Untranslated Region.* J Virol, 2015. **90**(5): p. 2332-44.
189. Moisy, D., et al., *HMGB1 protein binds to influenza virus nucleoprotein and promotes viral replication.* J Virol, 2012. **86**(17): p. 9122-33.
190. Zainal, N., et al., *Resveratrol treatment reveals a novel role for HMGB1 in regulation of the type 1 interferon response in dengue virus infection.* Sci Rep, 2017. **7**: p. 42998.
191. Borde, C., et al., *Stepwise release of biologically active HMGB1 during HSV-2 infection.* PLoS One, 2011. **6**(1): p. e16145.

192. Ma, Y., et al., *Peptidomic Analysis on Mouse Lung Tissue Reveals AGDP as a Potential Bioactive Peptide against Pseudorabies Virus Infection.* Int J Mol Sci, 2022. **23**(6).
193. Gustafsson, R., *Human Herpesvirus 6A Induces Dendritic Cell Death and HMGB1 Release without Virus Replication.* Pathogens, 2021. **10**(1).
194. Zhu, X., L. Sun, and Y. Wang, *High mobility group box 1 (HMGB1) is upregulated by the Epstein-Barr virus infection and promotes the proliferation of human nasopharyngeal carcinoma cells.* Acta Otolaryngol, 2016. **136**(1): p. 87-94.
195. Sprague, L., et al., *High Mobility Group Box 1 Influences HSV1716 Spread and Acts as an Adjuvant to Chemotherapy.* Viruses, 2018. **10**(3).
196. Kang, S.K., et al., *HMGB1 Knockout Decreases Kaposi's Sarcoma-Associated Herpesvirus Virion Production in iSLK BAC16 Cells by Attenuating Viral Gene Expression.* J Virol, 2021. **95**(16): p. e0079921.
197. Carrozza, M.J. and N. DeLuca, *The high mobility group protein 1 is a coactivator of herpes simplex virus ICP4 in vitro.* J Virol, 1998. **72**(8): p. 6752-7.
198. Dembowski, J.A. and N.A. DeLuca, *Selective recruitment of nuclear factors to productively replicating herpes simplex virus genomes.* PLoS Pathog, 2015. **11**(5): p. e1004939.
199. Mitsouras, K., et al., *The DNA architectural protein HMGB1 displays two distinct modes of action that promote enhanceosome assembly.* Mol Cell Biol, 2002. **22**(12): p. 4390-401.
200. Yetming, K.D., et al., *The BHLF1 Locus of Epstein-Barr Virus Contributes to Viral Latency and B-Cell Immortalization.* J Virol, 2020. **94**(17).
201. Song, M.J., et al., *The DNA architectural protein HMGB1 facilitates RTA-mediated viral gene expression in gamma-2 herpesviruses.* J Virol, 2004. **78**(23): p. 12940-50.
202. Shamay, M., et al., *A protein array screen for Kaposi's sarcoma-associated herpesvirus LANA interactors links LANA to TIP60, PP2A activity, and telomere shortening.* J Virol, 2012. **86**(9): p. 5179-91.
203. Kagele, D., et al., *Analysis of the interactions of viral and cellular factors with human cytomegalovirus lytic origin of replication, oriLyt.* Virology, 2012. **424**(2): p. 106-14.
204. Manska, S. and C.C. Rossetto, *Identification of cellular proteins associated with human cytomegalovirus (HCMV) DNA replication suggests novel cellular and viral interactions.* Virology, 2022. **566**: p. 26-41.
205. Agresti, A. and M.E. Bianchi, *HMGB proteins and gene expression.* Curr Opin Genet Dev, 2003. **13**(2): p. 170-8.
206. Bartok, E., et al., *iGLuc: a luciferase-based inflammasome and protease activity reporter.* Nat Methods, 2013. **10**(2): p. 147-154.
207. Fan, W., et al., *beta-catenin has potential effects on the expression, subcellular localization, and release of high mobility group box 1 during bovine herpesvirus 1 productive infection in MDBK cell culture.* Virulence, 2021. **12**(1): p. 1345-1361.
208. Chen, R., R. Kang, and D. Tang, *The mechanism of HMGB1 secretion and release.* Exp Mol Med, 2022. **54**(2): p. 91-102.
209. Liu, T., et al., *NF-kappaB signaling in inflammation.* Signal Transduct Target Ther, 2017. **2**: p. 17023-.
210. Singh, H. and D.K. Agrawal, *Therapeutic Potential of Targeting the HMGB1/RAGE Axis in Inflammatory Diseases.* Molecules, 2022. **27**(21).

211. Davis, K., et al., *Poly(ADP-ribosyl)ation of high mobility group box 1 (HMGB1) protein enhances inhibition of efferocytosis.* Mol Med, 2012. **18**(1): p. 359-69.
212. Yang, Y., et al., *Programmed cell death and its role in inflammation.* Mil Med Res, 2015. **2**: p. 12.
213. Patel, M.C., et al., *Serum High-Mobility-Group Box 1 as a Biomarker and a Therapeutic Target during Respiratory Virus Infections.* mBio, 2018. **9**(2).
214. Hsu, K.M., et al., *Murine cytomegalovirus displays selective infection of cells within hours after systemic administration.* J Gen Virol, 2009. **90**(Pt 1): p. 33-43.
215. Katzenstein, D.A., G.S. Yu, and M.C. Jordan, *Lethal infection with murine cytomegalovirus after early viral replication in the spleen.* J Infect Dis, 1983. **148**(3): p. 406-11.
216. Sacher, T., et al., *The role of cell types in cytomegalovirus infection in vivo.* Eur J Cell Biol, 2012. **91**(1): p. 70-7.
217. Zhang, S., et al., *MCMV exploits the spleen as a transfer hub for systemic dissemination upon oronasal inoculation.* Virus Res, 2016. **217**: p. 47-54.
218. Reddehase, M.J. and N.A.W. Lemmermann, *Cellular reservoirs of latent cytomegaloviruses.* Med Microbiol Immunol, 2019. **208**(3-4): p. 391-403.
219. Calogero, S., et al., *The lack of chromosomal protein Hmg1 does not disrupt cell growth but causes lethal hypoglycaemia in newborn mice.* Nat Genet, 1999. **22**(3): p. 276-80.
220. Harvey, D.M. and A.J. Levine, *p53 alteration is a common event in the spontaneous immortalization of primary BALB/c murine embryo fibroblasts.* Genes Dev, 1991. **5**(12B): p. 2375-85.
221. Darlington, G.J., et al., *Expression of liver phenotypes in cultured mouse hepatoma cells.* J Natl Cancer Inst, 1980. **64**(4): p. 809-19.
222. Muscolino, E., et al., *Herpesviruses induce aggregation and selective autophagy of host signalling proteins NEMO and RIPK1 as an immune-evasion mechanism.* Nat Microbiol, 2020. **5**(2): p. 331-342.
223. Tischer, B.K., G.A. Smith, and N. Osterrieder, *En passant mutagenesis: a two step markerless red recombination system.* Methods Mol Biol, 2010. **634**: p. 421-30.
224. van Diemen, F.R., et al., *CRISPR/Cas9-Mediated Genome Editing of Herpesviruses Limits Productive and Latent Infections.* PLoS Pathog, 2016. **12**(6): p. e1005701.
225. Schommartz, T., et al., *Functional Dissection of an Alternatively Spliced Herpesvirus Gene by Splice Site Mutagenesis.* J Virol, 2016. **90**(9): p. 4626-4636.
226. Huebener, P., et al., *High-mobility group box 1 is dispensable for autophagy, mitochondrial quality control, and organ function in vivo.* Cell Metab, 2014. **19**(3): p. 539-47.
227. Birnboim, H.C. and J. Doly, *A rapid alkaline extraction procedure for screening recombinant plasmid DNA.* Nucleic Acids Res, 1979. **7**(6): p. 1513-23.
228. Ramakrishnan, M.A., *Determination of 50% endpoint titer using a simple formula.* World J Virol, 2016. **5**(2): p. 85-6.
229. Zurbach, K.A., T. Moghbeli, and C.M. Snyder, *Resolving the titer of murine cytomegalovirus by plaque assay using the M2-10B4 cell line and a low viscosity overlay.* Virol J, 2014. **11**: p. 71.

Appendix

List of abbreviations

aa	amino acid
AIM2	absent in melanoma 2
AmpR	ampicillin resistance
ASC	apoptosis-associated speck-like protein containing a CARD
ATP	adenosine triphosphate
BAC	bacterial artificial chromosome
BAK	Bcl-2 Antagonist Killer
BAX	Bcl-2 Associated X protein
BCA	Bicinchoninic Acid
BlastR	blasticidin restance
BoHV-1	bovine herpesvirus 1
BSA	bovine serum albumin
CMV	cytomegalovirus
ctrlAb	control antibody
DENV	dengue virus
DMEM	Dulbecco’s modiefied Eagle medium
dNTP	deoxynucleoside triphosphate
doxy	doxycycline
dpi	days post infection
E	Early
EBV	Epstein-Barr virus
EGFP	enhanced green fluorescent protein
eHMGB1	extracellular HMGB1
ELISA	enzyme-linked immunosorbent assay
ER	endoplasmic reticulum
ERT2	mutant estrogen ligand-binding domain
FCS	fetal calf serum
GFP	green fluorescent protein
GSDMD	gasdermin D
HCMV	human cytomegalovirus
HCV	hepatitis C virus

HMGB	high-mobility group box protein
hpi	hours post infection
HRP	horseradish peroxidase
HSV	herpes simplex virus
iBMDM	immortalized bone marrow-derived macrophages
IDR	intrinsically disordered region
IE	immediate early
IL	interleukin
i.p.	Intraperitoneal
KanR	kanamycin resistance
KSHV	Karposi’s sarcoma-associated herpesvirus
L	late
LDH	lactate-dehydrogenase
LLPS	liquid-liquid phase separation
LPS	lipopolysaccharide
mAb	Monoclonal antibody
MAPK	mitogen-activated protein kinase
MCMV	murine cytomegalovirus
MLKL	mixed lineage kinase domain-like
MOI	multiplicity of infection
MOMP	mitochondrial outer membrane permeabilization
NES	nuclear export signal
NF-κB	nuclear factor kappa B
NLRP3	NLR family pyrin domain-containing 3
NLS	nuclear import signal
oriLyt	origin of lytic replication
PAGE	polyacrylamide gel electrophoresis
PAMP	pathogen-associated molecular pattern
PBS	phosphate-buffered saline
PCD	programmed cell death
PEI	polyethylenimine
PFA	paraformaldehyde
PTM	posttranslational modification
PuroR	puromycin resistance

RAGE	receptor for advanced glycation end products
RC	replication compartment
RFLP	restriction fragment length polymorphism
RHIM	RIP homotypic interacting motif
RIPA	radioimmunoprecipitation assay
RIPK	receptor-interacting protein kinase
ROS	reactive oxygen species
RSV	respiratory syncytial virus
RTA	replication and transcription activator
Scr	scramble
SDS	sodium dodecyl sulfate
shRNA	short hairpin RNA
TAE	Tris-acetate-EDTA
TBE	Tris-borate-EDTA
TBS-T	Tris-buffered saline with Tween20
$TCID_{50}$	median tissue culture infectious dose
TLR	toll-like receptor
TNF	tumor necrosis factor
TNFR	tumor necrosis factor receptor
UBC	ubiquitin C
UTR	untranslated region
vICA	viral inhibitors of caspase-8 activation
WT	wild-type

List of figures

Publications

I. Oral presentations at scientific meetings

- 16th Mini-Herpes Virus Workshop, Hannover, Germany, 2023
- LCI Summer School, Fintel, Germany, 2023
- LIV Scientific Retreat, Hamburg, Germany, 2023

II. Poster presentations at scientific meetings

- 32nd Annual Meeting of the Society for Virology (GfV), Ulm, Germany, 2023
- LCI Summer School, Koppelsberg, Germany, 2022

Acknowledgements / Danksagungen

I would like to express my sincere gratitude to my supervisors, Prof. Dr. Wolfram Brune and Dr. med. Peter Hübener. Your guidance and support have been instrumental throughout my research journey. Thank you for challenging me to think critically and for providing invaluable feedback that has enriched my work. I appreciate the time and effort you dedicated to my development, and I am grateful for the opportunity to learn from both of you through the past four years.

I would like to extend my sincere appreciation to the reviewers of my doctoral thesis and the members of the examination board for their time and expertise.

Thank you to all past and present members of the Virus-Host Interaction research unit. Your support and encouragement have been invaluable in keeping me motivated. The daily conversations and collaboration with each of you have helped me grow both professionally and personally.

Special thanks go to Dr. Eléonore Ostermann. You accompanied me from the first to the last day of my doctoral journey. I truly appreciate the countless hours you dedicated to my development, your invaluable training and advice, and our many “subgroup recap sessions.” I’m also deeply grateful for your patience and effort you put into the proofreading of my thesis, which surely tested your nerves. Thank you for everything!

I would like to extend my heartfelt thanks to Michaela, not only for her invaluable help and support as a colleague but especially for being my indestructible friend in the lab. Thank you for all the tears and laughter, and for the countless joyful moments we’ve shared over the years. Although I am moving on now, I will always cherish the memories of us singing in the cell culture room, dancing through the lab, and crafting Christmas decorations in the kitchen.

Zu guter Letzt möchte ich meiner Familie danken. Ohne eure bedingungslose Unterstützung, euer Verständnis und eure Geduld wäre dieser Weg nicht möglich gewesen. Ihr habt mich in jeder Phase meines Studiums begleitet, mich motiviert und mir immer den Rücken gestärkt. Dafür bin ich euch unendlich dankbar.

Affidavit / Eidesstattliche Versicherung

Hiermit versichere ich an Eides statt, die vorliegende Dissertationsschrift selbst verfasst und keine anderen als die angegebenen Hilfsmittel und Quellen benutzt zu haben. Sofern im Zuge der Erstellung der vorliegenden Dissertationsschrift generative Künstliche Intelligenz (gKI) basierte elektronische Hilfsmittel verwendet wurden, versichere ich, dass meine eigene Leistung im Vordergrund stand und dass eine vollständige Dokumentation aller verwendeten Hilfsmittel gemäß der Guten wissenschaftlichen Praxis vorliegt. Ich trage die Verantwortung für eventuell durch die gKI generierte fehlerhafte oder verzerrte Inhalte, fehlerhafte Referenzen, Verstöße gegen das Datenschutz- und Urheberrecht oder Plagiate.

I hereby declare and affirm that this doctoral dissertation is my own work and that I have not used any aids and sources other than those indicated. If electronic resources based on generative artificial intelligence (gAI) were used in the course of writing this dissertation, I confirm that my own work was the main and value-adding contribution and that complete documentation of all resources used is available in accordance with good scientific practice. I am responsible for any erroneous or distorted content, incorrect references, violations of data protection and copyright law or plagiarism that may have been generated by the gAI.

_____ _____

Hamburg, den Unterschrift